# DESIGN OF CONTROL SCHEMES FOR DISTILLATION COLUMN

**A THESIS**

***Submitted in partial fulfilment of the***
***requirements for the award of the degree***
***of***
DOCTOR OF PHILOSOPHY
***in***
ELECTRICAL ENGINEERING

***by***

**AMIT KUMAR SINGH**


**DEPARTMENT OF ELECTRICAL ENGINEERING**
**INDIAN INSTITUTE OF TECHNOLOGY ROORKEE**
**ROORKEE – 247667 (INDIA)**
**JULY 2014**

# INDIAN INSTITUTE OF TECHNOLOGY ROORKEE
# ROORKEE

## CANDIDATE'S DECLARATION

I hereby certify that the work which is being presented in this thesis entitled **DESIGN OF CONTROL SCHEMES FOR DISTILLATION COLUMN** in partial fulfilment of the requirements for the award of the Degree of Doctor of Philosophy and submitted in the Department of Electrical Engineering of the Indian Institute of Technology Roorkee, Roorkee is an authentic record of my own work carried out during a period from January 2010 to June 2014 under the supervision of Dr. Barjeev Tyagi, Associate Professor, Department of Electrical Engineering and Dr. Vishal Kumar, Assistant Professor, Department of Electrical Engineering of Indian Institute of Technology Roorkee, Roorkee.

The matter presented in this thesis has not been submitted by me for the award of any other degree of this or any other Institute.

(**AMIT KUMAR SINGH**)

This is to certify that the above statement made by the candidate is correct to the best of our knowledge.

Date: (Dr. Barjeev Tyagi) (Dr. Vishal Kumar)

---

The Ph.D. Viva-Voce Examination of **Mr. AMIT KUMAR SINGH**, Research Scholar, has been held on……..

Signature of Supervisors Signature of External Examiner

Chairman, DRC Head of the Department

## ABSTRACT

Distillation is defined as a process in which a liquid or vapor mixture of two or more substances is separated into its component fractions of desired purity, by the application and removal of heat. The objective of present research work is to develop a control scheme for distillation column through dynamic simulations and experimentation. To fulfill this objective, an existing laboratory set-up of distillation column is used. The set-up is a continuous binary type distillation column (BDC) and contains a vertical column that has nine equally spaced trays mounted inside of it. Mixture of methanol and water is taken as feed to the column. The distillation column is interfaced with auxiliary components and transducers to facilitate monitoring and control of various parameters of the column. A reboiler is connected to the vertical shell through pipes. A controller unit is interfaced to the reboiler heat input for controlling the temperature profile of the distillation column.

Due to inherent complexity of distillation process, it is difficult to achieve the simultaneous control of top and bottom composition. To overcome this difficulty Wood and Berry developed a linear model of BDC. The Wood and Berry model of distillation column is a simplified linear model and may not represent the BDC exactly therefore; a mathematical model that uses the fundamental physical and chemical laws along with valid normal assumptions has been utilized in this thesis work. Distillation column is divided into three different sections from the modeling point of view. I$^{st}$ section is reboiler section, II$^{nd}$ section is Tray section, and III$^{rd}$ section is condenser section. The balance equations are obtained by applying material and energy conservation laws to these sections. All these equations are solved to develop the model. The manipulated variables are reflux flow and reboiler heat duty. To validate the model, results obtained from this model have been compared with the results obtained from the experimental set-up. In experimental set-up, reflux flow-rate and reboiler heat duty have been varied similarly as in case of the equations based model. It is observed from the results that this equations based model is in good agreement with the experimental outputs. The results obtained in this study prove that this equation based model could be use to represent the existing experimental set-up of BDC. This equations based model has been used for the analysis and implementation of different control schemes to hold the product composition nearly to the set point under different types of disturbances i.e. disturbance in heat input, reflux ratio and feed flow.

As neural network method does not require a deep mathematical knowledge of the system to develop the system's model accurately, in this thesis, a neural network model is proposed for BDC. The neural model gives methanol composition as output based upon the knowledge of the six inputs namely; tray temperature, reflux flow-rate, feed flow-rate, reboiler duty, reflux drum top pressure and reboiler bottom pressure. For the training of the neural network, the data has been acquired by the operation of experimental set-up of BDC. Two

neural network topologies namely; Feed Forward Neural Network (FFNN) and Recurrent Neural Network (RNN) are utilized for the development of the neural network model.

Inferential control scheme is the technique in which secondary variables are used as the controlled variables. For the laboratory set-up of BDC, it is found by the sensitivity analysis that at constant pressure, the temperature of fourth tray is an exact indicator of the corresponding concentration of methanol output. Therefore; temperature of the tray is used as a secondary variable. By using the experimental results obtained with laboratory set-up, a relation has been established between the controller current and the tray temperature by curve-fitting method. This relation has been utilized to control the temperature of the tray. A PID controller is used to control the temperature of the tray. The parameters of the PID controller have been tuned using the Genetic Algorithm in MATLAB® /Simulink environment. This PID controller has also been implemented on the experimental set-up of BDC in the laboratory. The results obtained show that the simulated and hardware PID controller are in good agreement to each other.

Model Predictive Control (MPC) is one of the main process control techniques explored in the recent past for various chemical engineering applications, therefore; the linear MPC (LMPC) scheme utilize the equations based model of BDC and the nonlinear Neural Network based Model Predictive Control (NN-MPC) scheme utilize the ANN based model of BDC to control the methanol composition. In NN-MPC scheme, a three layer feed forward neural network model has been developed which is used to predict the methanol composition over a prediction horizon using the MPC algorithm for searching the optimal control moves. The training data is acquired from the existing laboratory set-up of BDC. Two cases have been considered, one is for reference tracking and another is for feed flow disturbance rejection. The performance of the control schemes are compared on the basis of performance parameters namely rise time, settling time and MSE. NN-MPC and LMPC schemes are also compared with conventional PID controller. The results show the improvement in rise time and MSE with NN-MPC scheme as compared to LMPC and conventional PID controller for both the cases.

The neural network has the ability to represent arbitrary non-linear relations and can be trained even for an uncertain system. These qualities have been exploited by many researchers in the past. In the present work, direct inverse control (NN-DIC) and internal model control (NN-IMC) schemes have been developed to control the final composition of methanol. Forward model and inverse model of BDC have been developed utilizing the ANN approach. In developing the NN-DIC scheme, inverse model is utilized. In NN-IMC scheme, both forward and inverse models are used. Two input variables, reflux flow-rate and reboiler heat duty are used as manipulated variables. The results obtained show the improvement in

the rise time, settling time and MSE with NN-IMC scheme as compared to NN-DIC and NN-MPC schemes.

Soft computing is a collection of various approaches like fuzzy system, neural networks and genetic algorithm. It is useful to tackle imprecision and uncertainty involved in a complex nonlinear chemical system. Recent reviews on soft computing around the world indicate that the number of soft computing based engineering applications is increasing. Neuro-fuzzy is one of the extensively used soft computing approaches. It is a hybridization of artificial neural networks and fuzzy inference system. Adaptive Neuro-Fuzzy inference system (ANFIS) is an example of Neuro-Fuzzy systems in which a fuzzy system is implemented in the framework of adaptive neural networks. ANFIS constructs an input-output mapping based on both the human knowledge (in the form of fuzzy rules) and the generated input-output data pairs. In this work, ANFIS controller is applied on the ANN based model of BDC. The controller controls the methanol composition in BDC by the variation of reflux flow-rate and reboiler heat duty. The performance of ANFIS controller has been compared with NN-IMC control scheme. The obtained result shows the improvement in the rise time, settling time and MSE with ANFIS scheme as compared to NN-IMC scheme.

The present thesis concludes that the discussed models namely; equation based model and ANN based model have been developed and validated for existing experimental set-up of BDC. A PID controller tuned by GA is studied in simulation and, subsequently, it is implemented on the experimental set-up of BDC in laboratory. The results obtained show that the simulated and hardware PID controller are in good agreement to each other. The developed equation based model and ANN based models are utilized to control the methanol composition by the application of different control schemes namely; LMPC, NN-MPC, PID, NN-DIC, NN-IMC and ANFIS. A comparison is conducted among these control schemes based on performance parameters namely; rise time, settling time, overshoot and MSE. Overall, ANFIS control scheme shows a superior performance over the above studied control schemes by presenting a shorter rise time, shorter settling time and smaller MSE.

## ACKNOWLEDGEMENTS

I express my deepest sense of gratitude towards my supervisors Dr. Barjeev Tyagi, Associate Professor, Department of Electrical Engineering and Dr. Vishal Kumar, Assistant Professor, Department of Electrical Engineering of Indian Institute of Technology Roorkee, Roorkee, for their patience, inspiring guidance, constant encouragement, moral support, and keen interest in minute details of the work.

My deepest gratitude and sincere thanks to Dr. Indra Gupta, Associate Professor, Department of Electrical Engineering, Indian Institute of Technology Roorkee, Roorkee without whose encouragement and support my Ph.D would not have been possible. I am thankful to Dr. G. N. Pillai, Chairmen DRC, Department of Electrical Engineering, Indian Institute of Technology Roorkee, Roorkee and Prof. S. P. Srivastava, Professor and Head, Department of Electrical Engineering, Indian Institute of Technology Roorkee, Roorkee for their invaluable direction, encouragement and support, and above all the noblest treatment extended by them during the course of my studies at IIT Roorkee.

I am grateful to Dr. Vijender Singh, Associate Processor, Division of Instrumentation and Control Engineering, Netaji Subhas Institute of Technology, New Delhi for his moral support, encouragement and suggestions for my research work. I am also grateful to the Ministry of Human Resources and Development, Government of India, AICTE, New Delhi for sponsoring me for doctoral research work.

I extend my sincere thanks to all research scholars especially to Dr. Jignesh Makwana, Mr. Bhargav Vyas, Mrs. Gitanjali Mehta, Mr. Ashok Manori, Mr. Anubhav Agrawal, Mr. shailendra Bhaskar, Mr. Nagendra Gautam, Mr. Arvindo Panda, Mr. KS Sajan for sharing and supporting me during my research work. I am also thankful to Mr. Nikesh and Mr. Om Krishan for their help and involvement in my research work. I am extremely thankful to Mr. Kaushal Kumar, Mr. Ravi Kumar and Mr. Jatin Patel, for supporting me during my research work.

I express my sense of gratitude to Mr. Rajendra Singh, the staff of Reliability and Testing Laboratory, Mr. Dinesh Mohan, Technical Officer, Embedded Systems lab, and Mr. Amir Ahmed, Caretaker, Workshop, Department of Electrical Engineering, Indian Institute of Technology Roorkee, Roorkee for their co-operation and assistance.

I am also very grateful to my B.Tech & M.Tech group friends Mr. Anurag Singh, Mr. Devansh Kataria, Mr. Saurabh Mishra, Mr. Prashant Singh, Mr. Siddharth Singh, Mr. Vivek Sharma, Mr. Mayank Srivastava, Mr. Shashank Garg, Mr. Amit Kumar, Mr. Sheersh Garg, Mr, Nikhil Raj, Mr. Mohit Srivastava, Mr. Sorav Dutta, Mr. Durgesh Kumar and Mr. Pramod Maurya for their help and co-operation during my study.

I owe a debt of gratitude to my parents, my brothers, Mr. Sachin Chauhan, Mr. Anuj chauhan, Mr. Sumit chauhan, my maternal uncle, Mr. videsh kumar, family members, sister-

in-law, mother in-law, father in-law and brother-in-law for their consistent encouragement, moral support, patience and care. I have no words to express the appreciation for my wife Mrs. Mayanka Singh, who stood by me at every moment, kept encouraging me in low moments and keeping myself free from almost all the liabilities of home issues during my work.

Last but not the least; I am thankful to the almighty who gave me the strength and health for completing the work.

**(Amit Kumar Singh)**

## CONTENTS

## LIST OF FIGURES

## LIST OF TABLES

## LIST OF ACRONYMS

| | |
|---|---|
| ANN | Artificial Neural Network |
| ANFIS | Adaptive Neuro Fuzzy Inference System |
| BDC | Binary Distillation Column |
| BP | Back Propagation |
| CSTR | Continually Stirred Tank Reactor |
| DIC | Direct Inverse Control |
| DMC | Dynamic Matrix Control |
| DNN | Dynamic Neural Networks |
| ETBE | Ethyl Tert-Butyl Ether |
| FFNN | Feed-forward Neural Network |
| FIS | Fuzzy Inference System |
| FLC | Fuzzy Logic Controller |
| FPGA | Field Programmable Gate Array |
| FSR | Finite Step Response |
| GA | Genetic Algorithm |
| GD | Gradient Descent |
| GDM | Modified Gradient Descent |
| GNN | Grouped Neural Network |
| IGA | Improved Genetic Algorithm |
| IMC | Internal Model Control |
| KKT | Karush-Kuhn-Tucker |
| LM | Levenberg–Marquardt |
| LSE | Least Square Estimate |
| MIMO | Multiple Input Multiple Output |
| MLP | Multi Layer Perceptron |
| MOGA | Multi Objective Genetic Algorithm |
| MPC | Model Predictive Control |
| MRAC | Model Reference Adaptive Control |
| MSE | Mean Squared Error |
| NNDIC | Neural Network based Direct Inverse Control |
| NNIMC | Neural Network based Internal Model Control |
| NNMPC | Neural Network based Model Predictive Control |
| PCA | Principle Component Analysis |
| PID | Proportional-Integral-Derivative |
| PLC | Programmable Logic Controller |

| | |
|---|---|
| PLS | Partial Least Squares |
| QDMC | Quadratic Matrix Control |
| RBFNN | Radial Basis Feed-forward Neural Network |
| RBS | Radial Basis Function |
| RMSE | Root Mean Squared Error |
| RNN | Recurrent Neural Networks |
| RTD | Resistance Temperature Detector |
| SCR | Silicon Controlled Rectifier |
| SDBP | Steepest Descent Back Propagation |
| SQP | Sequential Quadratic Programming |
| SRC | Step Response Coefficients |
| SSQ | Sum of Squares |
| SVD | Singular Value Decomposition |
| ZN | Ziegler-Nichols |

## LIST OF SYMBOLS

| | |
|---|---|
| $\alpha$ | Relative volatility |
| $\eta_{1,j}^{v}$ | Vaporization efficiency of component j in reboiler, |
| $n_{ij}$ | Murphree stage efficiency based on vapor phase of component j on tray i |
| c,σ | Parameters of gaussian membership function |
| $\mu_A(I)$ | Gaussian membership function for fuzzy set A of input I, |
| $Y_i^k$ | Output of ANFIS for layer k, node i |
| $\eta$ | Update rate |
| $\tau_i$ | Integral time, seconds |
| $\tau_d$ | Derivative time, seconds |
| $\Delta u_R$ | Change in reflux flow-rate |
| $\Delta u_S$ | Change in reboiler heat duty |
| $a_{1,k}$ | Step response coefficient for the input, $u_R$ |
| $a_j$ | Lower bound of PID parameters |
| A | Dynamic matrix |
| $A_i$, $B_i$, $C_i$ | Fuzzy sets |
| $A_{net}$ | Net area of the tray, $ft^2$ |
| B | Total bottom product rate, kg-mole/hr, |
| b | Neural network bias |
| $b_j$ | Upper bound of PID parameters |
| D | Distillate flow-rate, kg-moles/hr, |
| $F_i$ | Total feed flow-rate injected to tray-i, kg-moles/hr |
| $G_C(z)$ | Transfer function of controller |
| $G_P(z)$ | Transfer function of process |
| $\tilde{G}_P(z)$ | Neural network model of $G_P(z)$ |
| $h_1$ | Total molar enthalpy of liquid entering from tray-1 to reboiler, kJ/kmole, |
| $h_B$ | Total molar enthalpy of liquid leaving reboiler, kJ/kmole |
| $H_B$ | Total molar enthalpy of vapor leaving reboiler, kJ/kmole, |
| $H_C$ | Control horizon |
| $h_D$ | Total molar enthalpy of liquid leaving the reflux drum, kJ/kmole , |
| $h_i$ | Total molar enthalpy of liquid leaving tray I, kJ/kmole, |
| $H_i$ | Total molar enthalpy of vapor leaving tray I, kJ/kmole |
| $hl_{ij}$ | Pure component enthalpy of component j in liquid, kJ/kmole, |
| $H_{NT}$ | Total molar enthalpy of vapor leaving the last tray NT, kJ/kmole, |
| $H_P$ | Prediction horizon |

| | |
|---|---|
| $Hv_{ij}$ | Pure component enthalpy of component j in liquid, kJ/kmole |
| $h_w$ | Height of the weir, ft |
| I | Controller current, mA |
| $I_1$, $I_2$, $I_3$ | Inputs to ANFIS |
| J | Optimization function |
| $k_{1,j}$ | Equilibrium constant of component j in reboiler |
| $K_D$ | Derivative constant |
| $K_I$ | Integral constant |
| $K_P$ | Proportional constant |
| $L_1$ | Total liquid flow-rate from tray-1 entering to reboiler, kg-moles/hr, |
| $L_i$ | Total liquid flow-rate leaving tray-i, kg-moles/hr, |
| $L_{i+1}$ | Total liquid flow-rate entering to tray i, kg-moles/hr, |
| $l_w$ | Length of the weir, ft |
| $M_i$ | Molar liquid hold up on tray i, kmole |
| $M_B$ | Liquid molar hold up in reboiler, kmole, |
| $M_D$ | Liquid molar hold up in the reflux drum, kmole, |
| $M_{Di}$ | Average molar density of liquid on tray I, kmole/ft$^3$ |
| $n_i$ | The output of the first layer of neural network |
| n | Number of bits in chromosome |
| $p_i$, $q_i$, $r_i$, $s_i$ | Consequent parameters for ANFIS |
| $Q_B$ | Reboiler heat duty, kW |
| $Q_C$ | Condenser duty, kW |
| R | Total liquid flow-rate entering to the tray NT from reflux drum, kg-moles/hr, |
| S | Steam Flow-rate, kg-moles/hr, |
| $T_1$ | Measured temperature of tray, °C |
| $T_{ref}$ | Reference temperature of tray, °C |
| $T_s$ | Samling interval, seconds |
| $u_F$ | Feed flow-rate input, kg-moles/hr, |
| $u_{PB}$ | Reboiler bottom pressure input, kPa |
| $u_{PT}$ | Reflux drum top pressure input, kPa |
| $u_R$ | Reflux flow-rate input, kg-moles/hr, |
| $u_S$ | Reboiler duty input, kW |
| $u_{T1}$ | Tray temperature input, °C |
| $V_B$ | Total vapor flow-rate leaving reboiler, kg-moles/hr, |
| $V_i$ | Total vapor flow-rate leaving tray-i, kg-moles/hr, |
| $v_i$ | The output of the hyperbolic tangent sigmoid function, |
| $V_{i-1}$ | Total vapor flow-rate entering to tray i, kg-moles/hr, |

| | |
|---|---|
| $V_{NT}$ | Total vapor flow-rate leaving the tray NT, kg-moles/hr, |
| w | Neural network weights |
| $W_C$ | Weighting coefficient to penalize relative big changes in manipulated variable |
| $W_P$ | Weighting coefficient for the relative error between set-point and actual value |
| x | Composition of highly volatile component in liquid, mole fraction |
| $x_B$ | Bottom composition, mole fraction |
| $x_{B,j}$ | Liquid fraction of component j in bottom product ,% mole fractions, |
| $x_D$ | Methanol composition, mole fraction |
| $x_{DSP}$ | Set-point of methanol composition, mole fraction |
| $x_{D,j}$ | Liquid fraction of component j in reflux drum, % mole fractions |
| $x_{Dm}$ | Output of the neural network model |
| $x_{Fij}$ | Liquid fraction of component j in feed on tray i ,% mole fractions, |
| $x_{ij}$ | Liquid fraction of component j, leaving the tray i , % mole fraction |
| $x_j$ | Real value of the parameter |
| X* | Least square estimate of X |
| y | Composition of highly volatile component in vapor, mole fraction |
| $y_{B,j}$ | Vapor fraction of component j in bottom product ,% mole fractions, |
| $y_{ij}$ | Vapor fraction of component j leaving the tray i ,% mole fractions, |
| $y_{ij}^*$ | Equilibrium vapor fraction of component j on tray i |
| $y_{NT,j}$ | Vapor fraction of component j leaving tray NT ,% mole fractions, |
| $\overline{w}_{i,j,k}$ | Normalized firing strength |

# Chapter 1: INTRODUCTION

*This chapter introduces the research work carried out in this thesis. It describes the distillation process and discusses the existing laboratory experimental set-up of distillation column. The literature survey of modelling and control schemes of the distillation column has also been performed. In the end, scope of work, author's contribution and thesis outlines are explained.*

## 1.1 Introduction to Distillation Process

Distillation is a process in which a liquid or vapour mixture of two or more substances is separated into its component fractions of desired purity, by the application and removal of heat. The objective of separation is achieved by the creation of two phases which differ on the basis of volatilities, gravity or phase state. Because the different components of the mixture have different volatilities, each component will part itself between the liquid and vapor phases to a different extent. Trays or packing are used to bring the two phases into intimate contact. The end result is that the lower volatile components will be concentrated in the lower sections of the column, with the highly volatile components concentrated in the higher sections of the column. Distillation column is the required equipment for carrying out the process of distillation. Distillation columns are made up of several components, each of which is used either to transfer heat energy or enhance material transfer. A typical distillation column contains following major components:

- **Vertical shell:** In vertical shell, the separation of feed components is carried out.
- **Column internals:** Trays or plates are used to enhance component separations.
- **Reboiler:** Reboiler is used to provide the necessary vaporization for the distillation process.
- **Condenser:** It is used to cool and condense the vapor leaving from the top of the column.
- **Reflux drum:** It is used to hold the condensed vapor from the top of the column so that liquid (reflux) can be recycled back to the column.

Distillation columns can be classified on the basis of their operation, nature of processing feed and the types of column internals.

## 1.2 Types of Distillation Column

On the basis of the operation, the distillation columns are classified in the following two types:

**Batch columns:** The feed to the column is supplied batch-wise in these types of distillation columns. The column is charged with a 'batch' and then the distillation process is carried out. The next batch of feed is supplied after distillation of the current batch is completed.

**Continuous columns:** In contrast to the batch column, continuous column consists a continuous feed stream without any interruption. These columns are capable of handling high throughputs and are more in use out of the two types.

On the basis of nature of processing feed, distillation column can be classified in two categories:

**Binary column**: In binary column, the feed mixture contains only two components.

**Multi-component column**: In this type of distillation column, feed mixture contains more than two components.

On the basis of column internal architecture, distillation columns can be classified as:

**Tray column**: In this type of column, the trays are used to hold up the liquid to provide better contact between vapour and liquid. Different types of trays are used; bubble cap trays and sieve trays are the examples of these types of trays.

**Packed column**: In the packed column, instead of trays, 'packings' are used to enhance the contact between vapor and liquid.

### 1.3 Basic Operation of Distillation Column

The liquid mixture that is to be processed is known as feed. Normally the feed is input at the middle tray of the column known as the ‘feed tray’. The feed tray divides the column into two sections, top (enriching or rectification) section and bottom (stripping) section.

**Rectifying Section**: In this section, vapor rising is washed with liquid flowing down from the top to remove lower volatile component.

**Stripping Section:** In this section, liquid has been removed from the highly volatile stream by partial vaporization in the reboiler.

The feed flows down the column where it is collected at the bottom in the reboiler. Heat is supplied to the reboiler to vaporise the liquid. The source of heat is steam. In refineries, the heating source may be the steam exhausted from other columns. The vapor moves up in the column and as exits from the top of the unit where a condenser is used for condensation of the vapor. The condensed vapor is stored in a holding vessel known as the reflux drum. Some part of this condensed liquid is fed back to the top of the column and this is called the reflux. The condensed vapor which is the output of the system is known as the distillate or top product.

On each tray, the mass is transferred in such a way that the higher volatile component passes from the liquid to the vapor and the lower volatile component passes from the vapor to the liquid state. Thus there is an increase in the concentration of the higher volatile component in the vapor as it passes up in the column from tray to tray. There is also an increase in the concentration of the lower volatile component in the liquid as it passes down in the column from tray to tray.

### 1.4 Constructional Details of Laboratory Set-up of Distillation Column

The schematic of laboratory set-up of Binary Distillation Column (BDC) is shown in Figure 1.1. It consists of the following components:

- **Vertical Column:** The distillation column has been built as a vertical cylindrical column. There are nine equally spaced trays mounted inside the column. Every tray has one conduit on alternate side, called down comer. Due to the gravity, the liquid flows down from each tray to the next tray through these down comers. A weir is present on one side of each tray to maintain liquid level at a suitable height. In the present laboratory set-up, bubble cap type of trays has been placed.
- **Reboiler:** In order to create and sustain the two phases, needed for the separation, the heat exchange to the column must be regulated. The reboiler is a heat transfer unit which is connected to the vertical column through suitable piping to heat the liquid for vaporization. It has three electric heaters of 4kW, 2 kW and 2 kW capacities.

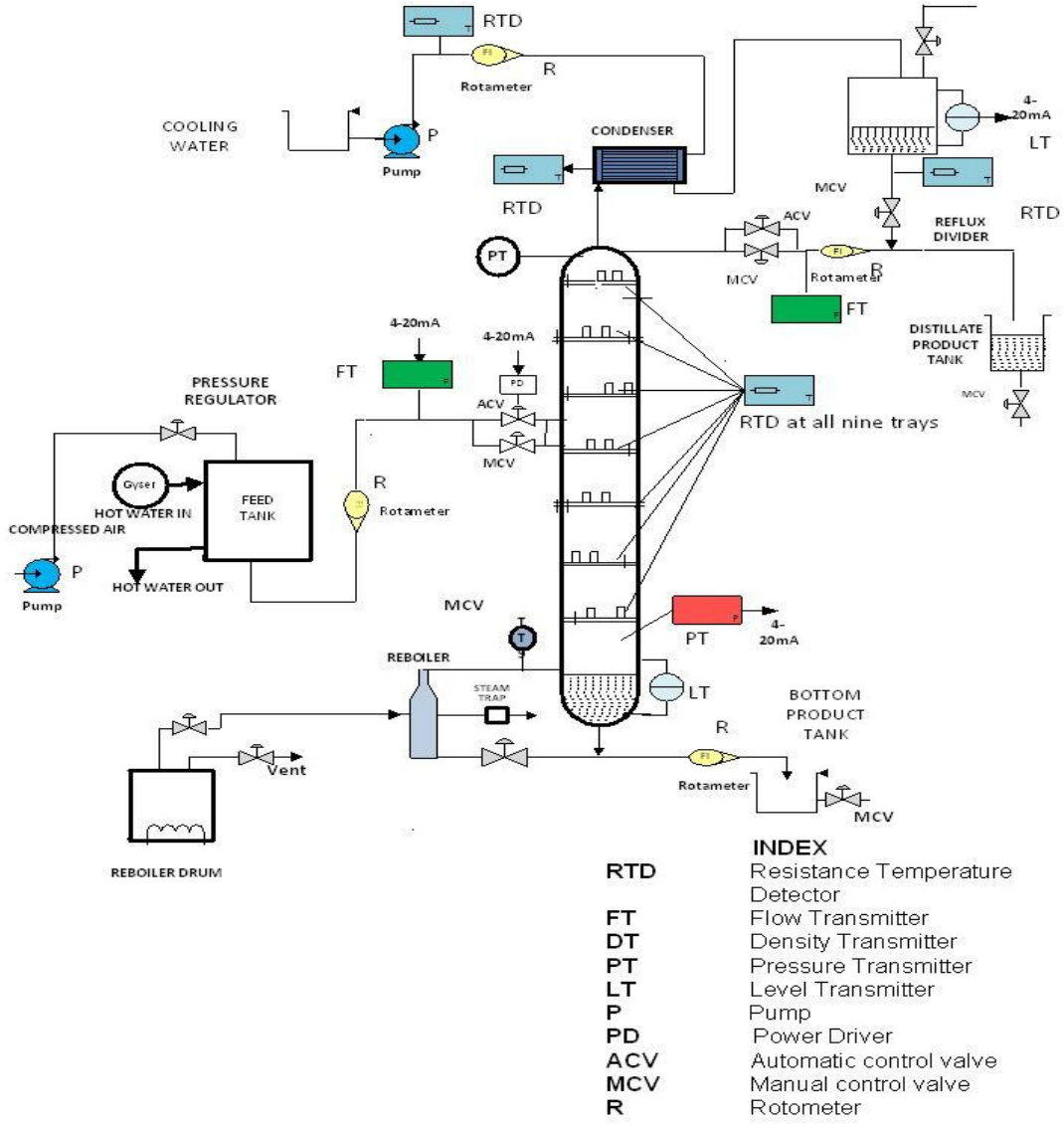


Fig. 1.1 Laboratory Set-up of BDC with Instrumentation

- **Condenser**: The condenser is a heat exchanger connected to the column through the piping. The primary function of the condenser is to remove heat from the vapor coming out of the highest stage of the column for the condensation. Water is used as coolant in the condenser.
- **Feed Tanks:** Feed tanks are used to store and supply the feed to the distillation column. There are two feed tanks in the existing column.
- **Rota-meters:** There are three rota-meters to measure the liquid flow-rate and to control the feed flow, bottom product and cooling water.
- **Pressure Regulator:** It is used to regulate the pressure in the distillation column.
- **Automatic Control Valve:** This valve is used to fix and control the flow of feed mixture. It can be placed to control the liquid flows at other points also. This control valve is electric type and accepts input in the range of 4-20 mA current signal.
- **Compressor:** The compressor is provided to develop necessary pressure for circulating the feed.
- **Tanks:** Three tanks are provided to store cooling water, distillate and bottom product.
- **Controller Unit:** The controller unit controls the heat input to control the tray temperature at the desired set point.
- **Reflux Divider Unit:** This unit is used to control the reflux ratio through reflux flow in the steady state condition.

## 1.5 Transducers used in Distillation Column

Following transducers are interfaced with the laboratory set-up to facilitate the monitoring and the control of various parameters of the column.

- **Temperature Transducer:** Total twelve Resistance Temperature Detectors (RTD) are provided for sensing the temperature at all the trays, reflux drum, and condenser inlet and outlet. Out of twelve RTD's, nine are fitted in the trays, one in reflux drum, one in condenser inlet and one in condenser outlet.
- **Level Sensor:** The level sensor is used to sense the level of reflux in reflux drum.
- **Pressure Sensor:** These sensors are used to measure the vapour pressure at the top and at the bottom of the distillation column.

## 1.6 Modeling of Distillation Column

The following are the different models of distillation column discussed in the literature.

### 1.6.1 Mathematical Modeling and Validation of BDC

An accurate mathematical model is the need of the process control. The mathematical modelling of distillation process is based on the mass and enthalpy equations. Different techniques have been used for distillation process modelling by the researchers.

A robust mathematical model based on mass balance and relative volatility is developed by Bonsfills and Puigjaner [1]. The model was tested in a variety of situations using a batch

distillation pilot plant. For validation of batch distillation column, Mehlhorn *et al.* [2] developed a simulation model. Its novelty consists in the use of both the non-equilibrium and the equilibrium model which makes it a better integrated model. Simulation results have been compared with experimental results and it shows that there is a good agreement between simulation and experimental results. It also verifies that the mathematical model is compatible with experimental set-up of distillation column. A model for efficient utilization of resources is developed and validated by Babu and Ramakrishna [3] using technology, management and waste emissions (TMW) process.

Darnon *et al.* [4] proposed a method to overcome the difficulty of limitation of downstream processing which requires a lot of experimentation. The approach is based on non steady state mass balance equations. On the assumption of constant transmission rates, these equations can be solved analytically. When these assumptions are not accurate, a numerical resolution is proposed. The simulation results are compared with the experimental results obtained with a synthetic bio-solution. Operation of a conventional batch distillation column can be conveniently described in three parts: 1) startup period, 2) production period and 3) shutdown period. For standard separation processes, the production period is the most time consuming. However, for high purity separations, the startup time may also be significant. Sorensen and Skogestad [5] presented the optimal operation taking the start-up time into consideration. Alternative ways of reducing the duration of the startup period were discussed.

A new approach is addressed by Gupta *et al.* [6] to calculate the effective thermal conductivity of poly dispersed packed beds. The proposed approach is validated with the experimental measurements of binary and ternary beds. The effect of the thermal variations on the inlet temperature to predict the variations of key output variables is studied by H. Ben Bacha *et al.* [7]. Such variables include water temperature, air temperature, humidity in the evaporation and condensation chambers and the amount of produced distilled water. A series of experiments was conducted to validate the dynamic model of the distillation module. Experimental results were compared with the simulation results. It was shown that the developed model is able to predict accurately the trends of the heat and mass characteristics of the evaporation and condensation chambers. Schoenmakers and Bessling [8] developed the simulation model based on equilibrium and applied to a large industrial set-up. The scale-up from the mini plant is used for the experimental validation for conventional distillation, but it is complicated for reactive distillation. Reference plant experience on an industrial scale is necessary to overcome these problems. The combination of a chemical reaction and a distillation separation in one apparatus shows several advantages compared to the separately performed processes. Several possible models of different complexity have been compared by Sundmacher *et al.* [9] for the reactive distillation process. These models consider multiple chemical main and side reactions which are always present in the industrial

production. The simulation results are compared with the experimental results for the validation of the developed models for two packed laboratory scale columns. Wang *et al.* [10] reported the model parameters for binary mixtures and studied the feasibility of these parameters. This method is used for obtaining reasonably reliable vapor-liquid equilibrium at constant temperature or at constant pressure. In 2003, Sundmacher and Qi [11] presented a comparative study on the conceptual design of reactive distillation process configurations. The reversible reactions are considered for an ideal binary mixture as a sample model system. The design aspects are discussed in terms of operating parameters.

A detailed approach for modeling and simulation of catalytic distillation including all major aspects of the description of column hydraulics, mass and energy transfer, chemical reactions and thermodynamic non-idealities is presented [12] in the principle component analysis (PCA). PCA is used by Zullo [13] to identify and monitor the operating modes of continuous distillation plants. The PCA is used to reduce dimensionality and to remove the collinearity of the original data set. Tapp *et al.* [14] developed an experimental technique for measurement of the residue curves. The modified form of time dependent profiles of the apparatus is developed which is mathematically equivalent to the position dependent profiles in a continuous distillation column. This method facilitates to simulate a distillation column profile in a small batch apparatus. The accuracy of the apparatus is determined by the comparison of experimental results and simulations. Doma *et al.* [15] developed a methodology for identifying MIMO step response models while the process is operating under multivariable control. The identification of MIMO step response models is achieved by adding an external signal considering one variable at a time. The approach is applied to a distillation tower in a petroleum refinery. Lith *et al.* [16] developed a simple model, describing the product quality and production over time of an experiment batch distillation column, including the start-up time. The knowledge about dynamics having general validity is used and additional information about the specific column behavior is derived from the measured process data. Deshpande [17] has discussed the detailed mathematical modeling of distillation process.

Henrion and Moller [18] have dealt with a continuous distillation process under stochastic rate of inflows collected in the flow tank. A pilot plant has been built and operation was optimized by Schneider *et al.* [19] with the help of synthesis methods for the validation and verification of the structure alternatives of simulation tools. Luyben [20] has explained the mathematical modeling of distillation process for simulation using different examples. The different algorithms are presented by using different aspects of mathematical modeling. The conventional Luyben algorithm is used by John and Lee [21] for the dynamic simulation of reactive distillation unit with ethyl tert-butyl ether (ETBE) synthesis. The unit has twenty stages and five feed components. Akanksha *et al.* [22] developed a diffusion–convection–reaction model taking momentum, mass and heat transfer effects into account. The resultant

equations were solved using a finite difference backward implicit scheme. The results indicated that the predicted conversion was in close agreement with the experimental results. The fundamental dynamic model approach has been used by Can *et al.* [23] for binary distillation column. Bansal *et al.* [24] developed a dynamic distillation model for separation of benzene and toluene. This model consists of differential-algebraic equations for trays, reboiler, condenser and reflux drum. Diehl *et al.* [25] developed the differential algebraic first principle model for binary mixture of methanol and n-propanol. This model was described by means of material and energy balances, hydrodynamic effects, equilibrium relationships for each tray, reboiler and the condenser. The model reduction techniques have been used in references [26]-[27] to derive a simplified dynamic model from complex higher order models. Higler *et al.* [28] applied the non-equilibrium model for a complete three-phase distillation. The model consists of a set of mass and energy balances for each of the three possible phases present. The results obtained for the non-equilibrium model are in good match with the experimental data for the water-ethanol-cyclohexane system. Bian and Henson [29] proposed a nonlinear model for high purity distillation column in separation of benzene-toluene. A new computational mass transfer model is proposed by Li and Lee [30] for the distillation process. This model is developed by utilizing the fluctuating mass flux for the closure of turbulent mass transfer equation in order to obtain the concentration profile and the separation efficiency of distillation column. Muntean *et al.* [31] has proposed a general modeling framework to provide a fast and easy solution for modeling of distillation columns.

### 1.6.2 ANN Modeling of BDC

ANN can provide good empirical models of complex nonlinear processes which are useful for many purposes including process control. The ANN is used for various applications. Some of the applications of ANN in the process modelling are presented here. In 1991 and 1992, Marmol *et al.* [32, 33] described the model of multi-component batch distillation. Two approaches were explored to estimate the distillate composition: a rigorous steady state model and a quasi-dynamic non-linear model. The models developed provide the estimation of distillate composition using only one temperature measurement. Bhagat [34] has discussed briefly the neural networks. Two examples were taken to demonstrate this practical application. In the first one, the change in concentration of outlet stream with respect to the change in inlet stream concentration was studied. The second example involved the identification of degree of mixing in a reactor or vessel. In 1994, Morris *et al.* [35] examined the contribution of various network methodologies to the process modelling. Feed forward networks with sigmoidal activation functions, radial basis function networks and auto associative networks were reviewed and studied using data from industrial processes. In 1995, Macmurray and Himmelblau [36] described the ANN modeling of packed distillation column. This modelling is an interesting example of complex modeling because the column exhibits a change in the sign of the gain under various operating conditions. It is

demonstrated that the ANN model is as good as or better than a simplified first principles model when used for model predictive control.

A group of feed-forward neural networks, each providing the prediction of an individual process output at a future step, is used as the dynamic prediction model for the model-based predictive control (MPC) scheme by Ou and Rhinehart [37]. These ANNs are trained and implemented in parallel. Therefore, the complexity and effort in the training stage is decreased and compounded error propagation is eliminated from the prediction. A new strategy of compensating for the process-model mismatch under this grouped-NN model structure is also developed. Effectiveness of the scheme as a general nonlinear MPC is demonstrated by simulation results.

A novel multilayer discrete-time neural network is presented for the identification of multi-input multi-output (MIMO) nonlinear dynamical systems [38]. The major novelty of this approach is a rigorous proof of identification error convergence which reveals a requirement for a new identifier structure and nonstandard weight tuning algorithms. The NN identifier includes modified delta rule weight tuning and exhibits a learning-while-functioning feature instead of learning-then-functioning, so that the identification is on-line with no explicit off-line learning phase needed. A new approach has been presented to control nonlinear discrete dynamic systems, which relies on the identification of a discrete model of the system by ANN [39]. A locally equivalent optimal linear model is obtained from the ANN model at every operating point the system goes through during the control task. A study has been given regarding Nonlinear system identification via discrete-time recurrent single layer and multilayer neural networks [40]. Gupta *et al.* [41] discussed the performance of Recurrent Neural Networks (RNNs) using Compensatory Neuron Model (CNM).The simulation results show that the proposed model performs significantly better than the existing model when used with RNNs. Singh *et al.* [42, 43] has applied the Levenberg–Marquardt (LM) approach for the development of ANN model of distillation process. The developed model predicts the composition of distillate using column pressure, reboiler duty, and reflux flow along with the temperature profile of the distillation column as inputs.

## 1.7 Control Schemes

A control action is called effective when it hold the measured output near to the desired set point. For distillation column control, product composition should be around desired value under all types of disturbances in feed, reflux and feed input. The following control schemes for the control of distillation column are discussed in the literature.

### 1.7.1 PID Control Scheme and Tuning

The PID controller [44] is consists of proportional, integrative and derivative elements. It is widely used in feedback control of industrial processes. Ziegler-Nichols method is mostly used to acquire the tuning parameters of PID controllers [45]. This method requires open loop characteristics of the plant to determine the controller parameters. Zhen-Yu Zhao [46]

has developed a fuzzy gain scheduling scheme to determine the PID controller parameters. The comparison of results by Quadratic Matrix control (QDMC) and conventional PI controller to distillation column has been done by Hsie and Mcavoy [47]. A computational algorithm is presented by Nagar *et al.* [48] for the design of digital controllers. The adopted design procedure is based on the matching frequency of open loop system with a reference model. The controller parameters are obtained by formulating the design problem as unconstrained optimization problem.

Porter and Jones [49] have utilized genetic algorithms to optimize the parameters of PID controllers. Skogestad [50] has presented analytic tuning rules which result in a good closed-loop behavior. The integral term has been modified to improve disturbance rejection for integrating processes. Upreti [51] has presented a new optimal control technique to provide good quality, robust solutions for chemical engineering problems, which are generally non-linear and highly constrained. The technique neither uses any input of feasible control solution, nor any auxiliary condition. The technique generates optimal control by applying the genetic operations of selection, crossover, and mutation on an initial population of random, binary-coded deviation vectors. Gupta and Garg [52] have found the Multi Objective Genetic Algorithm (MOGA) more meaningful and relevant for solving industrial problems. One of the MOGA algorithms was the elitist non-dominated sorting genetic algorithm (NSGA-II). Several bio-mimetic adaptations have been developed to improve the rate of convergence. Some of these are heat exchanger networks, industrial catalytic reactors etc. Chen *et al.* [53] have presented a method of PID controller parameters optimization based on Improved Genetic Algorithm (IGA).

### 1.7.2 Neural Network based Schemes

Considering the complexity and non-linear behaviour of the distillation process, ANN based approaches are more suitable to maintain the product quality at the desired level. Joseph and Brosilow [54] developed an inferential control scheme by using the estimated composition to determine valve position directly, or by manipulate the set point of a temperature controller as in parallel cascade control. In this inferential control scheme, selected tray temperatures are used as secondary outputs. The measurements of secondary outputs and manipulated variables are used to estimate the effect of unmeasured disturbances in the feed on product quality to achieve improved composition control. Up to 1958, the digital computers for calculations were not utilized up to its strength. For general multi-component mixtures, solution becomes difficult because the coefficients depend in a highly non-linear fashion on compositions. Amundson and Pontinen [55] introduced the use of digital computers to solve this distillation column problem.

A number of applications of ANNs to process control problems have been reported. Piovoso et al. [56] have compared ANN modeling to other modeling approaches for Internal Model Control and it was reported that ANNs give better performance in the case of

process/model mismatch. Nahas *et al.* [57] proposed a neural network based nonlinear internal model control (NIMC) strategy for SISO processes. The neural network model is identified from input−output data using a three-layer feed forward network trained with a conjugate gradient algorithm. The NIMC controller consists of a model inverse controller and a robustness filter with a single tuning parameter. The proposed strategy includes time delay compensation in the form of a Smith predictor and ensures offset-free performance. Pottman and Seborg [58] used Radial Basis function Neural Network (RBFNN) for non-linear control. It was found that the ANN based controllers are better than the other controllers in terms of their ease of design and their robustness.

In the late 1980s, ANNs were applied to map the measured output to the control input. It was established that standard multi layer feed forward network with one hidden layer are capable of approximating any measurable function [59]. Some basic concepts relating to ANNs are explained as well as how these can be used to model the process. The need for modelling is pointed out for closed loop control. It is concluded that the accuracy of ANN modelling is fully comparable with the accuracy achieved by more traditional modelling schemes [60]. A noval technique using ANN is proposed for the adaptive control of nonlinear systems [61]. The ability of ANNs to model nonlinear functions and the inverses is exploited. The use of nonlinear function inverses raises questions of the existence of the inverse operators. These are investigated and results are given characterising the invertibility of a class of nonlinear dynamical systems. The control structure used is internal model control. It is used to directly incorporate networks modelling the plant and its inverse within the control strategy. The potential of the proposed method is demonstrated by an example. Hunt and Sbarbaro [62] observed that ANN is suitable for the identification and control of nonlinear plants. Narendra and Parthasarathy [63] explained how neural networks, trained by a back propagation algorithm for adjustment of parameters, can be effectively used for identification and control of nonlinear dynamic systems. The use of multi-layer ANN trained by back propagation algorithm for dynamic modeling and control of chemical processes have been discussed by Bhat and Avoy [64]. Two approaches were proposed for modeling and control of nonlinear systems. The first approach utilizes a trained NN model of the system in a model based control work frame and the second approach utilizes an inverse model of the plant extracted using NN in the internal model control structure. Willis *et al.* [65] discussed ANN models from the process engineering point of view and explained some of the approaches. Some of the industrial applications have been considered for use of ANN in modeling and control applications whereby an ANN is trained to characterize the behavior of the systems, namely industrial, continuous and fed-batch fermenters, and a commercial scale, industrial, high purity distillation column. A scheme has been presented by Nguyen and Widrow [66] for use of ANNs to solve highly nonlinear control problems. Noriega and Wang [67] presented a direct adaptive ANN control strategy for unknown nonlinear systems. Chen et al. [68]

proposed an improved differential evolutionary algorithm to encode prior knowledge simultaneously into networks in training process. Different classifications are found in the literature for neuro-controllers [69-71]. In general the inversion of nonlinear models is not an easy task and analytical solutions may not exist, so solutions have to be found numerically. There are several strategies for obtaining the inverse model so that the nonlinear performance can be fully exploited in order to cope with a complex plant [72]. Few researchers applied ANNs to generalize well known nonlinear control methods [73]. Since early 2000s, in some of the research works, it is reported that even after ANN compensation, the resultant dynamics was nonlinear and the process was controlled using nonlinear control methods [74]. The ANN based internal model control (NN-IMC) is one of those methods [75]. Two ANN models are utilized in this scheme. One model is trained to learn forward dynamics of the process (forward model) while another model is trained to learn the inverse dynamics of the process (inverse model). Inverse model is utilized as a controller to the process in NN-IMC scheme. Singh *et al.* [76] utilized forward and inverse models in two approaches namely: Neural Network based Direct Inverse control (NN-DIC), and Neural network based internal model control (NN-IMC) to control the methanol composition in BDC. Recently ANN based control schemes are used in various industrial applications by researchers [77, 78].

### 1.7.3 Model Predictive Schemes

Model Predictive Control (MPC) is a multivariable control algorithm to predict the future control action and future control trajectories by using the past control actions and the available current output variables [79]. MPC uses a dynamic model of the plant to predict the future actions of manipulated variables on the plant output. The future moves of the manipulated variables can be determined by minimising the difference between the set point and the predicted output. MPC has been widely used in various industrial fields, such as chemicals, food processing, automotive, and aerospace engineering, etc. MPC has come a long way since its inception almost five decades ago. Hussain [80] has carried out an extensive review on MPC. A survey on industrial MPC technology has been carried out in reference [81]. For the successful implementation of MPC, the existence of an accurate process model is a must. Distillation processes have been traditionally controlled using linear system analysis even though these are inherent nonlinear process. One solution to get the accurate model is the identification of distillation process by using the neural networks [82-84].

Neural network based model predictive control (NN-MPC) is one of the latest approaches where MPC scheme is implemented by using the neural network model of the process. NN-MPC has been widely used in the field of chemical engineering by. Konakom *et al.* [85] applied the NN-MPC scheme for reactive distillation column. Arumugasamy and Ahmad [86] presented a paper which surveys the concept of Feed forward Neural Networks used in MPC for various Chemical and Biochemical processes.

### 1.7.4 ANFIS Scheme

Adaptive Neuro-Fuzzy Inference System (ANFIS), proposed by Jang [87] is one of the examples of Neuro-Fuzzy systems in which a fuzzy inference system is implemented in the framework of adaptive networks. The input output mapping of ANFIS is based on both the human knowledge (in the form of fuzzy if then rules) and on generated input output data pairs by using a hybrid algorithm which is a combination of gradient descent and least square estimation. ANFIS works well with optimization techniques. It can be used in modeling and controlling studies, and also for estimation purposes.

Belarbi *et al.* [88] proposed a fuzzy neural network that learns rules of inference for a fuzzy system by classical back-propagation. The network has been trained off-line in a closed loop simulation to design Fuzzy Logic Controller (FLC). Another network was used as a design model to back -propagate the error signal. Controller rules were extracted from the trained network to build the rule base of the FLC. The framework was used for the estimation and control of a batch pulp digester. The controlled variable was estimated with same type of FNN by the measurements of the batch temperature and concentration of the alkali. FLC with nine rules showed good degree of robustness in the face of parameter variations and changes in operating conditions. To predict the controlled variable for the continuous digester, Leiviska [89] has applied linguistic equations (fuzzy models) and NN models by using the actual training data collected from a continuous digester house.

Oh *et al.* [90] has introduced an identification method in the form of Fuzzy-Neural Networks for nonlinear models. Buragohain and Mahanta [91] have proposed an ANFIS based model for complex ill-defined real world systems for optimization of the training of the neural network. The proposed model is experimentally validated by using it for gas furnace and thermal power plant. Fernandez *et al.* [92] has applied the ANFIS modeling and indirect control of the heavy and light product composition in a binary methanol-water distillation column by using the adaptive Levenberg–Marquardt approach. The results obtained demonstrate the potential of the adaptive ANFIS scheme for the dual control of composition both for changes in set points with null stationary error even in the presence of disturbances. Fernandez *et al.* [93] have suggested the use of inferential composition estimators to assist the monitoring and control of continuous distillation columns. In this paper, an ANFIS predictor is used to estimate the product compositions in a binary methanol-water continuous distillation column from available on-line temperature measurements.

## 1.8 Author's Contribution

The aim of present research work is to develop the suitable models and control schemes for the distillation process. The various contributions made through this work are summarized as follows:

- A detailed literature survey of distillation process, modeling of distillation column and the various control schemes developed for the output control has been carried out.

- The equations based model which is based on the fundamental physical and chemical laws along with valid normal assumptions has been validated experimentally. A neural network based model is also developed for the distillation column with the use of experimental data. Two neural network topologies namely; FFNN and RNN have been utilized for the model development.
- Temperature of the tray is used as a secondary variable to develop the inferential control scheme to control the composition of methanol output of BDC. A PID controller is used to control the temperature of the tray. The parameters of the PID controller have been tuned using the Genetic Algorithm.
- Different control schemes namely; PID, LMPC and NN-MPC are developed to control the methanol composition for BDC. These control schemes are evaluated on the basis of rise time, settling time and mean squared error.
- The forward and inverse models of BDC have been developed utilizing the ANN approach. These models are used in ANN based Direct Inverse Control (NN-DIC) and ANN based Internal Model Control (NN-IMC) schemes to control the methanol composition.
- The ANFIS control scheme is utilized to control the composition of methanol output in BDC by the variation of reflux flow-rate and reboiler heat duty. Two separate ANFIS controllers are designed to control the reflux flow and reboiler heat duty respectively.

## 1.9 Organization of Thesis

The thesis is organized in the following chapters:

**Chapter 1:** The distillation process and laboratory set-up of distillation column with all the auxiliary components and instrumentation is introduced in this chapter. All the key parts of the experimental set-up are briefly described to give a clear idea of the process. A detailed literature review is given regarding modeling and control schemes applied on the distillation column. The author's objective and contribution is also defined in the chapter.

**Chapter 2:** In this chapter, equation based model is developed for the existing experimental set-up of distillation column. In the equation based modeling, a model of BDC is constructed based on mass balance and constant relative volatility with valid assumptions. Experiments on the experimental set up are carried out in order to validate the model. The Validation of the proposed model has been verified with a step change in reflux flow-rate and reboiler heat duty. A neural network based model has also been developed for the distillation column with the use of experimental data. Two neural network topologies namely; FFNN and RNN have been utilized for the model development.

**Chapter 3: I**n this chapter, secondary measurement is used to compute the output methanol composition of distillation column. The temperature of selected tray is chosen as the secondary measurement variable. A relation is established between the controller current and the tray temperature by curve-fitting method. This relation is used as a distillation

column model for the application of the controller. GA tuned PID control technique is used to control the temperature of the tray.

**Chapter 4:** Here, in this chapter, LMPC and NN-MPC Methodologies are implemented on the developed models of BDC to control the methanol composition. The performance of LMPC and NN-MPC are also Compared with conventional PID controller. In NN-MPC scheme, a three layered feed forward neural network is developed to model the distillation process. Then this model is used to predict the future process response in the MPC algorithm for controlling the methanol composition in distillation process. These control schemes are compared for two cases one for reference tracking and another for disturbance rejection.

**Chapter 5:** In this chapter, two neural network based control schemes; Neural Network based Direct Inverse Control (NN-DIC) and Neural Network based Internal Model Control (NN-IMC) are introduced to cover both well-established and emergent methods. These approaches are simulated and their performances are assessed. These control schemes are used to produce an efficient control to get the desired methanol composition. The main goal is to control a single output variable, methanol composition, by changing two manipulated variables, reflux flow-rate and steam flow-rate.

**Chapter 6:** Here, ANFIS controller has been applied on the non-linear ANN based model of BDC. Experimental work has been done on experimental set-up of nine trays BDC. In distillation column, a mixture of methanol (30%) and water (70%) is used as a feed. In this study, ANFIS controller is designed to control the methanol composition by the variation of reflux flow-rate and reboiler heat duty. Two ANFIS controllers are designed to control the Reflux flow and reboiler heat duty respectively. ANFIS controllers are evaluated for two cases; one is for reference tracking and another is for disturbance rejection case. Performance of ANFIS controller is further compared with the NN-IMC controller.

**Chapter 7:** The conclusion and future scope of the work is discussed in this chapter. The work carried in this thesis has been summarised and conclusions have been made. The scope for future extension of work has also been discussed.

# Chapter 2: DEVELOPMENT AND VALIDATION OF MODEL OF BINARY DISTILLATION COLUMN

*In this chapter, a BDC model based on the fundamental physical and chemical laws with few assumptions has been proposed. The model has been validated with the experimental set-up of distillation column. A neural network based model has also been developed for the distillation column with the use of experimental data. Two neural network topologies namely Feed Forward Neural Network and Recurrent Neural Network have been utilized for the model development.*

## 2.1 Introduction

Distillation is one of the most important processes in chemical engineering because it is most frequently used for separation of gases or liquids in the chemical and petroleum industries. Several models have been reported for distillation column in the literature. These models can be categorized under two major groups (i) fundamental models, which are derived from mass, energy and momentum balance equations involved in the process (ii) empirical models which are derived from input-output data of the process.

Several works have been carried out to develop the fundamental models of the distillation column. Wood and Berry have presented a linear model for a binary distillation column [94]. The fundamental dynamic model approach has been used by Can et al. for binary distillation column [23]. Bansal et al. have developed the dynamic distillation model for separation of benzene and toluene [24]. This model consists of differential-algebraic equations for the trays, reboiler, condenser and reflux drum. Diehl et al. have developed the first principle model for a binary mixture of methanol and n-propanol [25]. This model is described by the means of material and energy balances, hydrodynamic effects, and equilibrium relationships for each tray, reboiler and condenser.

In the present work, an equation based model has been developed. This equation based model has been validated for the existing laboratory set-up of BDC. The modelling of BDC has been described in the following sections.

## 2.2 Mathematical Modeling of Binary Distillation Column

Fig. 2.1 shows the schematic of a typical distillation unit with a single feed and two product streams. Feed is a mixture of methanol and water. In binary distillation unit, the methanol composition in the top and bottom is controlled by manipulating the reflux flow-rate and the steam flow-rate respectively. It is difficult to achieve the simultaneous control of top and bottom composition due to inherent complexity in distillation process. A linear model of BDC has been proposed by Wood and Berry to overcome this difficulty [94]. The model represents an approximation of the dynamical behavior of a BDC separating methanol from water. In this dynamic model, the distillate and bottom methanol weight fraction are expressed as a function of the reflux and reboiler steam flow-rate.

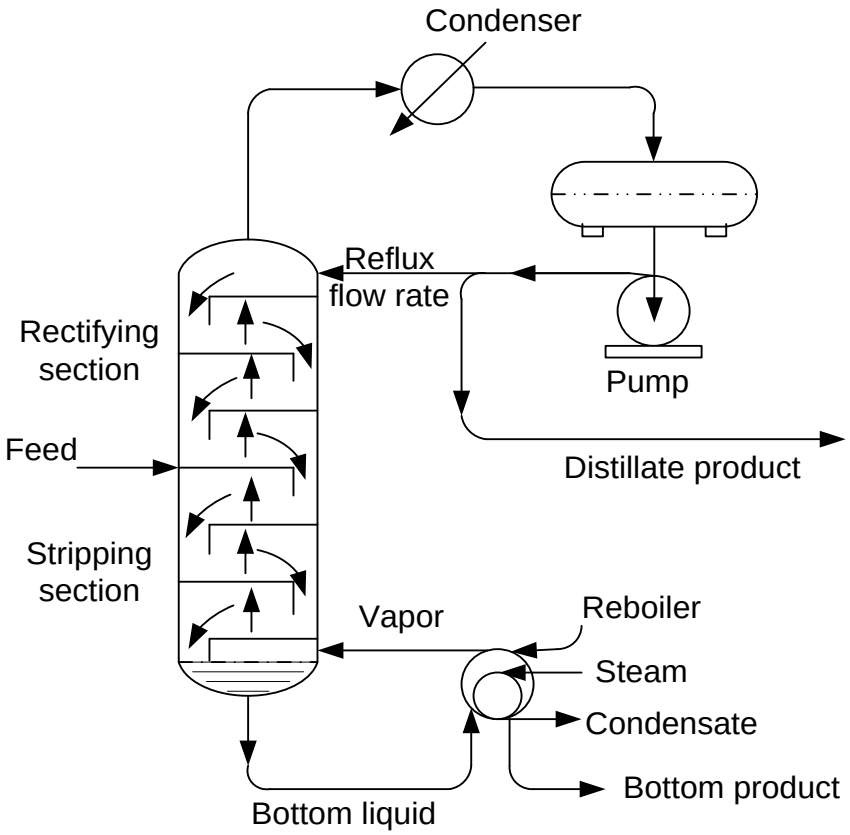


Fig. 2.1 Schematic of a BDC

Wood and Berry model does not represent the real characteristics of the laboratory set-up of BDC exactly. Therefore; in the present work an equation based mathematical model is developed and validated for the existing laboratory set-up of BDC. The mathematical model is easy to use for the design of distillation column control schemes. To develop the equation based model, the following information has been taken directly from the existing experimental set-up of BDC:

(1) Liquid composition on each tray
(2) Liquid flow-rates from each tray
(3) Temperature of each tray
(4) Condenser and reboiler duties

An extremely rigorous model that includes every phenomenon would be so complex that it may lose its practical applicability. To simplify the mathematical equations used in the development of the model, the following assumptions have been considered [95]:

1) The relative volatility 'α' is constant throughout the column.

It is assumed for binary distillation process that the vapour leaving the tray is in equilibrium with the liquid on the tray. This means that the simple vapour - liquid equilibrium relationship can be used. This relation will remain same throughout the process.

$$y = \frac{\alpha x}{1+(\alpha-1)x} \qquad 2.1$$

Where

α = Relative volatility

x= Composition of more volatile component in liquid, mole fraction,

y= Composition of more volatile component in vapour, mole fraction

2) The overhead vapour is totally condensed in the condenser.

3) The holdup of vapour is negligible throughout the system.

4) The molar flow-rates of the vapour and liquid through the stripping and rectifying sections are constant:

$V_i = V_{i+1} = \ldots = V_{N+1}$ ;

$L_{i+1}=L_{i+2}=\ldots.=L_{N+2}$

where i= 1,……N (N= total number of trays)

$V_i$ = Total vapour flow-rate leaving tray i, kg-moles/hr,

$L_i$ = Total liquid flow-rate leaving tray i, kg-moles/hr,

5) Reboiler and condenser are also considered as a tray. Numbering of the trays is started from the bottom i. e. boiler is considered as the first tray and condenser is considered as the last tray. This means that if there are N number of column trays then boiler is $I^{st}$ tray and condenser is $(N+2)^{th}$ tray.

From the modeling point of view, the distillation column is divided into three different sections as shown in Fig. 2.2.

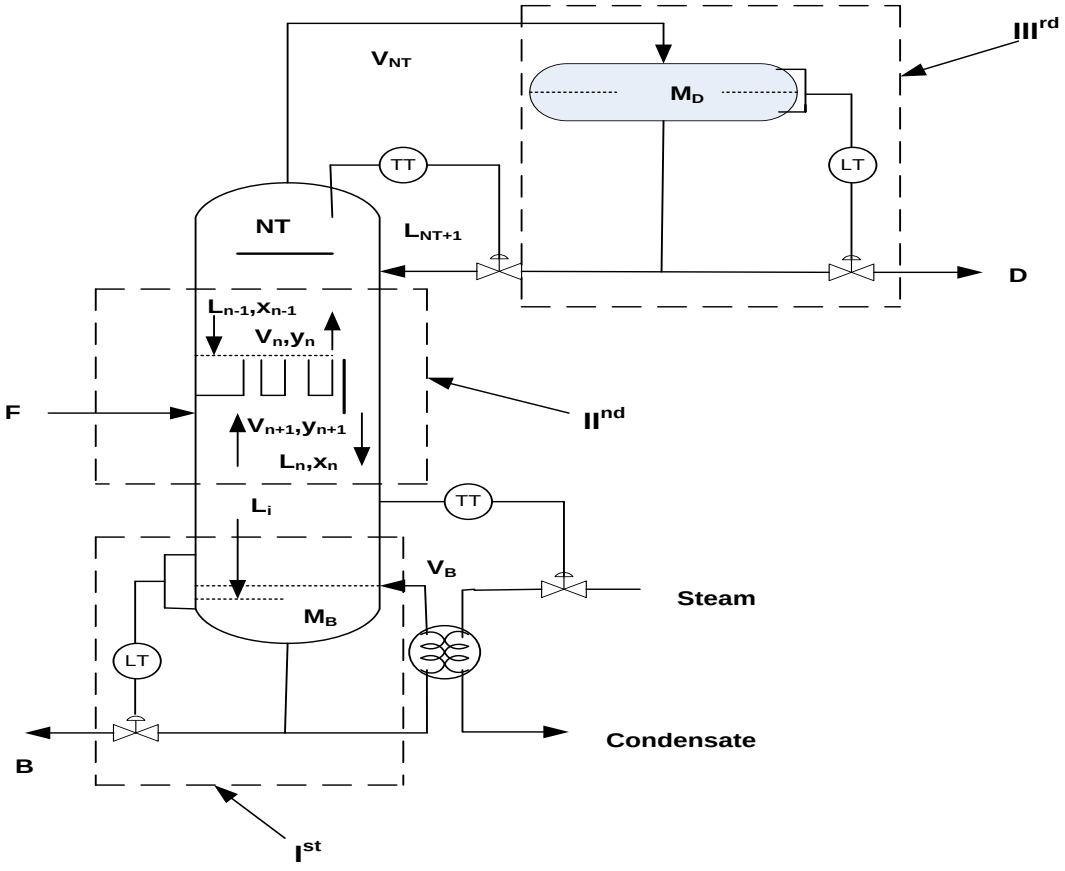


Fig. 2.2 Distillation column used in modelling

I[st] section is reboiler section, II[nd] section is Tray section, and III[rd] section is condenser section. The mass and energy balance equations are obtained by applying conservation laws to each tray, condenser and reboiler [95].

### 2.2.1 Reboiler Section

**Component material balance Equations**

The schematic diagram of reboiler is shown in Fig. 2.3. It is assumed that the level remains constant in reboiler at all times. Thus the molar holdup in reboiler has been considered to be constant i.e. $dM_B/dt=0$,

$$B=L_1-V_B \qquad 2.2$$

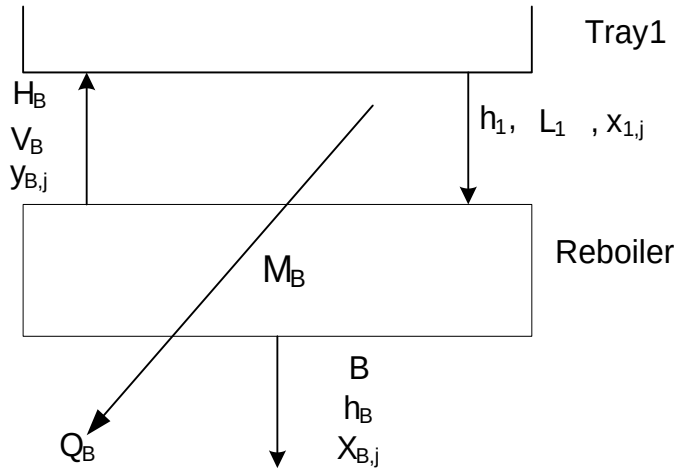


Fig. 2.3 Modeling of reboiler

Component material balance around reboiler is given as:

$$M_B \frac{dx_{B,j}}{dt} = L_1 x_{1,j} - V_B y_{B,j} - (L_1 - V_B) x_{B,j} \qquad 2.3$$

Where

$M_B$= Liquid molar hold up in reboiler, kmoles,

$L_1$= Total liquid flow-rate from tray-1 entering to reboiler, kg-moles/hr,

$x_{B,j}$ = Liquid fraction of component j in bottom product ,% mole fractions,

$V_B$ = Total vapour flow-rate leaving reboiler, kg-moles/hr,

$y_{B,j}$ = Vapour fraction of component j in bottom product ,% mole fractions,

B = Total bottom product rate, kg-moles/hr,

The vapour fraction of component j from reboiler is given as:

$$y_{B,j} = \eta^{v}_{1,j} k_{1,j} x_{B,j} \qquad 2.4$$

Where

$\eta^{v}_{1,j}$ = vaporisation efficiency of component j in reboiler,

$k_{1,j}$ = Equilibrium constant of component j in reboiler

**Total enthalpy balance equations**

The enthalpy is defined as the sum of internal energy and the product of pressure and volume. Total enthalpy balance equation for reboiler is given as:

$$M_{B.}\frac{dh_B}{dt} = L_1 h_1 - V_B H_B - (L_1 - V_B)h_B + Q_B \qquad 2.5$$

Where

$h_1$ = Total molar enthalpy of liquid entering from tray-1 to reboiler, kJ/kmole,

$h_B$ = Total molar enthalpy of liquid leaving reboiler, kJ/kmole ,

$H_B$ = Total molar enthalpy of vapour leaving reboiler, kJ/kmole,

$Q_B$ = Reboiler heat duty, kW

### 2.2.2 Tray Section

In the second section, modelling for general $i^{th}$ tray is considered. Material balance and energy balance equations are written for this section.

**Component material balance Equations**

The schematic diagram of general tray-i is shown in Fig. 2.4.

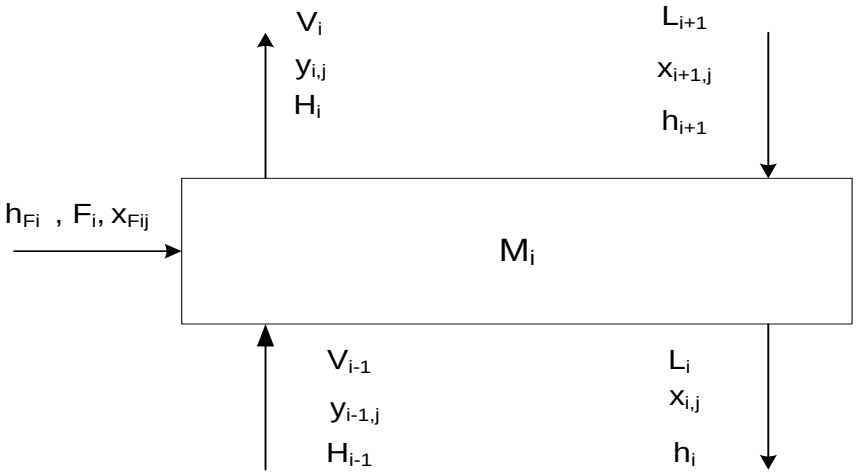


Fig. 2.4 Modeling of general tray-i

Component material balance Equation for $i^{th}$ tray is given as:

$$\frac{d(M_i x_{ij})}{dt} = L_{i+1}x_{i+1,j} - L_i x_{ij} - V_i y_{ij} + V_{i-1}y_{i-1,j} + F_i x_{Fij} \qquad 2.6$$

$y_{ij}$ is calculated as

$$y_{ij} = \eta_{ij}(y_{ij}^{*} - y_{i-1,j}) + y_{i-1,j} \qquad 2.7$$

Where

$M_i$= Molar liquid hold up on tray i, kmole

$x_{ij}$ = Liquid fraction of component j, leaving the tray i , % mole fraction

$L_i$ = Total liquid flow-rate leaving tray-i, kg-moles/hr,

$V_i$ = Total vapour flow-rate leaving tray-i, kg-moles/hr,

$F_i$ = Total feed flow-rate injected to tray-i, kg-moles/hr,

$x_{Fij}$ = Liquid fraction of component j in feed on tray i ,% mole fractions,

$y_{ij}$ = vapour fraction of component j leaving the tray i ,% mole fractions,

$n_{ij}$ = Murphree stage efficiency based on vapour phase of component j on tray i

$y_{ij}^*$ = Equilibrium vapour fraction of component j on tray i

$L_i$ is an additional variable and it is related to $M_i$ through

$$L_i = 3.33 l_w \left[ M_i / \left( A_{net} . M_{Di} \right) - h_w \right] \frac{3600}{2.204} M_{Di} \qquad 2.8$$

Where

$l_w$ = Length of the weir, ft

$A_{net}$ = Net area of the tray, $ft^2$

$h_w$ = Height of the weir, ft

$M_{Di}$ = Average molar density of liquid on tray I, $kmole/ft^3$

Total Material Balance Equation for $i^{th}$ tray is given as:

$$\frac{dM_i}{dt} = L_{i+1} - L_i - V_i + V_{i-1} + F_i \qquad 2.9$$

Where

$L_{i+1}$ = Total liquid flow-rate entering to tray i, kg-moles/hr,

$V_{i-1}$ = Total vapour flow-rate entering to tray i, kg-moles/hr,

$F_i$ = Total feed flow-rate injected on tray i, kg-moles/hr,

**Enthalpy balance equation for tray i**

Enthalpy balance equation for tray i is given as:

$$\frac{d(M_i h_i)}{dt} = L_{i+1} h_{i+1} - L_i h_i - V_i H_i + V_{i-1} H_{i-1} + F_i h_{Fi} \qquad 2.10$$

Where

$h_i$ = Total molar enthalpy of liquid leaving tray I, kJ/kmole,

$H_i$ = Total molar enthalpy of vapour leaving tray I, kJ/kmole

Enthalpy on any tray is calculated by mixing rule and is given as:

$$h_i = \sum_{j=1}^{NC} hl_{ij} x_{ij} \qquad 2.11$$

$$H_i = \sum_{j=1}^{NC} Hv_{ij} y_{ij} \qquad 2.12$$

Where

$hl_{ij}$ = Pure component enthalpy of component j in liquid, kJ/kmole,

$Hv_{ij}$ = Pure component enthalpy of component j in liquid, kJ/kmole

### 2.2.3 Condenser Section

**Component material balance Equations**

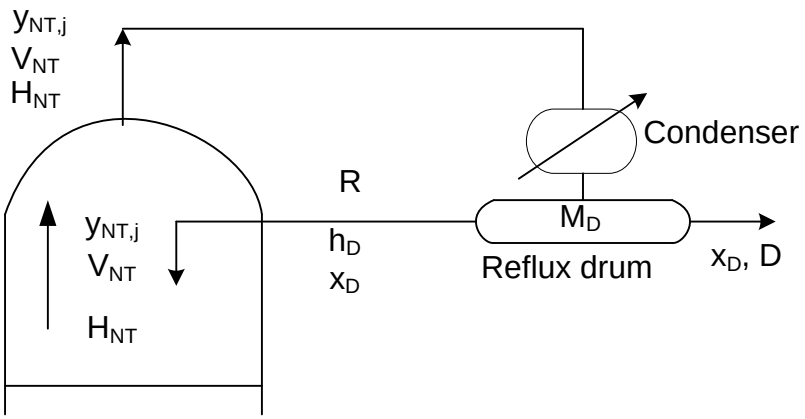


Fig. 2.5 Modeling of condenser

The schematic diagram of condenser is shown in Fig. 2.5. It is assumed that the reflux drum level remains constant in condenser at all the time. Thus Reflux drum level is considered constant. This means at any time

$$D=V_{NT}-R \qquad 2.13$$

Component material balance around condenser is given as:

$$M_D \frac{dx_{D,j}}{dt} = V_{NT} y_{NT,j} - V_{NT} x_{D,j} \qquad 2.14$$

Where

$M_D$= Liquid molar hold up in the reflux drum, kmole,

D = Distillate flow-rate, kmole/hr,

$x_{D,j}$ = Liquid fraction of component j in reflux drum, % mole fractions

$y_{NT,j}$ = Vapour fraction of component j leaving tray NT ,% mole fractions,

R = Total liquid flow-rate entering to the tray NT from reflux drum, kg-moles/hr,

$V_{NT}$ = Total vapour flow-rate leaving the tray NT, kg-moles/hr,

**Enthalpy balance equation**

The enthalpy balance equation for liquid and vapour for condenser is

$$M_D \frac{dh_D}{dt} = V_{NT} H_{NT} - V_{NT} h_D - Q_c \qquad 2.15$$

Where

$h_D$ = Total molar enthalpy of liquid leaving the reflux drum, kJ/kmole ,

$H_{NT}$ = Total molar enthalpy of vapour leaving the last tray NT, kJ/kmole,

$Q_C$ = Condenser duty, kW

### 2.3 Simulation Algorithm

All the above equations (2.1) to (2.15) have been utilized to determine the methanol composition. The steps involved to get the desired methanol composition are given in the form of a flow chart as shown in Fig. 2.6. This algorithm is simulated in the environment of MATLAB®/Simulink.

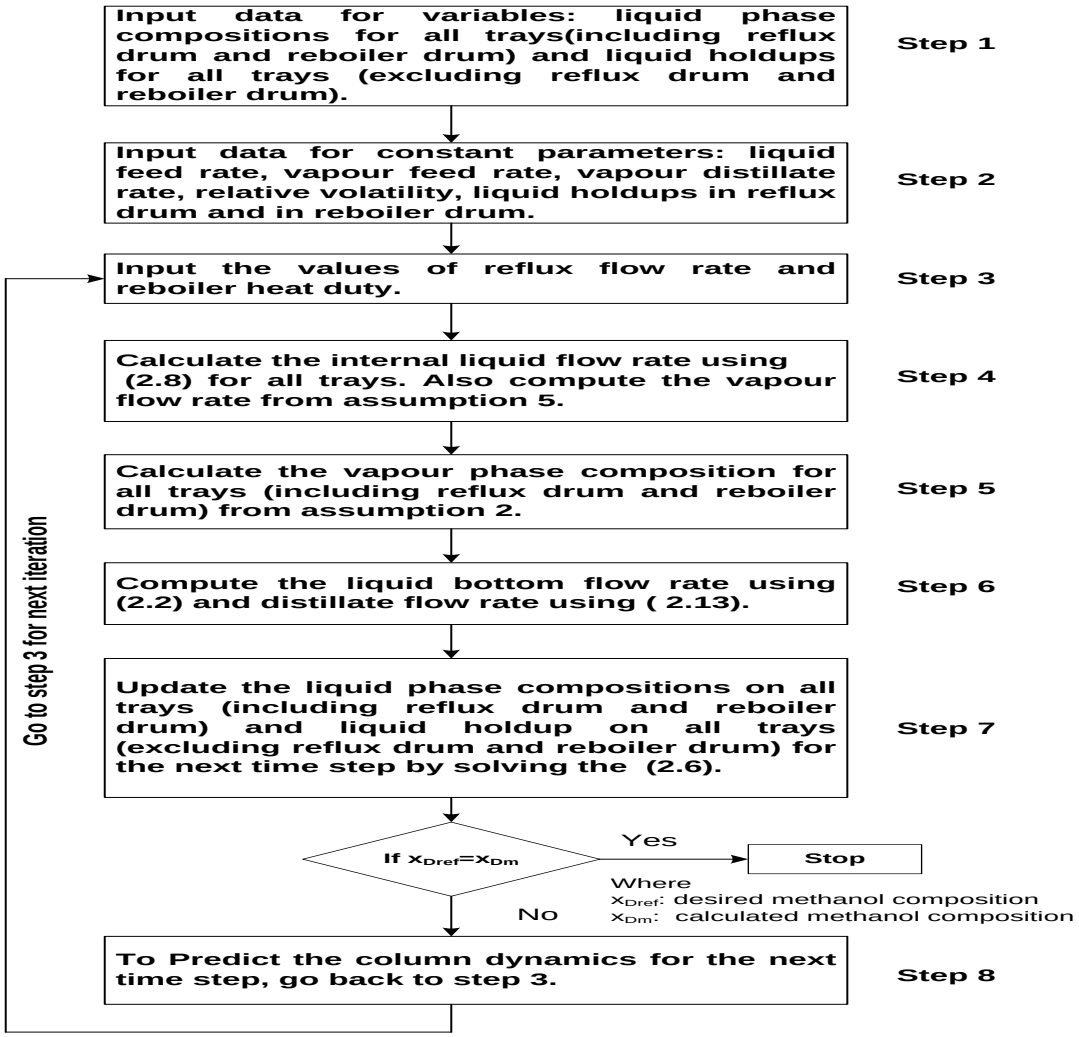


Fig. 2.6 Simulation Algorithm

## 2.4 Validation of Equation based Model

The experiments are carried out on the experimental set-up of BDC to separate the mixture of methanol and water. The details of BDC set-up is given in chapter-1. The composition of the feed mixture is taken as 70% water and 30% methanol. This mixture is fed at fifth tray of BDC set-up. Methanol is collected at the top of the column [35]. The feed mixture from the feed tray descends throughout the column until it reaches the bottom, where the heaters of reboiler heats and vaporizes this mixture. The vapour mixture rises up along the column and reaches to the condenser. The condensed vapour is received at the upper part of the column as the distillate. Then, the reflux is feeded back until a stable situation (temperature stabilises) is reached. At this moment the rate of vaporization is equal to the rate of condensation. This is thermal equilibrium condition and the output distillate temperature does not vary with time. BDC may show a high transition period until the thermal equilibrium condition is achieved. The existing laboratory set-up of BDC takes around 45 minutes to achieve the thermal equilibrium condition. The values of parameters of BDC set-up at thermal equilibrium condition are given in Table 2-1 and the temperature profile of all

the trays is shown in Table 2-2. At this condition, reflux flow-rate is at 3 kg-moles/hr, while the methanol composition is at 0.83 mol fraction. The equation based model is initialized with these values in order to validate with the experimental set-up of BDC.

Table 2-1 Parameters at thermal equilibrium condition

| | |
|---|---|
| Column pressure | 115.21 kPa |
| Feed flow-rate | 2.5 kg-moles/hr |
| Feed temperature | 34.5 °C |
| Heat input | 6 kW |
| Murphree vapour efficiency | 0.60 |
| Relative volatility | 1.5 |

Table 2-2 Temperature profile of trays at thermal equilibrium condition

| Temperature (°C) | | | | | | | | |
|---|---|---|---|---|---|---|---|---|
| Tray1 | Tray 2 | Tray 3 | Tray 4 | Tray 5 | Tray 6 | Tray 7 | Tray 8 | Tray 9 |
| 89.5 | 86.9 | 85.0 | 83.0 | 81.0 | 74.9 | 69.8 | 65.9 | 65.2 |

After the establishment of thermal equilibrium, the reflux flow-rate has been increased from 3.0 kg-moles/hr to 3.1 kg-moles/hr whereas, reboiler heat duty has been increased from 6 kW to 7 kW. The variation in output methanol composition is observed for this variation in reflux flow-rate and reboiler heat duty. The measurement of output methanol composition has been made at the interval of 1 minute. Now for the same parameter values the simulation has been performed using equation based model as explained in section 2.3 and the final methanol composition has been determined.

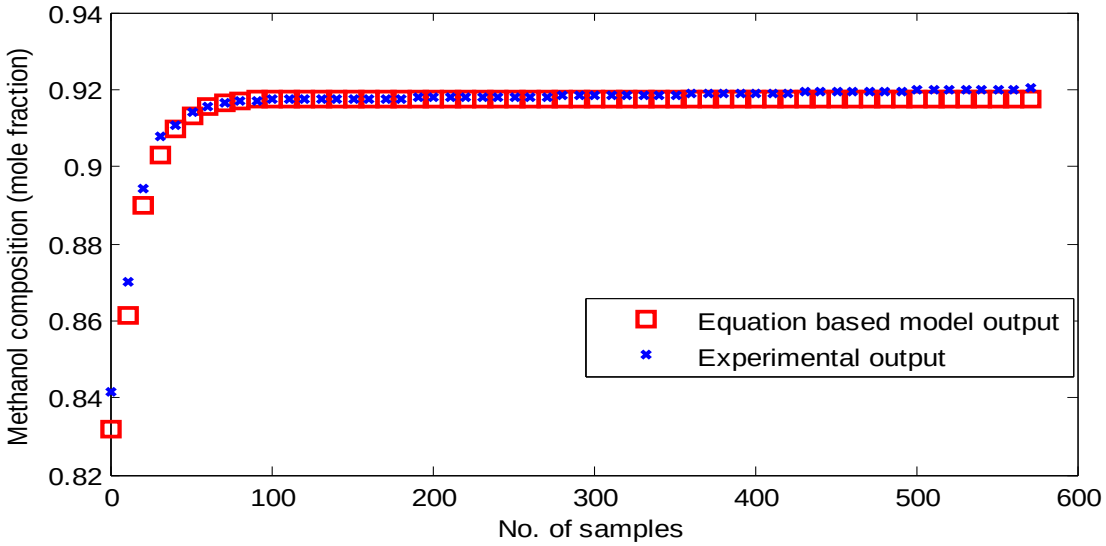


Fig. 2.7 Output of experimental set-up and equation based model

The comparison between the experimental set-up and equation based model is given in Fig. 2.7. The Mean Squared Error (MSE) between the experimental output and the equation based model output is shown in Fig. 2.8. It is observed from the above results that the output of equation based model closely matches with the experimental output; therefore,

this model can be used as a model for laboratory set-up of BDC for the analysis and control of the BDC.

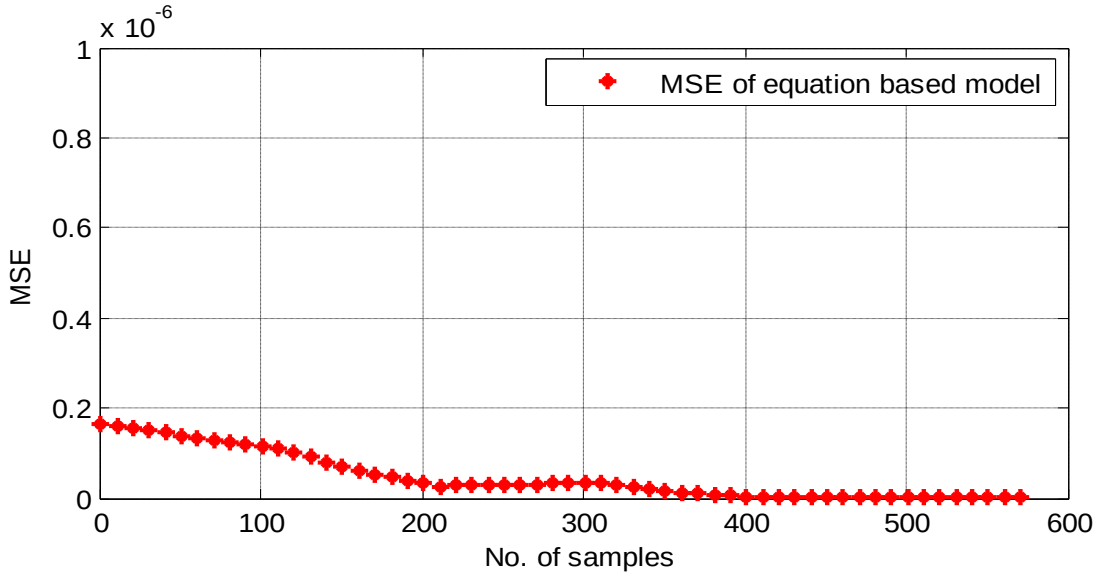


Fig. 2.8 MSE between experimental output and equation based model output

Mathematical models are inherently hard to build due to lack of knowledge of the process and measurements. Due to above reasons, many iterations and experiments are required to get an accurate mathematical model for distillation column. ANN based models are good alternatives to avoid these limitations, therefore; ANN based model of BDC has also been developed in the present work.

## 2.5 Artificial Neural Network based Model of BDC

In chemical process, parameter variations and uncertainty play an important role in the system dynamics and are difficult to be modelled accurately. In such cases, input-output characteristics are used for the modelling. Such methods do not require an in depth knowledge of internal mathematical relations. In this work a neural network model has been proposed to get the methanol composition in BDC. A neural network is composed of simple elements (artificial neurons) operating in parallel. The network function is determined by the connections (weights) between the elements. The neural network is trained to approximate a given function by adjusting the values of the connections between elements. Neurons are arranged in 'layers'. There are a variety of neural networks suitable for different purposes [35].

First step to develop the ANN model of BDC is to determine the inputs. The reboiler duty, reflux flow, feed flow, top and bottom pressure of the column along with the temperature of selected tray are taken as inputs while the output is methanol composition. A single hidden layer is taken in the present work. Number of neurons in hidden layer is selected on the basis of gradient and MSE. Selection of the proper topology is the next step in ANN modelling. Topology of ANN can be classified on the basis of the direction in which signal travels. ANN either allows signals to travel one way only; from input to output or; It

allows signal travelling in both directions by introducing loops in the network. The ANN which allows signals in only one direction is called Feed Forward Neural Network (FFNN) and the ANN which allows signals in both directions is called Recurrent Neural Network (RNN). In the following section both FFNN and RNN topologies are utilized for the development of the model for BDC.

### 2.5.1 Feed Forward Neural Network based Model (FFNN)

The FFNN model for BDC is given in Fig. 2.9 [96]. The suitable structure for FFNN model of BDC is determined on the basis of gradient and MSE. In the present model of BDC, the Tangent sigmoid function is considered as activation function for the hidden layer while linear activation function is considered for output layer.

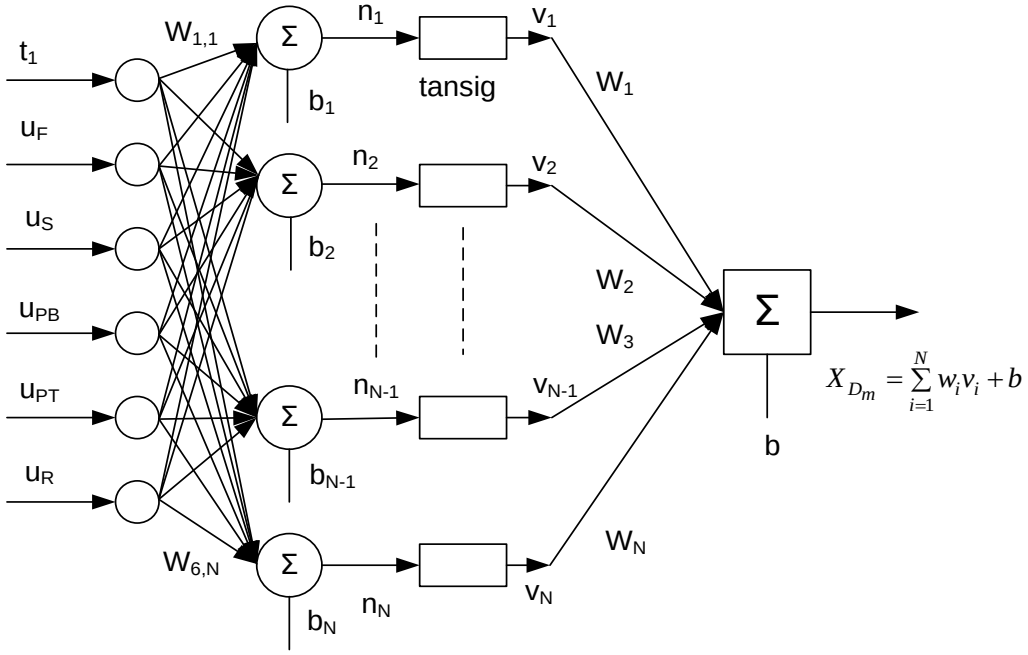


$t_1$ = Tray temperature
$u_F$ = Feed flow rate
$u_S$ = Reboiler duty
$u_{PB}$ = Reboiler bottom pressure
$u_{PT}$ = Reflux drum top pressure
$u_R$ = Reflux flow rate
$X_{Dm}$ = Methanol composition

$W_{j,i}$ = Weights between inputs and hidden neurons (j=1,…,6, i= 1,…,N)
$n_i$ = Output of the first layer
$b_i$ = Bias of the neurons in first layer
$v_i$ = Output of the tansig functions in hidden layer
$w_i$ = Weights between hidden neurons and output
b = Bias in the output neuron
N = No. of hidden neurons

Fig. 2.9 FFNN model of BDC

The output of the neural network model $x_{Dm}$ is the distillate output composition. The relationship between $n_i$, the output of the first layer, and the input variables is given as

$$n_i = \sum_{j=1}^{6} \sum_{i=1}^{N} (u_j w_{j,i} + b_i) \qquad 2.17$$

Where N is the number of neurons in hidden layer and $n_i$ is the weighted sum of the input variables, which is fed to hyperbolic tangent sigmoid transfer function which is given as:

$$f(x) = \frac{\sinh x}{\cosh x} = \frac{e^x - e^{-x}}{e^x + e^{-x}} \qquad 2.18$$

The output of the hyperbolic tangent sigmoid function is $v_i$,

$$v_i = \frac{e^{n_i} - e^{-n_i}}{e^{n_i} + e^{-n_i}} \qquad 2.19$$

For FFNN model, $n_i$ multiplies with the corresponding weight and sum up with the bias. A pure linear function is considered as the activation function for the output. For FFNN model, the output of the activation function is the distillate composition $x_{Dm}$ as shown

$$x_{Dm} = \sum_{i=1}^{N} w_i v_i + b \qquad 2.20$$

In the next section, RNN topology has been utilized for the ANN model development.

### 2.5.2 Recurrent Neural Network based Model (RNN)

In the RNN topology the output of the recurrent network is a function not only of the weights, biases, and network input, but also depends on the outputs of the network at previous instant [96]. The RNN model of BDC is given in Fig. 2.10.

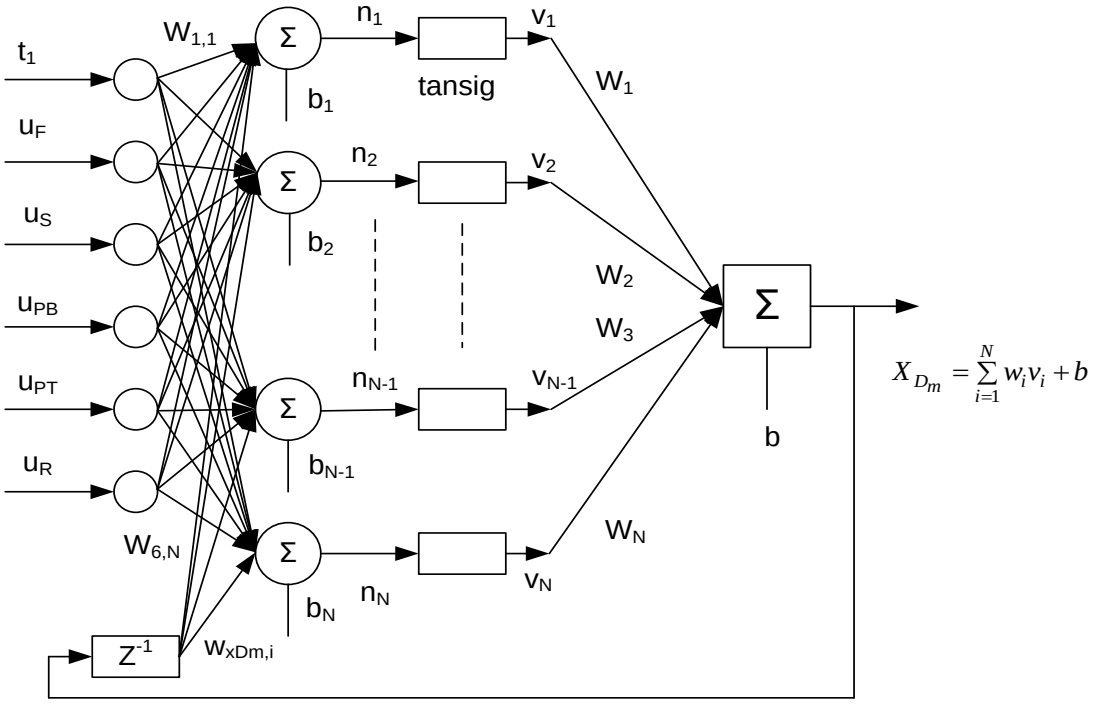


$t_1$ = Tray temperature
$u_F$ = Feed flow rate
$u_S$ = Reboiler duty
$u_{PB}$ = Reboiler bottom pressure
$u_{PT}$ = Reflux drum top pressure
$u_R$ = Reflux flow rate
$X_{Dm}$ = Methanol composition

$W_{j,i}$ = Weights between inputs and hidden neurons (j=1,…,6, i= 1,…,N)
$n_i$ = Output of the first layer
$b_i$ = Bias of the neurons in first layer
$v_i$ = Output of the tansig functions in hidden layer
$w_i$ = Weights between hidden neurons and output
$b$ = Bias in the output neuron
N = No. of hidden neurons

Fig. 2.10 RNN model of BDC

The suitable structure for RNN model of BDC is determined on the basis of gradient and MSE. For RNN model, the output of the first layer $n_i$ is given as

$$n_i = \sum_{j=1}^{6}\sum_{i=1}^{N}(u_j w_{j,i} + b_i) + \sum_{i=1}^{N} x_{Dm}(k-1) w_{xDm,i} \quad 2.21$$

$n_i$ is fed to hyperbolic tangent sigmoid transfer function. The output of the hyperbolic tangent sigmoid function is $v_i$,

$$v_i = \frac{e^{n_i} - e^{-n_i}}{e^{n_i} + e^{-n_i}} \quad 2.22$$

The distillate output is given as

$$x_{Dm} = \sum_{i=1}^{N} w_i v_i + b \quad 2.23$$

The output $x_{Dm}$ is fed back to the input of the second layer. The difference between the output of the plant and the output of the network is called the prediction error 'e' is given in (2.24), where $x_{Dr}$ is the value of the output of the real BDC and $x_{Dm}$ is the output of the ANN model of the BDC.

$$e = x_{Dr} - x_{Dm} \quad 2.24$$

The Mean Square of the Error (MSE) 'ε' is minimized for the adjustment of weights and biases in the network.

$$\varepsilon = \frac{1}{2}\left[x_{Dr} - x_{Dm}\right]^2 \quad 2.25$$

The Gradient Descent method has been used for the minimization of MSE. The weights ($w_{j,I}$ , $w_{xDm,I}$ , $w_i$) and biases ($b_i$,b) are updated as shown below in this iterative method.

$$w_{j,i}(k+1) = w_{j,i}(k) - \eta \frac{\partial \varepsilon}{\partial w_{j,i}} \quad 2.26$$

$$w_i(k+1) = w_i(k) - \eta \frac{\partial \varepsilon}{\partial w_i} \quad 2.27$$

$$w_{x_{Dm},i}(k+1) = w_{x_{Dm},i}(k) - \eta \frac{\partial \varepsilon}{\partial w_{x_{Dm},i}} \quad 2.28$$

$$b_i(k+1) = b_i(k) - \eta \frac{\partial \varepsilon}{\partial b_i}; \quad 2.29$$

$$b(k+1) = b(k) - \eta \frac{\partial \varepsilon}{\partial b} \quad 2.30$$

Where η= learning rate and,

$$\frac{\partial \varepsilon}{\partial w_{xDm,i}} = \frac{\partial \varepsilon}{\partial x_{Dm}} \cdot \frac{\partial x_{Dm}}{\partial w_{xDm,i}}; \frac{\partial \varepsilon}{\partial w_{j,i}} = \frac{\partial \varepsilon}{\partial x_{Dm}} \cdot \frac{\partial x_{Dm}}{\partial w_{j,i}}; \frac{\partial \varepsilon}{\partial w_i} = \frac{\partial \varepsilon}{\partial x_{Dm}} \cdot \frac{\partial x_{Dm}}{\partial w_i};$$

$$\frac{\partial \varepsilon}{\partial b_i} = \frac{\partial \varepsilon}{\partial x_{Dm}} \cdot \frac{\partial x_{Dm}}{\partial b_i}; \frac{\partial \varepsilon}{\partial b} = \frac{\partial \varepsilon}{\partial x_{Dm}} \cdot \frac{\partial x_{Dm}}{\partial b}$$

In the next section, both the above topologies are utilized to develop the neural network model for BDC. The training performance of FFNN and RNN models are evaluated on the basis of gradient and MSE.

### 2.5.3 Neural Network Training

The proposed ANN model of BDC has two layers namely: input (hidden) layer and output layer. Number of neurons in the hidden layer affects the performance of the training. Number of neurons which gives the minimum MSE (between the trained output and desired target output) is the desired number of neurons in the hidden layer.

The data for training and testing of FFNN and RNN have been acquired experimentally from the BDC set-up available in the laboratory. The BDC set-up is interfaced with a computer and the Input–output data samples for training and testing are acquired from various transducers connected in BDC by using Labview® software with National Instruments modules (FP-RTD-122, FP-AI-110 and FP-1600). The data samples are acquired when the thermal equilibrium condition has been established. Total 579 data samples are recorded for each input and output at the sampling interval of one minute. The operating range of inputs and output is given in Table 2-3.

Table 2-3 Range of Inputs and output

| I/O | Process Variable | Minimum value | Maximum value |
|---|---|---|---|
| Inputs | $u_R$: Reflux flow-rate (kg-mole/hr) | 2.9 | 3.11 |
| | $u_S$: Reboiler heat duty (kW) | 5.5 | 7.0 |
| | $u_{T1}$ : Tray temperature(Deg C) | 75 | 85 |
| | $u_F$ : Feed flow-rate(kmole/hr) | 2.5 | 3.5 |
| | $u_{PT}$ : Reflux drum top pressure(kPa) | 101.42 | 106 |
| | $u_{PB}$ : Reboiler bottom pressure(kPa) | 115.21 | 120 |
| Output | $x_{Dm}$: Distillate Composition (mole fraction) | 0.84 | 0.98 |

60 % experimentally acquired data has been taken for the training whereas, 20 % data for the validation and 20 % data for testing. Table 2-4 shows the gradient value and the MSE for FFNN and RNN architectures with different number of hidden neurons. These two parameters are utilized for the selection of the ANN structure. Considering the convergence, the number of hidden neurons taken in the range of 6 to 22. Training of the network off the range of the number of neurons shows the non-convergence.

It is observed that the value of gradient and MSE is minimum when the number of hidden neurons of the FFNN structure is 14. The best structure of FFNN is 6-14-1 with learning rate 0.80; whereas, the most suitable structure of RNN on the basis of minimum gradient and MSE is 6-18-1 with learning rate 0.65.

Table 2-4 Training performance of FFNN and RNN

| Architecture | Gradient | | MSE for RNN | | | MSE for FFNN | | |
|---|---|---|---|---|---|---|---|---|
| | RNN | FFNN | Training | Testing | Validation | Training | Testing | Validation |
| 6-6-1 | 8.09e-8 | 7.08e-7 | 4.62e-7 | 6.18e-6 | 5.76e-7 | 5.38e-7 | 8.04e-7 | 1.21e-7 |
| 6-8-1 | 2.51e-8 | 4.40e-6 | 2.51e-8 | 1.81e-7 | 1.31e-7 | 1.12e-7 | 4.40e-6 | 4.02e-6 |
| 6-10-1 | 7.65e-8 | 6.63e-7 | 8.37e-8 | 2.30e-7 | 5.72e-8 | 6.50e-7 | 9.54e-7 | 5.24e-7 |
| 6-12-1 | 4.60e-8 | 7.74e-7 | 4.60e-8 | 4.04e-8 | 3.89e-8 | 2.78e-7 | 5.55e-7 | 4.32e-7 |
| 6-14-1 | 4.27e-8 | 1.13e-7 | 4.27e-8 | 1.27 e-7 | 3.49e-8 | 4.19e-7 | 1.13e-7 | 1.12e-7 |
| 6-16-1 | 4.57e-8 | 3.13e-6 | 4.57e-8 | 1.34 e-7 | 4.42e-8 | 3.86e-6 | 4.32e-6 | 2.32e-6 |
| 6-17-1 | 3.58e-8 | 4.64e-7 | 3.58e-8 | 9.37e-8 | 5.95e-8 | 3.00e-6 | 4.64e-7 | 3.04e-7 |
| 6-18-1 | 2.36e-8 | 1.08e-5 | 2.36e-8 | 6.12e-8 | 8.94e-8 | 2.10e-7 | 2.13e-5 | 1.92e-5 |
| 6-20-1 | 2.42e-7 | 5.53e-7 | 7.60e-7 | 1.17e-6 | 6.94e-7 | 1.52e-7 | 3.64e-7 | 2.65e-7 |
| 6-22-1 | 5.80e-8 | 5.63e-6 | 5.80e-8 | 1.49e-7 | 3.92e-8 | 6.98e-6 | 5.63e-6 | 4.89e-6 |

To obtain the methanol composition from the developed ANN model of BDC, the value of four inputs namely, Feed flow-rate, First tray temperature, Reflux drum top pressure and reboiler bottom pressure are fixed at the initial values as given in Table 2-1 while, the remaining two inputs namely: reflux flow-rate and reboiler heat duty are varied similarly as in the case of equation based model and experimental setup.

## 2.6 Validation of Neural Network based Model

To validate the ANN based model, the outputs obtained from FFNN and RNN models are compared with the experimental output in terms of the methanol mole fraction in product streams. The results given in Fig. 2.11 show the great agreement between predicted and experimental methanol composition. The MSE for FFNN and RNN models is shown in Fig. 2.12.

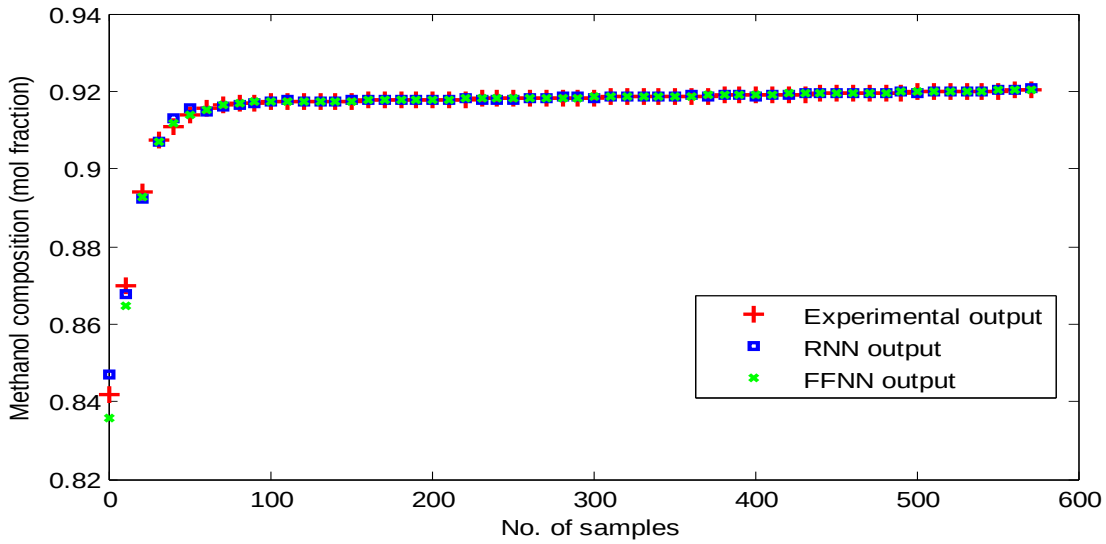


Fig. 2.11 Output of FFNN and RNN models with experimental results

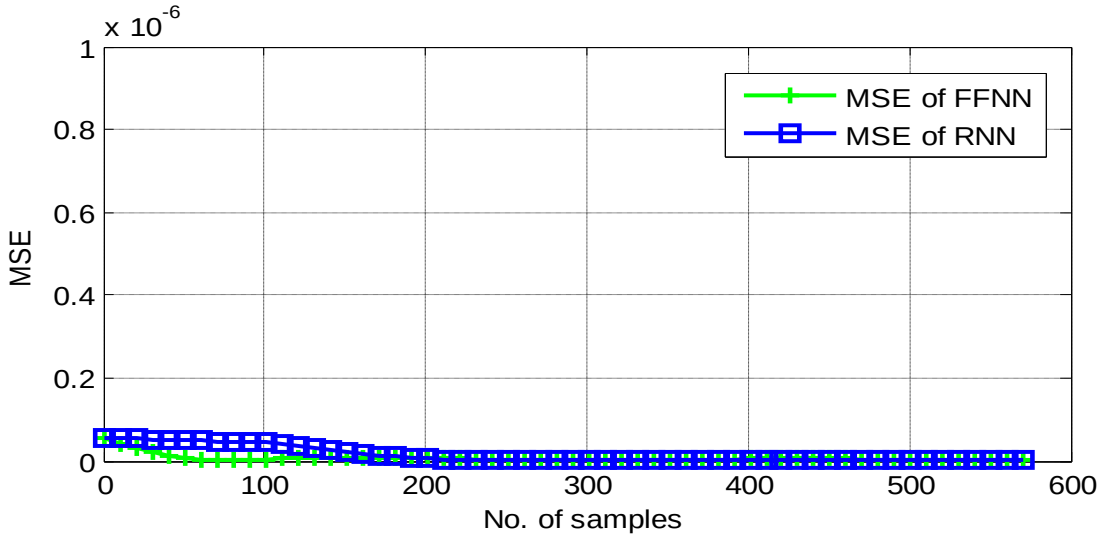


Fig. 2.12 MSE of FNN and RNN models with experimental results

The performance of FFNN and RNN topologies are also compared with the equation based model as shown in Fig. 2.13. The MSE between the outputs of the models is given in Fig. 2.14.

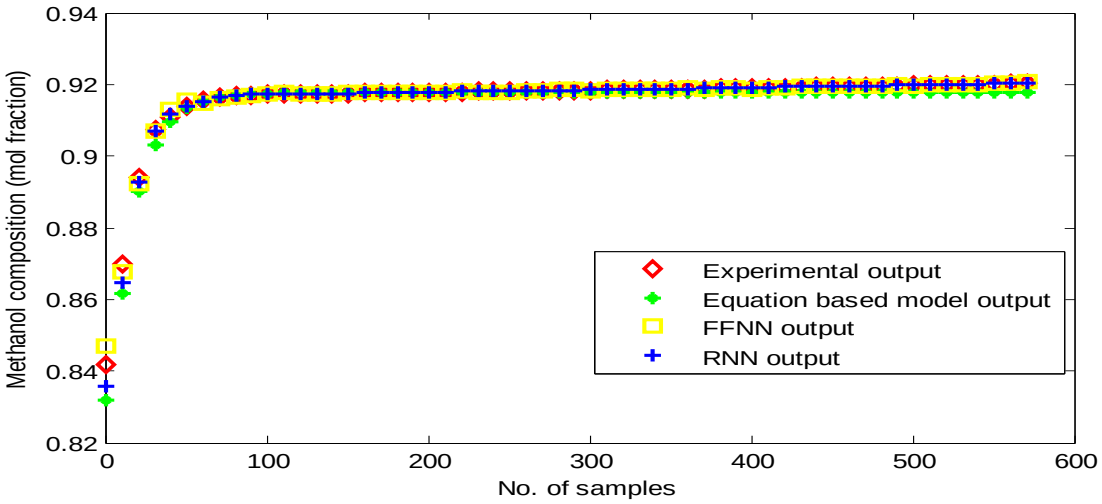


Fig. 2.13 Output of equation based model and ANN models

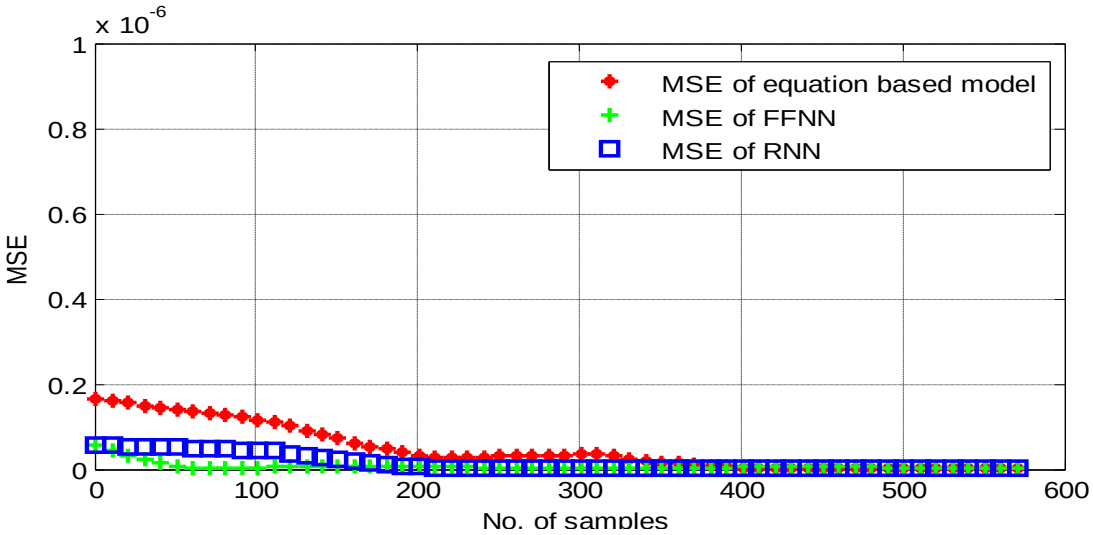


Fig. 2.14 MSE of equation based model and ANN models

It is observed that both the ANN and equation based models are in good agreement with the experimental results. The insignificant values of MSE validate both the developed models and can be used for purpose of analysis and controller designing.

## 2.7 Conclusion

This chapter presents the modelling of distillation column. An equation based model is validated for existing experimental setup of BDC. Experiments on the laboratory set up are carried out in order to acquire data to validate the model. The result shows that the equation based model is in good agreement with the experimental set-up. ANN based model has also been developed for BDC. Two ANN topologies namely: FFNN and RNN have been used for the modelling. The training of the developed ANN based model of BDC has been carried out by the data acquired from experiments performed on the laboratory set-up of BDC. The ANN models are also compared with the equation based model of BDC.

# Chapter 3: DESIGN OF INFERENTIAL PID CONTROL SCHEME FOR TRAY TEMPERATURE CONTROL OF BDC

*In this chapter, inferential control scheme is used to control the methanol composition of BDC. Temperature of the selected tray is used as a secondary variable. A relation is established between the tray temperature and controller current by curve fitting method. This relation is utilized to design a PID controller which controls the temperature of the tray and hence the composition of methanol.*

## 3.1 Introduction

A major problem to measure the product quality (e.g. methanol composition) is the lack of on-line instrumentation (e.g. online chromatograph). Other problems that are associated with online measurement are higher cost, substantial measurement delay and infrequent feedback. Inferential control scheme is a method which has been designed to overcome this problem [54]. Inferential control scheme utilized the secondary variables measurement (e.g. temperature, pressure, flow, etc.) which are associated with a process in spite of primary variable (product quality). Changes in some of the secondary variables are indicative of changes in product quality. Thus by monitoring suitable secondary variables, it is often possible to get the desired value of the primary variable.

In BDC, at constant pressure, the tray temperatures of BDC reflect the output methanol composition, therefore; the tray temperature can be used as a secondary variable for controlling the output methanol composition. The selection of the tray for temperature control has been made on the basis of sensitivity. The sensitivity is defined as the cause- effect relationship for any process. In the present work, temperature sensitivity has been determined by creating the disturbances in feed flow, heat input and reflux flow. Temperature profile of the BDC trays can be controlled through the most sensitive tray [97]. The most sensitive tray can be selected by utilizing the sensitivities for BDC. In the following section sensitivity analysis has been carried out to select the most temperature-sensitive tray.

## 3.2 Tray Selection using Sensitivity Analysis

Experimentation has been performed on laboratory set-up of BDC to select the most temperature-sensitive tray with respect to reflux flow-rate, feed flow-rate and heat input. The BDC set-up has been run for distillation of methanol from water-methanol mixture at the initial thermal equilibrium state. At this moment the rate of vaporization is equal to the rate of condensation. This is thermal equilibrium condition and the output distillate temperature does not vary with time. The values of parameters of BDC set up at thermal equilibrium condition are given in Table 3-1. At this condition, reflux flow-rate is at 3 kg-moles/hr while the methanol composition is at 0.83 mol fraction.

Table 3-1 BDC Parameters at thermal equilibrium condition

| | | | |
|---|---|---|---|
| Column pressure | 115.21 kPa | Heat input | 6 kW |
| Feed flow-rate | 2.5 kg-moles/hr | Murphree vapour efficiency | 0.60 |
| Feed temperature | 34.5 °C | Relative volatility | 1.5 |

Temperatures of different trays have been recorded till the thermal equilibrium condition has been established and temperature differences between the successive trays have been calculated. Temperature and temperature difference between the trays are shown in Table 3-2. It is observed from the table that the maximum change occurred between tray-3 and tray-4 Therefore; it is concluded that the change of temperature is highest between tray-3 and tray-4.

Table 3-2 Temperature and Temperature difference between trays

| Tray no. | Temperature of trays at Initial equilibrium state(°C) | Temperature difference b/w successive trays (°C) |
|---|---|---|
| Tray-1 | 92 | 2 |
| Tray-2 | 90 | |
| Tray-3 | 88 | 2 |
| Tray-4 | 80 | 8 |
| Tray-5 | 76 | 5 |
| Tray-6 | 71 | 5 |
| Tray-7 | 68 | 3 |
| Tray-8 | 66 | 2 |
| Tray-9 | 64 | 2 |
| Reflux section | 62 | 2 |

To determine the temperature sensitivities with respect to reflux flow-rate (δT/δR), feed flow-rate (δT/δF) and heat input (δT/δH) respectively, the perturbation has been created in the reflux flow-rate, feed flow-rate and heat input considering one at a time and keeping all other process variables constant.

First, an increment of 1% is made in reflux flow-rate (ΔR) and the temperature of all the trays of the column are recorded at equilibrium state. The change in reflux flow is done by the rota-meter connected in reflux flow line. These temperatures have been compared with the initial equilibrium state temperatures and change in temperatures (ΔT) is reported in Table 3-3. It is observed from this table that the maximum drop in temperature occurred in tray-4.

Table 3-3 Temperature sensitivity w.r.t. reflux flow

| Tray no. | Temperature of trays when ΔR=1% ($T_1$) (°C) | Temperature of trays at Initial equilibrium state $T_2$ (°C) | Change in temperature $\Delta T = \lvert T_1 - T_2 \rvert$ (°C) | ΔT/ΔR |
|---|---|---|---|---|
| Tray-1 | 91 | 92 | 1 | 1 |
| Tray-2 | 86.5 | 90 | 3.5 | 3.5 |
| Tray-3 | 82 | 88 | 6 | 6 |
| Tray-4 | 70 | 80 | 10 | 10 |
| Tray-5 | 68 | 76 | 8 | 8 |
| Tray-6 | 62 | 71 | 9 | 9 |
| Tray-7 | 61.5 | 68 | 6.5 | 6.5 |
| Tray-8 | 61 | 66 | 5 | 5 |
| Tray-9 | 61 | 64 | 3 | 3 |

Now, the feed flow is increased by 1% (ΔF) from its initial value at thermal equilibrium condition and the tray temperatures have been recorded after the establishment of equilibrium. This increment in feed flow is made by the rota-meter connected in BDC set-up. The change in tray temperatures with the initial equilibrium state is given in Table 3-4. These results show that maximum change in temperature occurred in tray-4.

Table 3-4 Temperature sensitivity w.r.t. feed flow

| Tray no. | Temperature of trays when ΔF=1% ($T_1$) (°C) | Temperature of trays at Initial equilibrium state $T_2$ (°C) | Change in temperature $\Delta T = \lvert T_1 - T_2 \rvert$ (°C) | ΔT/ΔF |
|---|---|---|---|---|
| Tray-1 | 91 | 92 | 1 | 1 |
| Tray-2 | 88.5 | 90 | 1.5 | 1.5 |
| Tray-3 | 86 | 88 | 2 | 2 |
| Tray-4 | 85.5 | 80 | 4.5 | 4.5 |
| Tray-5 | 72.5 | 76 | 3.5 | 3.5 |
| Tray-6 | 67 | 71 | 4 | 4 |
| Tray-7 | 65 | 68 | 3 | 3 |
| Tray-8 | 64 | 66 | 2 | 2 |
| Tray-9 | 62.5 | 64 | 1.5 | 1.5 |

Now, the heat input is incremented by 1kW and the effect of variation is observed on the temperature profile of the BDC. Heat input in BDC is changed by the manual switch of connected heater. Table 3-5 shows the change in tray temperatures from the initial equilibrium state. It is observed from the table 3-5 that the tray-4 is the most sensitive tray.

Table 3-5 Temperature sensitivity w.r.t. heat input

| Tray no. | Temperature of trays when ΔH=1% ($T_1$) (°C) | Temperature of trays at Initial equilibrium state $T_2$ (°C) | Change in temperature $\Delta T = \lvert T_1 - T_2 \rvert$ (°C) | ΔT/ΔH |
|---|---|---|---|---|
| Tray-1 | 93 | 92 | 1 | 1 |
| Tray-2 | 92 | 90 | 2 | 2 |
| Tray-3 | 91 | 88 | 3 | 3 |
| Tray-4 | 86 | 80 | 6 | 6 |
| Tray-5 | 80 | 76 | 4 | 4 |
| Tray-6 | 75 | 71 | 4 | 4 |
| Tray-7 | 71.5 | 68 | 3.5 | 3.5 |
| Tray-8 | 68.5 | 66 | 2.5 | 2.5 |
| Tray-9 | 66 | 64 | 2 | 2 |

It is evident from the above sensitivity analysis that the tray-4 is the most sensitive tray. The desired output i.e. methanol composition can be controlled by keeping the temperature of the tray at a given reference temperature. The reference temperature is the temperature corresponding to the desired methanol composition. The desired methanol composition in the present work is considered as 98% (0.98 mole fraction). In the next step, the suitable reference temperature of tray-4 has been determined in the following manner.

BDC set-up has been started with the minimum heat input. The feed flow has been set at 2.5 kg-mol/hr. At equilibrium point of BDC, tray-4 temperature and final methanol composition has been recorded. This process has been repeated by increasing the heat input (i.e. tray-4 temperature). At each equilibrium state, tray-4 temperature and final methanol composition has been recorded which is given in Table 3-6. It is observed from this table that the desired output of methanol composition 98%, is obtained when the $4^{th}$ tray temperature is 85 °C. Therefore, it is concluded that the reference temperature of the tray-4 is 85 °C when the feed flow is 2.5 kg-mol/hr. At the point when the temperature of tray-4 is 85°C, the tray-1 is at 95°C because it is the nearest tray to the reboiler. If the temperature of tray-4 is further increased from 85 °C, the temperature of tray-1 approaches to 100°C which is the boiling point of water and at this point water starts to vaporize, thus the methanol composition in output distillate decreases as shown in Table 3-6. After selecting the most temperature-sensitive tray and its reference temperature for the desired output, the objective is to control the temperature of this tray to obtain the given methanol composition.

Table 3-6 Output methanol composition vs. temperature of tray-4

| S. No. | Methanol Composition (%) | Temperature set point (°C) | S. No. | Methanol Composition (%) | Temperature set point (°C) |
|---|---|---|---|---|---|
| 1 | 83 | 80 | 11 | 97 | 86 |
| 2 | 85 | 80.5 | 12 | 96 | 88 |
| 3 | 88 | 81 | 13 | 95 | 89 |
| 4 | 90 | 82 | 14 | 94 | 90 |
| 5 | 92 | 82.5 | 15 | 93 | 91 |
| 6 | 94 | 83 | 16 | 92 | 92 |
| 7 | 95 | 83.5 | 17 | 91 | 94 |
| 8 | 96 | 84 | 18 | 90 | 96 |
| 9 | 97 | 84.5 | 19 | 89 | 97 |
| 10 | 98 | 85 | 20 | 88 | 98 |

In BDC, the measurement of methanol composition is difficult therefore it is estimated using the measurement of secondary variables. Inferential control scheme is the technique in which secondary variable is controlled to get the desired output. As discussed in sensitivity analysis, temperature of tray-4 in BDC is found the most suitable secondary variable to implement inferential control scheme.

### 3.3 Inferential Control Scheme for Tray-4 Temperature Control

The block diagram of inferential control scheme for BDC is shown in Fig. 3.1. A PID controller is designed to minimize the error between the reference temperature and measured temperature of tray-4. Genetic Algorithm (GA) is used to determine the optimal parameters of the PID controller $K_P$, $K_I$ and $K_D$ [49].

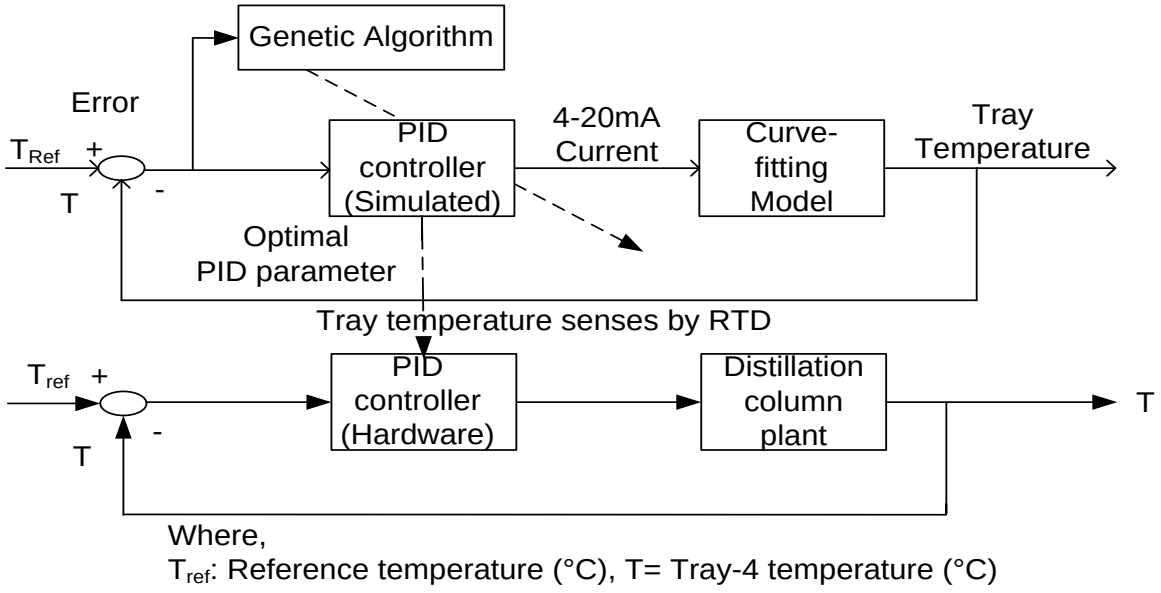


Fig. 3.1 Inferential PID control scheme for BDC

The schematic diagram of the temperature control scheme is shown in Fig. 3.2. In the laboratory set-up of BDC, a resistance temperature detector (RTD) has been used to measures the temperature of the tray. The output of the RTD is fed to the controller box. In the controller box actual measured temperature is compared with the reference temperature. The error (reference temperature-actual temperature) is fed into a Proportional-Integral-Derivative (PID) controller.

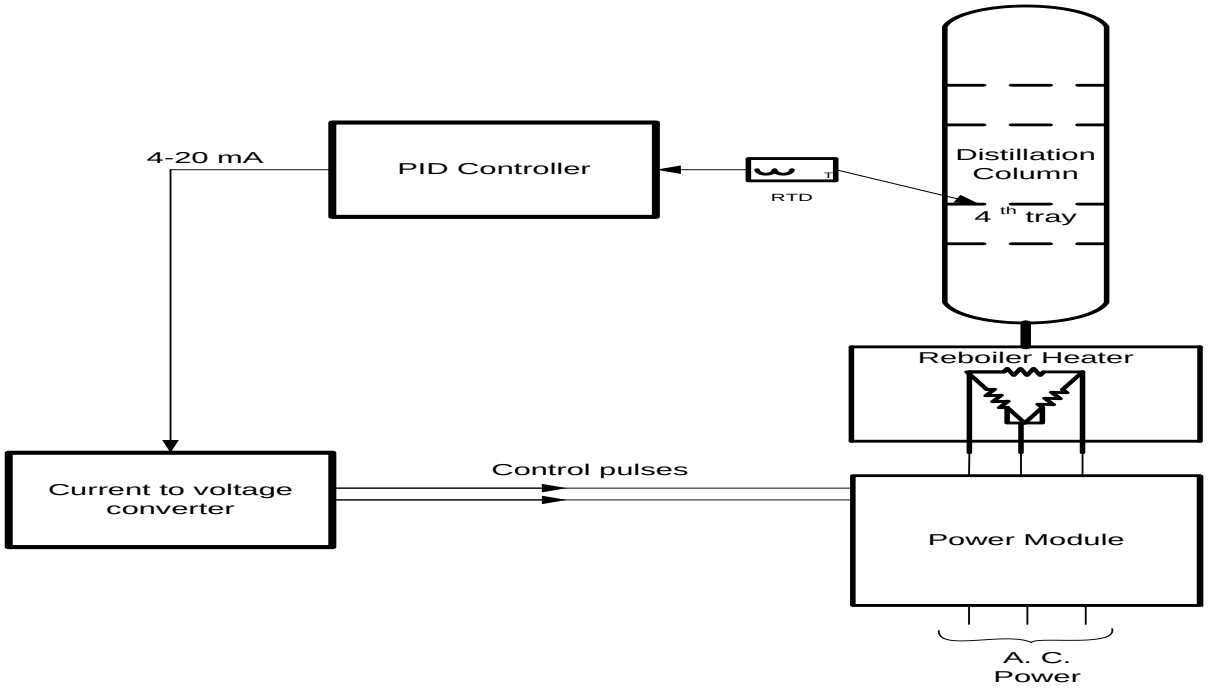


Fig. 3.2 Schematic diagram of tray temperature control

The output of the PID controller is a current signal of 4-20 mA when temperature varies between 0-200 °C. This signal is utilized to control the heat generated by the heater of reboiler. If actual temperature of tray-4 is less than the reference temperature, the controller output signal is used to increase the input power of the reboiler heater or vice-versa. The closed loop block diagram is shown in Fig. 3.3. The parameters of the PID controller should be selected optimally for the efficient operation of the BDC.

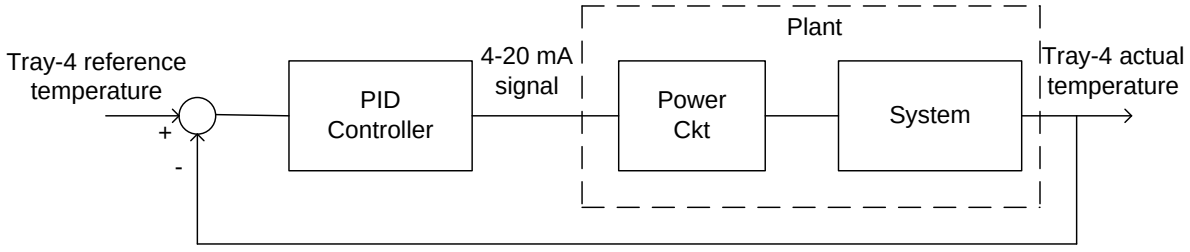


Fig. 3.3 Block diagram of tray-4 temperature control scheme

The dynamics of the plant shown in Fig.3.3 must be known to obtain the optimal parameters of PID. It is difficult to determine this dynamics for the experimental set-up

therefore; this dynamics has been determined experimentally in the following manner. Consider the open loop system as shown below in Fig. 3.4. For the experimentation the realization of this block diagram is shown in Fig. 3.5. The objective here is to develop the dynamics between plant input (current signal, *I*) and plant output (tray-4 temperature $T_4$).

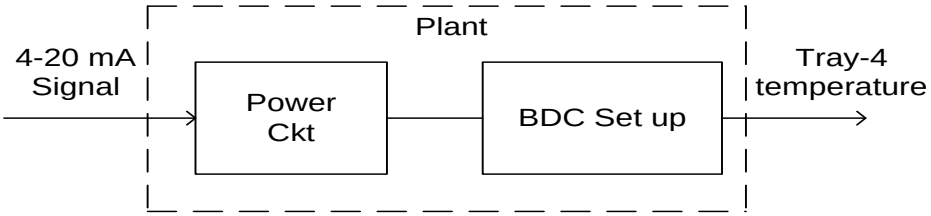


Fig. 3.4 Block diagram of open loop plant

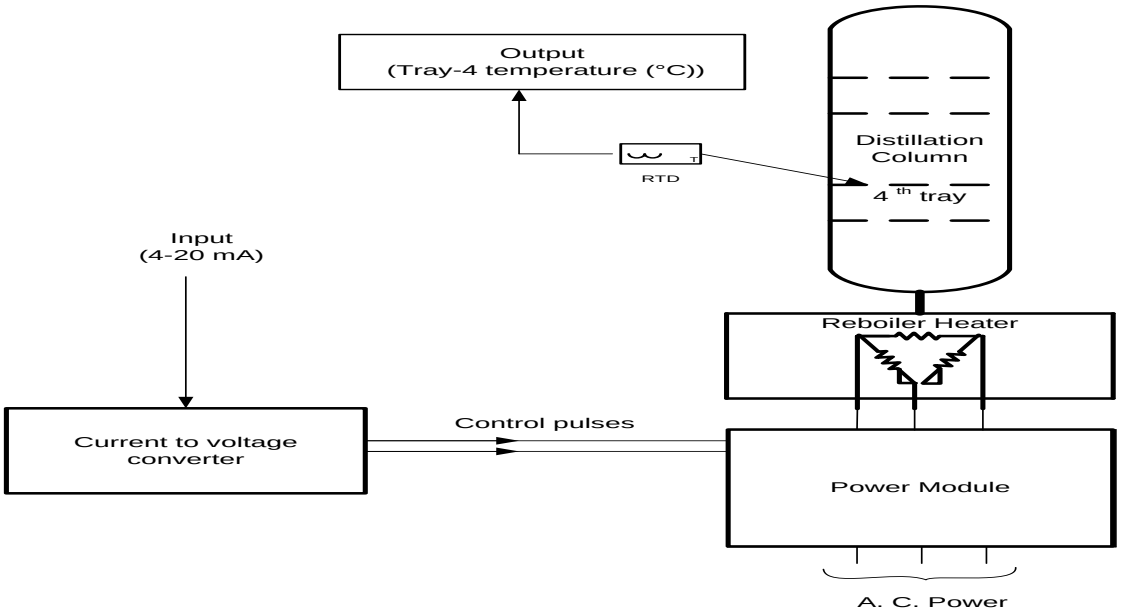


Fig. 3.5 Open loop diagram of distillation plant

The plant input current has been varied utilizing the circuit shown in Fig. 3.6. In this circuit, a 1-5 V DC variable power supply is used to get the 4-20 mA current signal. A 250 Ω resistor is utilized as this will give a voltage drop of 5 V DC at 20 mA and a minimum of 1 V DC at 4 mA.

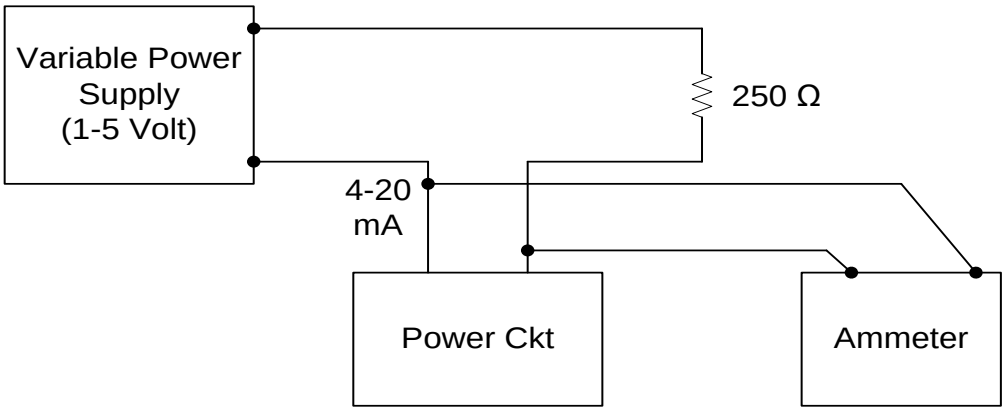


Fig. 3.6 Circuit for the variation of current signal

The sensitivity of power supply is 0.1 Volt. BDC plant has been started at minimum current 4mA. Now the current has been increased gradually and the tray-4 temperature has been recorded as given in Table 3-7.

Table 3-7 Recorded data between current and tray-4 temperature

| S. No. | Controller current (mA) | Tray-4 temperature (°C) | S. No. | Controller current (mA) | Tray-4 temperature (°C) | S. No. | Controller current (mA) | Tray-4 temperature (°C) |
|---|---|---|---|---|---|---|---|---|
| 1 | 4 | 0 | 15 | 9.6 | 70 | 29 | 15.2 | 140 |
| 2 | 4.4 | 5 | 16 | 10.0 | 75 | 30 | 15.6 | 145 |
| 3 | 4.8 | 10 | 17 | 10.4 | 80 | 31 | 16.0 | 150 |
| 4 | 5.2 | 15 | 18 | 10.8 | 85 | 32 | 16.4 | 155 |
| 5 | 5.6 | 20 | 19 | 11.2 | 90 | 33 | 17.0 | 160 |
| 6 | 6.0 | 25 | 20 | 11.6 | 95 | 34 | 17.4 | 165 |
| 7 | 6.4 | 30 | 21 | 12.0 | 100 | 35 | 17.8 | 170 |
| 8 | 6.8 | 35 | 22 | 12.4 | 105 | 36 | 18.2 | 175 |
| 9 | 7.2 | 40 | 23 | 12.8 | 110 | 37 | 18.6 | 180 |
| 10 | 7.6 | 45 | 24 | 13.2 | 115 | 38 | 19.0 | 185 |
| 11 | 8.0 | 50 | 25 | 13.6 | 120 | 39 | 19.4 | 190 |
| 12 | 8.4 | 55 | 26 | 14.0 | 125 | 40 | 19.8 | 195 |
| 13 | 8.8 | 60 | 27 | 14.4 | 130 | 41 | 20.0 | 200 |
| 14 | 9.2 | 65 | 28 | 14.8 | 135 | | | |

The following relation is achieved by utilizing the data between current and tray-4 temperature by using curve fitting method-

$$T_4 = 12.5 * I - 50 \qquad 3.1$$

This experimentally established relation (3.1) is utilized for determining the optimal parameters of PID controller. The output of the PID controller is a current signal ranging 4-20 mA. The PID controller [44] used in this work can be given as:

$$I(t) = \left[ K_P e(t) + K_I \int e(t)dt + K_D \frac{d}{dt} e(t) \right] \qquad 3.2$$

Where

$e(t) = T_{ref} - T_4$,

$I(t)$ : Current signal (mA)

$T_{ref}$ : Reference temperature of tray-4 (°C),

$T_4$ : Measured temperature of tray-4 (°C),

$K_P$ : Proportional constant,

$K_I$ : Integral constant,

$K_D$ : Derivative constant,

$K_P$, $K_I$ and $K_D$ are the parameters of PID controller. Proportional action $K_P$ improves the system rising time, and reduces the steady state error. However, the higher value of $K_P$ produces large overshoot and steady state error so integral action $K_I$ is used to eliminate the steady state error. Integral control reduces the steady state error but it may make the transient response worse, therefore, derivative gain $K_D$ will have the effect of increasing the damping in system to reduce the overshoot, and improve the transient response. Therefore, the determination of optimal values of PID parameters ($K_P$, $K_I$ and $K_D$) is must for the desired response. In this work, Genetic Algorithm (GA) is used to search the optimal values of PID controller.

The GA has some meaningful advantages over ordinary optimization tools [98]: (1) Genetic Algorithms search a population of points in parallel, not from a single point, (2) it does not require derivative information or any other auxiliary knowledge of the system but it needed only the objective function and corresponding fitness levels to influence the direction of the search. In this work, an objective function is required to find a PID controller that will minimise the error of the controlled system. In genetic algorithms, each chromosome in the population is passed into this objective function one at a time. A chromosome is a set of parameters which define a proposed solution to the problem that the genetic algorithm is trying to solve. In this work, the chromosome is represented as a finite bit string. Each chromosome consists of three separate strings constituting a P, I and D term. When the chromosome enters the objective function, it is split up into its three terms. The controlled system is then given a PID controller input initialize with the initial values of P, I and D. Error is assessed using error performance criterion MSE. The chromosome is assigned an overall fitness value according to the magnitude of the error, the smaller the error the larger the fitness value.

The basic operations include in GA are reproduction, crossover, and mutation, which perform the task of copying strings, exchanging portions of strings as well as changing some bits of strings respectively. Finally, the string which contains the largest value of fitness function is found and decoded from the last pool of mature strings. The general structure of GA is described in Appendix E. The steps involved in the tuning of PID controller for BDC using GA are described below.

**Step 1: Initialize the settings of GA parameters and generate an initial, random population of individuals**

GA is implemented with double vector type population with population size 20. The smaller population size optimizes the controller faster than bigger population size therefore; the initial parameters of GA are selected as [98] :

Population size: 20,

Crossover rate: 0.8,

Mutation rate: 0.01,

The Stopping criterion for GA search is error convergence. The value of converging error is set to $1x10^{-6}$. The selected upper and lower bounds of $K_P$, $K_I$ and $K_D$ are [0, 5], [0, 5] and [0 0.5] respectively. The initial population is set by encoding the PID parameters [$K_P$, $K_I$ and $K_D$] into binary strings known as chromosome. The length of strings depends on the required precision which is about 4 significant figures. The required bits string is calculated based on the following equation-

$$2^{n-1} < (b_j - a_j) \times 10^4 \leq 2^n - 1 \qquad 3.3$$

Where n is the number of bits, and $b_j$ and $a_j$ are upper and lower bound of PID parameters. For BDC, $K_P \in [0,5]$, $K_I \in [0,5]$ and $K_D \in [0,0.5]$. The required bits calculated based on (3.3) are equal to 16, 16 and 13 bits respectively. The total length of chromosome is 45 bits which can be represented as Fig. 3.7. A random value is selected for the Initialisation of chromosomes.

$$\underbrace{[0000101010001001]}_{16bits}\Big|\underbrace{[0000111000110010]}_{16bits}\Big|\underbrace{[0001010010001]}_{13bits}$$

Fig. 3.7 A chromosome representing PID parameters

**Step 2: Evaluate the fitness of each individual**

The fitness of each chromosome is evaluated by converting its binary string into a real value which represents the PID parameters. The conversion process of each chromosome is done by encoding into real numbers as follows:

$$x_j = a_j + decimal(substring_j) \times \frac{(b_j - a_j)}{2^n - 1} \qquad 3.4$$

Where, $x_j$ is the real value of the parameter.

The corresponding values of $K_P$, $K_I$ and $K_D$ are given below:

| Binary string | Decimal value |
|---|---|
| $K_P$: 0000101010001001 | 2697 |
| $K_I$: 0000111000110010 | 3634 |
| $K_D$: 0001010010001 | 657 |

Therefore, the real number becomes:

$$K_P = 0 + 2697 \times \frac{5-0}{2^{16}-1} = 0.21,$$

$$K_I = 0 + 3634 \times \frac{5-0}{2^{16}-1} = 0.11,$$

$$K_D = 0 + 657 \times \frac{0.5-0}{2^{13}-1} = 0.06$$

Each set of PID parameters is passed to PID controller. A complete response of the system for each PID set and its initial fitness value is computed using a defined objective function. In this work, the Mean Square Error (MSE) is chosen as the objective function as shown in (3.5).

$$MSE = \frac{1}{t}\int_{o}^{T} (e(t))^2 dt \qquad 3.5$$

Where

$e(t) = T_{ref}(t) - T_4$

**Step 3: Perform selection, crossover and mutation**

All individuals go through the selection process based on their fitness values. The probability of selection of an individual is higher if the fitness value is higher of that individual. Roulette method is utilized as a selection strategy to improve the searching performance of GA. Crossover is the next operation after selection process. For selection, single point crossover method is utilized in the present work. Two mating individuals are selected randomly and one single point is used to swap the right part of the two parents to generate the offspring. Mutation is the next operation after crossover. Mutation prevents the GA algorithm to be trapped in local minima and maintain the diversity in the population. Lower mutation rate is used otherwise search process will become random.

**Step 4: Repeat step 2 until end of generations**

After the completion of selection, crossover and mutation processes, a new set of PID parameters is sent to PID controller to compute a new fitness value. This process will go through steps 2 to 3 sequentially and repeat until the end of generations where the best fitness is achieved. The application of GA for determination of the optimal parameters of PID controller is shown in the form of a flow chart in Fig. 3.8.

In the next section, the results of implemented PID controller are discussed which is tuned by Genetic Algorithm (GA). GA requires several iterations to obtain the optimal solution. For the present work, the obtained optimal values of PID parameters $K_P$, $K_I$ and $K_D$ by GA are 1.9, 2.2 and 0.1 respectively and the minimum value of MSE is $2.978 \times 10^{-6}$. The convergences of the parameters are shown in Fig. 3.9.

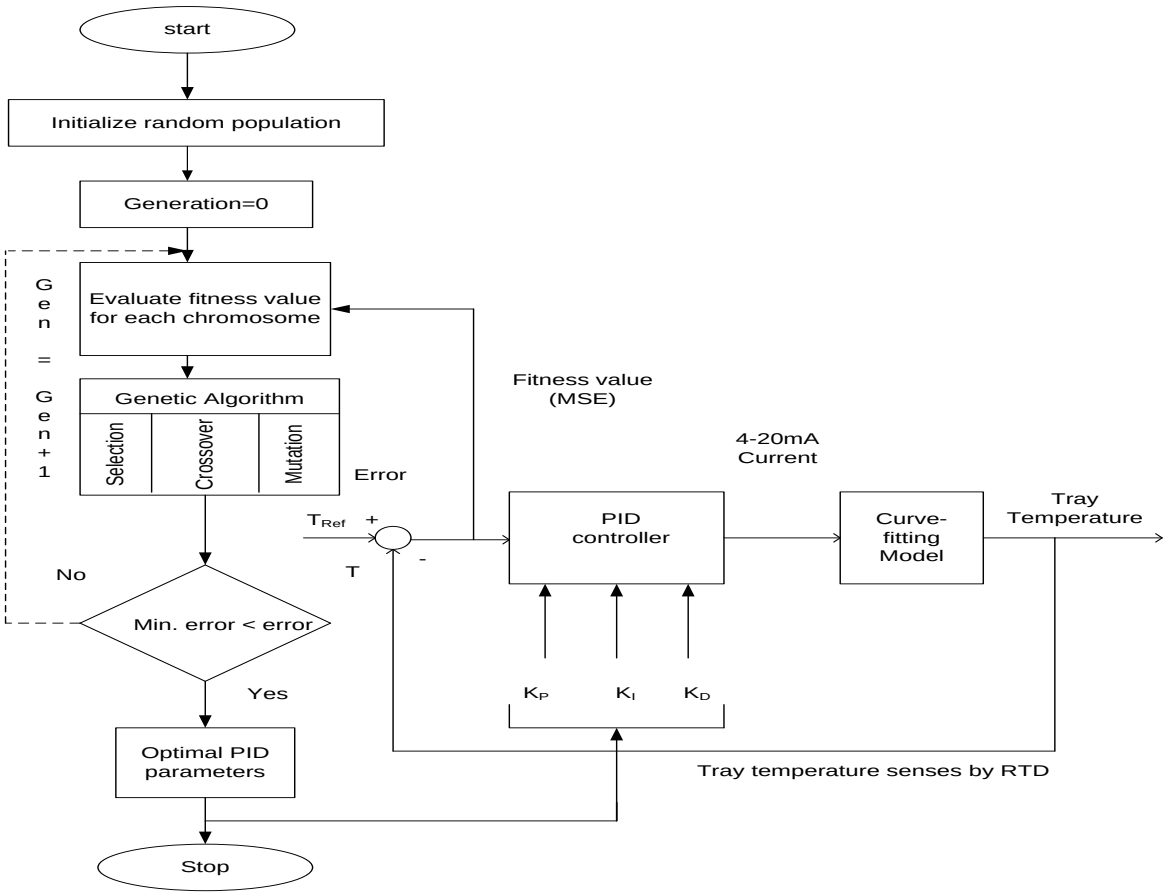


Fig. 3.8 Flow chart of GA algorithm for PID tuning

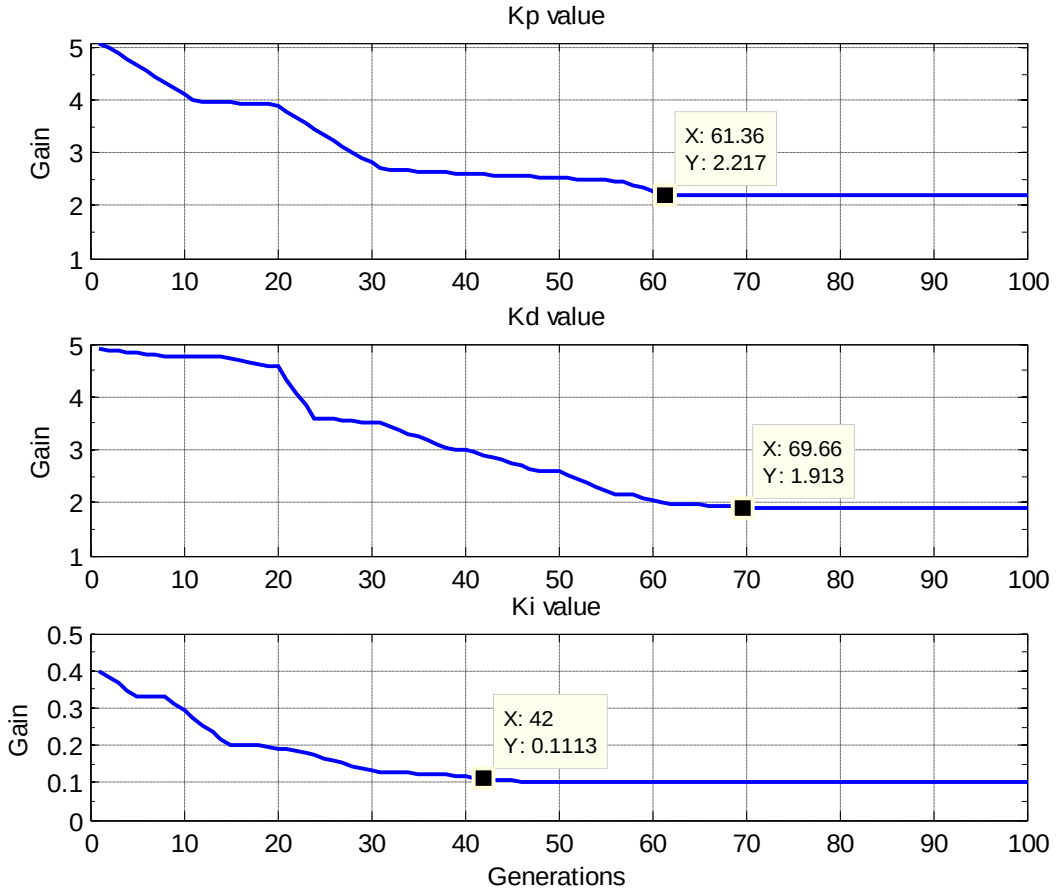


Fig. 3.9 Illustration of the Genetic Algorithm Converging through Generations

### 3.4 Performance of the Designed PID Temperature Controller

In this section, the performance of designed PID controller is evaluated for simulation and implementation phase. In the simulation phase, the parameters of PID controller are obtained by GA in the environment of MATLAB®/SIMULINK. The established relation between the tray-4 temperature and current (to the power circuit) is utilized to search the optimal PID parameters. In the implementation phase, Yokogawa PID controller (Model-UT320) is used to control the tray-4 temperature of laboratory set-up of BDC [99]. The obtained optimal PID parameters are incorporated in this controller and then the performance of the controller is evaluated.

#### 3.4.1 Simulation Results

In the simulation phase, the set-point of tray-4 temperature is 85°C. The performance of simulated PID controller is evaluated on the basis of rise time and settling time as shown in Fig. 3.10.

.

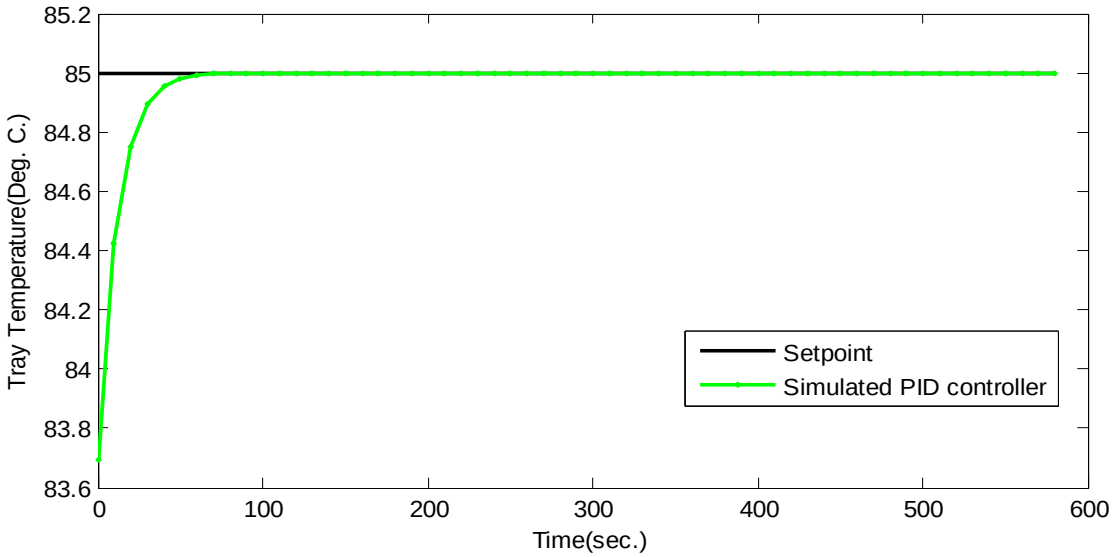


Fig. 3.10 Output of simulated PID controller

#### 3.4.2 Implementation Results

In this phase, the obtained parameters of PID controller are incorporated in the hardware PID controller attached with BDC set-up. The performance of hardware PID controller involves reference tracking and disturbances rejection cases.

##### 3.4.2.1 Reference Tracking

In this case, feed flow-rate is fixed at 2.5 kg-mole/hr and all the other parameters of BDC are at their rated value as shown in Appendix-A. It is observed from the sensitivity analysis that the desired output of methanol composition (98 %), is obtained when the 4$^{th}$ tray temperature is 85 °C. Therefore, the reference temperature of the tray-4 is kept at 85 °C when the feed flow is 2.5 kg-mol/hr. The performance of the hardware PID controller is compared with simulation results on the basis of rise time, settling time and MSE. The results

obtained show that rise time is 18.5 seconds and 140 seconds for simulated and hardware PID controllers respectively. The settling time is 90 seconds for simulated controller and 340 seconds for hardware controller as shown in Fig. 3.11.

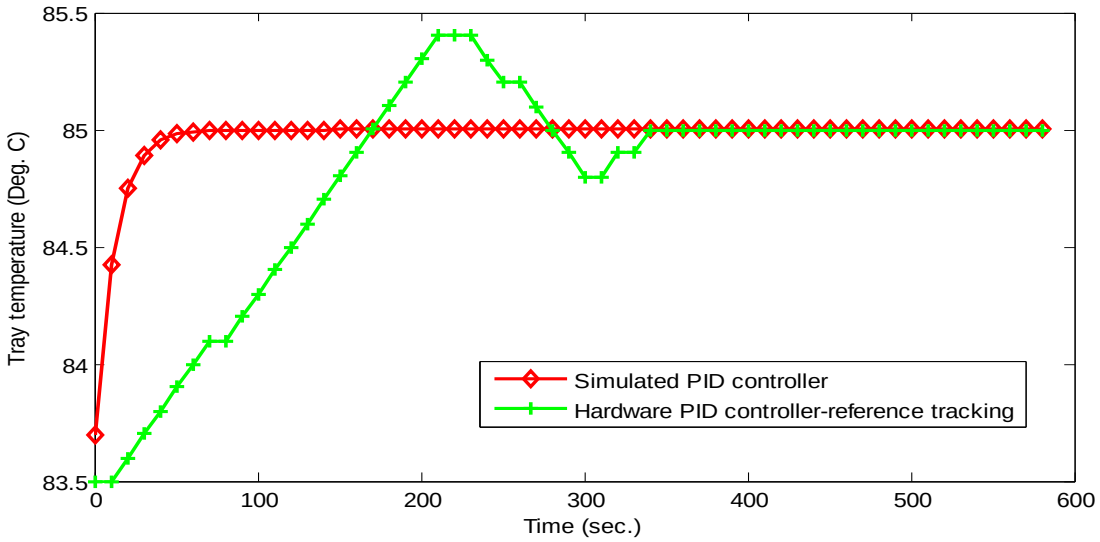


Fig. 3.11 Output of hardware PID controller for reference tracking

The rise time and settling time for hardware controller is seems to be much larger than the simulated controller. There are number of factors like time delays, disturbances, unmeasured variables, noise, nonlinearities, large time constant and multivariable interactions associated with the laboratory set-up of BDC, because of that the hardware PID controller takes longer time to approach the desired temperature of tray-4.The MSE for simulated and hardware controller is given in Fig. 3.12. MSE of hardware PID controller have oscillations due to the overshoot in the output.

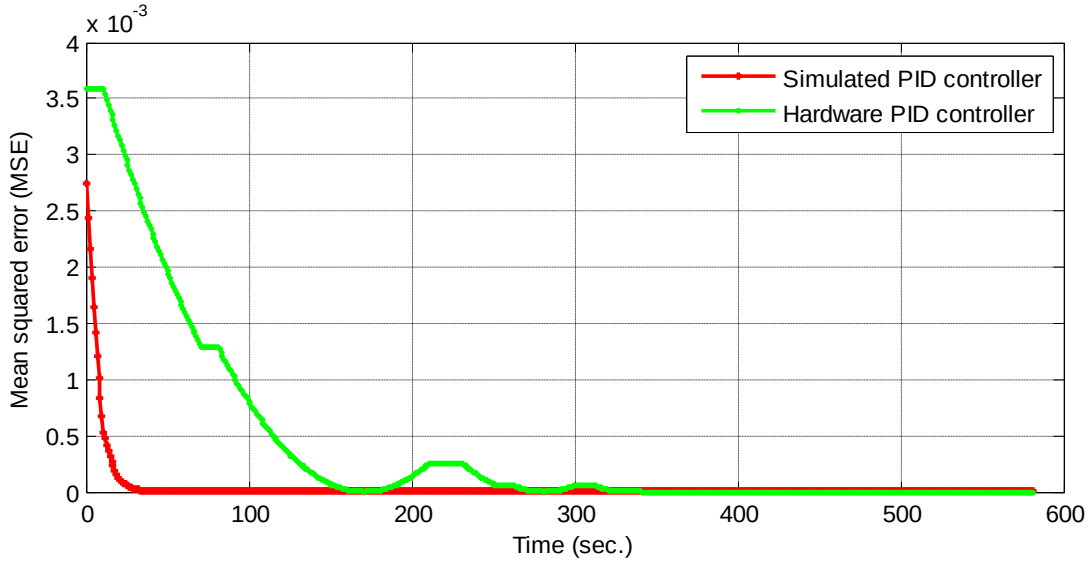


Fig. 3.12 MSE of Simulated and hardware PID controller for reference tracking

#### 3.4.2.2 Disturbance Rejection

In this case, 10% increment in the feed flow is made. This change in feed flow affects the thermal equilibrium of distillation process. The performance of hardware PID controller is compared with simulated PID controller and hardware PID controller (reference tracking case) as shown in Fig. 3.13.

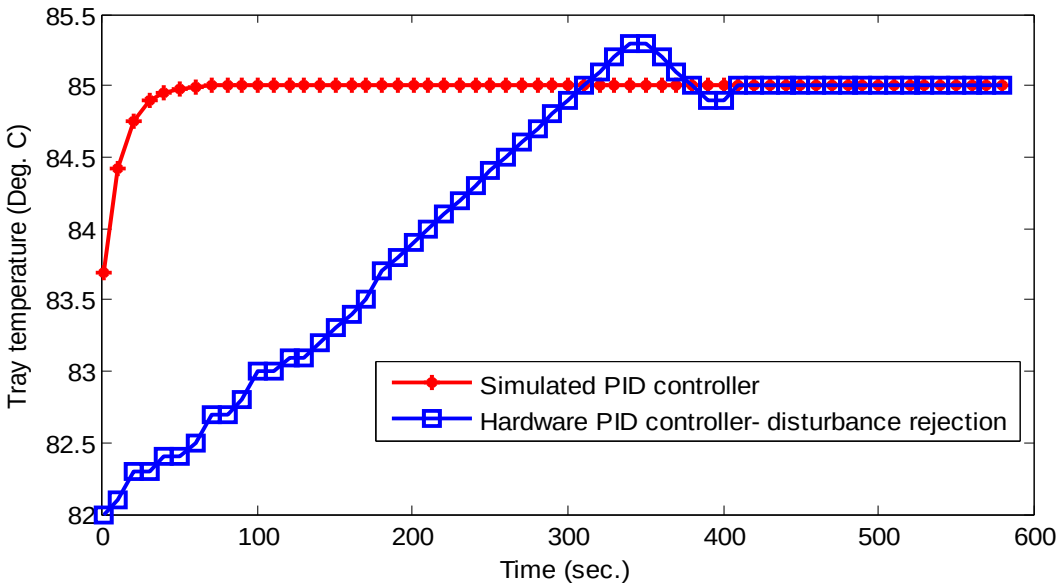


Fig. 3.13 Output of hardware PID controller for disturbance rejection

The rise time and settling time is 280 seconds and 410 seconds respectively. The comparison of MSE for both the controllers is shown in Fig. 3.14.

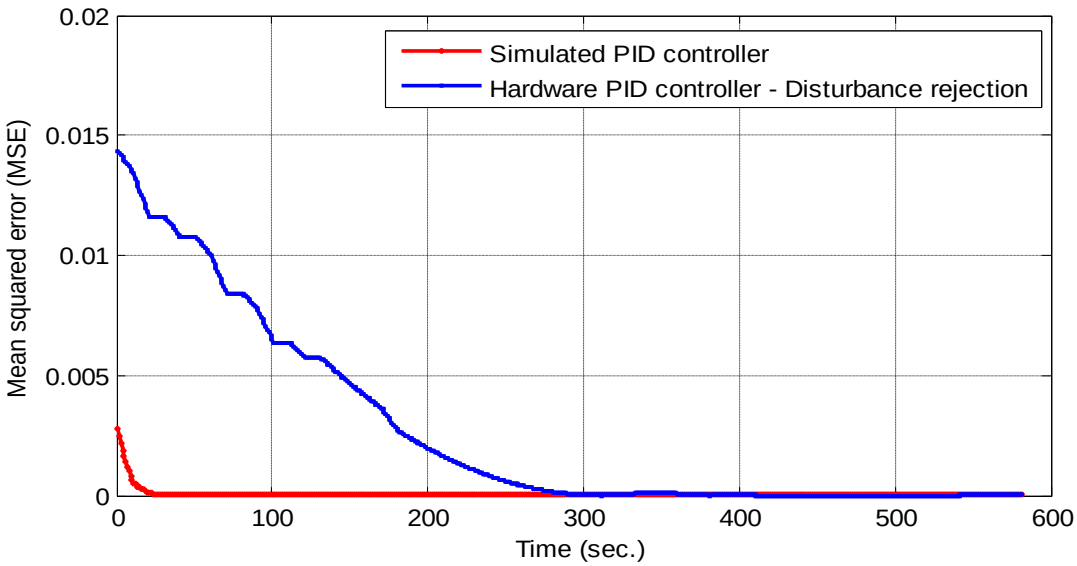


Fig. 3.14 MSE of simulated and hardware PID controller for disturbance rejection

## 3.5 Conclusion

In this chapter, inferential control scheme is utilized to control the methanol composition of BDC. Inferential control scheme is the technique in which secondary variable

is controlled to get the desired output. For the laboratory set-up of BDC it is found by the sensitivity analysis that the temperature of fourth tray is an exact indicator of the corresponding methanol composition. A relation between the controller current and the tray-4 temperature has been established and used to control the temperature of the tray by a PID controller. The optimal parameters of the PID controller have been determined using GA. The controller has been implemented in laboratory set-up of BDC using embedded PLC (Yokogawa PID controller). It is evident by the results that the rise time and settling time for hardware controller are larger than the simulated controller as there are various factors (i.e. associated time delay, larger time constant) involved in the distillation process.

# Chapter 4: LINEAR MODEL PREDICTIVE CONTROL AND NEURAL NETWORK BASED MODEL PREDICTIVE CONTROL SCHEME FOR BDC

*In this chapter, Linear Model Predictive Control (LMPC) and Neural Network based Model Predictive Control (NN-MPC) Methodologies are evaluated for the purpose of getting the desired methanol composition in distillation process. The equation based model and ANN based model of BDC as described in the second chapter, are utilized for the application of above control schemes. The performance of LMPC and NN-MPC schemes are also evaluated and compared with conventional PID controller.*

## 4.1 Introduction

A PID controller is connected with the experimental set-up of BDC to control the tray temperature. This PID controller is utilized in the inferential control scheme. There are few limitations associated with the experimental set-up of BDC. One limitation is that the close loop control is possible only for tray-temperature and another limitation is that the facility of direct measurement of distillate composition is not available. Due to these limitations, other control schemes can not be implemented on the experimental set-up of BDC. Therefore, equation based model and ANN based model (developed in chapter-2) are utilized to implement the various control schemes described in the following chapters.

Model Predictive Control (MPC) is a powerful technique for optimizing the performance of control systems, with several advantages:

- MPC can directly take the constraints on process inputs and outputs into account [100].
- MPC is more effective than the PID control, even in the case of a single loop without constraint control problem [101].

Because of the above advantages, MPC has been used widely in various industrial applications, such as chemical, food processing, aerospace engineering, etc. The existence of an accurate process model is the key for the successful implementation of MPC scheme. MPC scheme has come a long way since its inception almost five decades ago. Hussain [80] carried out an extensive review on MPC. A survey on industrial application of MPC has been performed by Qin et. al. [81].

Traditionally, the distillation process has been controlled by utilizing the linear model of the process despite of the fact that this is inherent nonlinear process. One of the ways to get the accurate model is identification of distillation process by using the neural networks. NN-MPC is the latest approach where MPC scheme is implemented by using the neural network model of the process. Arumugasamy *et al.* [86] have presented a review which surveys the concept of incorporating Feed forward Neural Networks into Model Based Predictive Control approach in various Chemical and Biochemical systems. Recently, NN-MPC has been utilized by many researchers [85] in the field of chemical engineering.

In this chapter, LMPC and NN-MPC are designed for the proposed ANN model of BDC to control the methanol composition as described in chapter 2, section 2.5. The performance of the LMPC and NN-MPC schemes have also been evaluated and compared with conventional PID controller.

## 4.2 Proportional-Integral-Derivative (PID) Control Scheme

The PID controller consists of proportional, integrative and derivative elements [44]. It is widely used in feedback control of industrial processes. In this work, the PID controller is designed to control the purity of methanol composition of BDC. Two PID controllers are designed in this work to control the two manipulated variables namely; reflux flow-rate and reboiler heat duty. The control scheme is shown in Fig. 4.1.

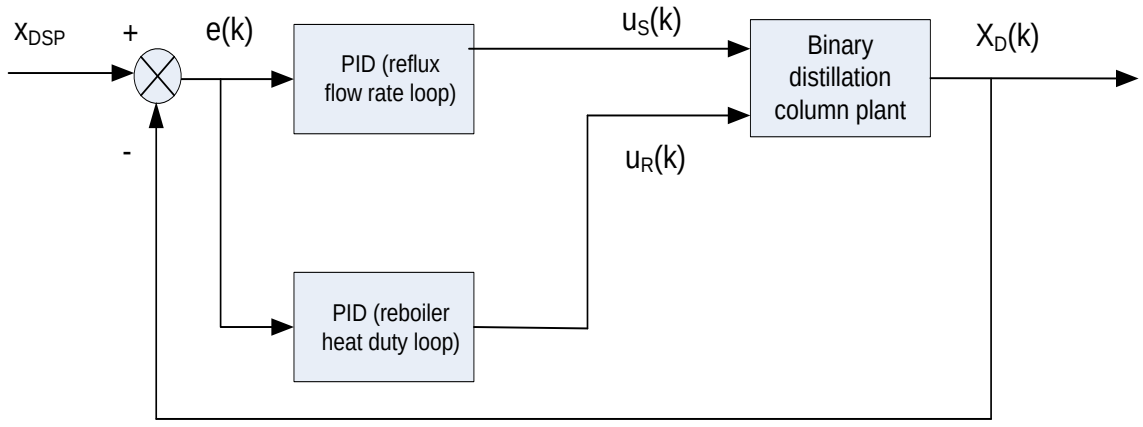


Fig. 4.1 PID control scheme for BDC

The structure of each PID controller [7] is considered as given in (4.1). $K_P$, $K_I$ and $K_D$ are the parameters of PID controller. Ziegler-Nichols method is used to get the parameters of each PID controller [45].

$$u(k) = \left[ K_P \cdot e(k) + \underbrace{K_P \cdot \left(\frac{T_s}{\tau_i}\right)}_{K_I} \cdot \sum_{i=0}^{m} e_i(k) + \underbrace{K_P \cdot \left(\frac{\tau_d}{T_s}\right)}_{K_D} \cdot (e(k) - e(k-1)) \right] \qquad 4.1$$

Where

$e(k) = x_{DSP}(k) - x_D(k)$,

$x_{DSP}(k)$: Desired methanol composition (mol fraction),

$x_D(k)$ : Measured methanol composition (mol fraction),

$\tau_i$ : Integral time(seconds),

$\tau_d$ : Derivative time (seconds),

$T_S$ : Sampling interval (seconds),

*u(k)* : Controller output (either $u_R(k)$ or $u_S(k)$),

m : No. of samples

*u(k)* is the output of the PID controller. *e(k)* is the difference between the desired methanol composition and actual methanol composition. The inputs are same for both the PID controllers but the outputs are different. Outputs of PID controllers are reflux flow-rate and reboiler heat duty respectively. Industrial process are normally stochastic in nature therefore, frequent tuning of PID controllers are required. PID controllers are also incapable to incorporate the non-linearities and parameter variation in the system. MPC has been designed in the following section to minimize these problems.

### 4.3 Model Predictive Control

Model Predictive Control is an approach where a process model is used to predict the future behaviour. Model Predictive Control is a multivariable control approach to predict the future control action by using the past control actions and the available present output variables [79]. MPC uses a dynamic model of the plant to predict the future actions of manipulated variables on the plant output. The future moves of the manipulated variables can then be determined by minimising the difference between the set-point and the predicted output. The structure of linear MPC is given in Fig 4.2. In this figure, distillation process is the actual plant. The ANN model with six inputs (reflux flow, reboiler heat duty, feed flow, top and bottom pressure of the column, tray temperature) and single output (methanol composition), developed in chapter 2, section 2.5 has been considered as the actual plant. In this work, four outputs namely: feed flow, top and bottom pressure of the column and tray temperature are kept constant at the values as given in Table 2-1.

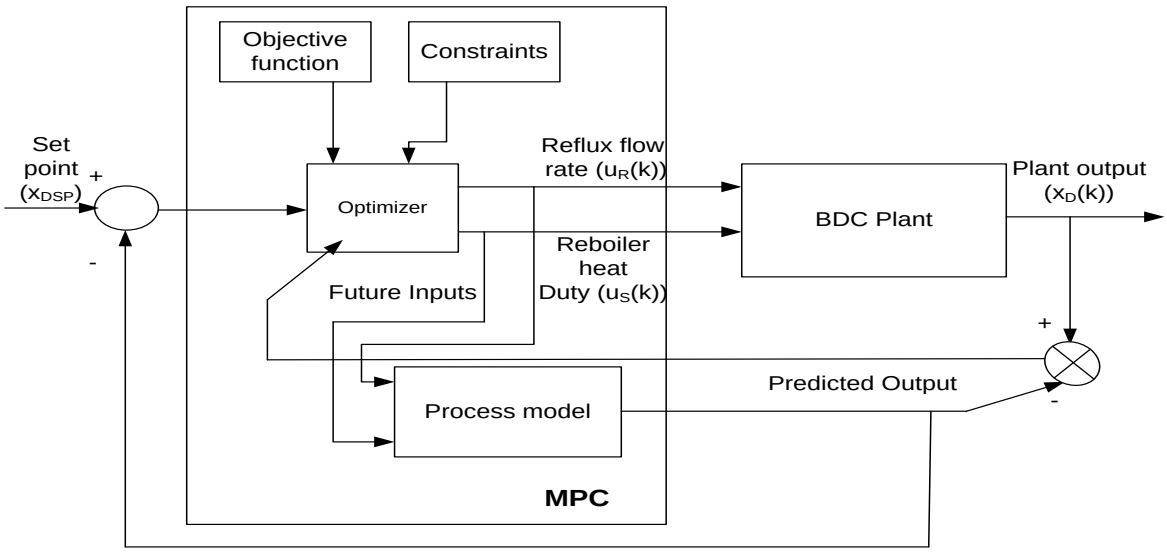


Fig. 4.2 MPC scheme for BDC

The two inputs reflux flow-rate ($u_R$) and reboiler heat duty ($u_S$) are the manipulated variables. The process model is the mathematical model or ANN based model of the actual plant which has been utilized to predict the output of the plant model. MPC can be categorized as linear or nonlinear based on the model considered for the plant.

In linear MPC, the linear equation based model developed in chapter 2, section 2.2 has been used as process model. The actual model of the BDC is nonlinear in nature therefore, ANN based model is used as the process model to implement NN-MPC scheme. For linear MPC, an optimum solution is obtained by using the least square method while; for NN-MPC, Sequential Quadratic Programming (SQP) is used to solve nonlinear constrained optimization problem [102]. These two approaches are explained in the following sections. The system model of the process is used to predict the system's future outputs based on the present value of the system output and future value of inputs. This information is used to obtain the control signal by minimizing an objective function. This objective or cost function considers the deviations from the set-point.

### 4.3.1 Linear Model Predictive Control (LMPC)

The first step to design the LMPC is to determine the Step Response Coefficients (SRC). SRC is determined in this work by using the Finite Step Response (FSR) of the BDC. Initially the thermal equilibrium is achieved without any control at time $t_0$. Now the reflux flow-rate ($u_R$) is increased by 5% while keeping the reboiler heat duty ($u_S$) same as at steady state. At this condition the output (methanol composition, $x_D$) has been determined and SRC are calculated as given below:

At any time $t \geq t_0$, reflux flow-rate can be written as:

$$u_R(t) = u_R + \Delta u_R \text{ for } t \geq t_0 \qquad 4.2$$

At this step change, measure $x_D(t)$ at regular intervals

$$x_{D_k} = x_D(t_0 + kh_s), \text{ k=1,2,…,N} \qquad 4.3$$

Where $h_s$=sampling interval, N is equal to the prediction horizon which is explained later.

The step response coefficient for the input $u_R$ are defined as:

$$a_{1,k} = \frac{x_{D_k} - x_{D_0}}{\Delta u_R} \qquad 4.4$$

Now, the reboiler heat duty input ($u_S$) is increased by 5% keeping the $u_R$ constant and similarly SRC for input $u_S$ has been determined. SRC for input $u_S$ is denoted as $a_{2,k}$. After obtaining the SRC for both the inputs, the dynamic matrix [A] is obtained by arranging the SRC in specify form of matrix as follows:

$$A \triangleq \left[ A_{1,i} \;\; A_{2,i} \right] \qquad 4.5$$

Where

$$\left[ A_{1,i} \right] \triangleq \begin{bmatrix} a_{1,1} & 0 & \cdots & 0 \\ a_{1,2} & a_{1,1} & 0 & \vdots \\ \vdots & \vdots & \ddots & 0 \\ a_{1,H_c} & a_{1,H_c-1} & \cdots & a_{1,1} \\ a_{1,H_c+1} & a_{1,H_c} & \cdots & a_{1,2} \\ \vdots & \vdots & \ddots & \vdots \\ a_{1,H_p} & a_{1,H_p-1} & \cdots & a_{1,H_p-H_c+1} \end{bmatrix} \text{ and,}$$

$$\left[A_{2,i}\right] \triangleq \begin{bmatrix} a_{2,1} & 0 & \cdots & 0 \\ a_{2,2} & a_{2,1} & 0 & \vdots \\ \vdots & \vdots & \ddots & 0 \\ a_{2,H_c} & a_{2,H_c-1} & \cdots & a_{2,1} \\ a_{2,H_c+1} & a_{2,H_c} & \cdots & a_{2,2} \\ \vdots & \vdots & \ddots & \vdots \\ a_{2,H_p} & a_{2,H_p-1} & \cdots & a_{2,H_p-H_c+1} \end{bmatrix}$$

$H_p$ is the prediction horizon and $H_c$ is control horizon. The number of future control moves which are calculated during each time step is called the control horizon ($H_C$). The number of future controlled variables that are calculated using the control horizon is called the prediction horizon ($H_P$). A step response model can be represented as given in (4.6).

$$\hat{x}_D(k+1) = \bar{x}_D(k) + \underbrace{\sum_{i=0}^{H_p-1} [A_{1,i} \quad A_{2,i}][\Delta u]_{k+1-i}}_{\hat{x}_D} \tag{4.6}$$

Where

$$\left[\Delta u\right] \triangleq \begin{bmatrix} \Delta u_R \\ \Delta u_S \end{bmatrix} \tag{4.7}$$

$\Delta u_R$ : Change in reflux flow-rate,

$\Delta u_S$ : Change in reboiler heat duty,

$\hat{x}_D(k+1)$ : The predicted value of the controlled variable at future instance k+1,

$\bar{x}_D(k)$ : The value of the controlled variable at the $k^{th}$ instant,

$\hat{x}_D$ : Future changes in the controlled variable due to past moves in Δu,

$\hat{x}_D$ can be written in matrix form:

$$[\hat{x}_D] = [A].[\Delta u] \tag{4.8}$$

The objective of the controller is to minimise the closed loop error (between the future controlled variables and the set point). The objective function to be minimized can be written as:

$$\min_{\Delta u_R, \Delta u_S} OBJ = \underbrace{w_p \sum_{k=0}^{H_P-1} (x_{DSP} - (\hat{x}_D(k+1) + \hat{x}_D))^2}_{Predicted\ errors} + \underbrace{w_c \sum_{k=0}^{H_C-1} [\Delta u]^2}_{Control\ moves} \tag{4.9}$$

Where

$x_{DSP}$ : Set-point of methanol composition,

$\hat{x}_D(k+1)$ : The predicted value of the controlled variable at future instance k+1,

Where Δu is the change in manipulated variable and $w_P$ and $w_C$ are the weights. The value of $w_P$ determine the importance placed on the controlled variable and the value of $w_C$

penalize the changes in manipulated variables. This objective function can be reorganized in the quadratic form as follows:

$$\min_{\Delta u} OBJ = \left[ e^k - A\Delta u \right]^T w_P \left[ e^k - A\Delta u \right] + (\Delta u)^T w_C (\Delta u) \qquad 4.10$$

Where $e^k = x_{DSP} - \hat{x}_D(k+1)$ and $[\hat{x}_D] = [A].[\Delta u]$

An optimum solution is obtained by using the least square method [79]. The optimum value of Δu determined by this method is given as:

$$\Delta u = (A^T w_P A + w_C)^{-1} A^T w_P e^k \qquad 4.11$$

Now using this Δu, value of $\hat{x}_D$ is updated using (4.8). The predicted value for the next step is given in (4.12).

$$\hat{x}_D(k+1) = \bar{x}_D(k) + \hat{x}_D \qquad 4.12$$

Where $\bar{x}_D(k)$ **:** The value of the methanol composition at the k[th] instant.

The steps involved in designing the LMPC controller are given in the form of flow chart as shown in Fig. 4.3.

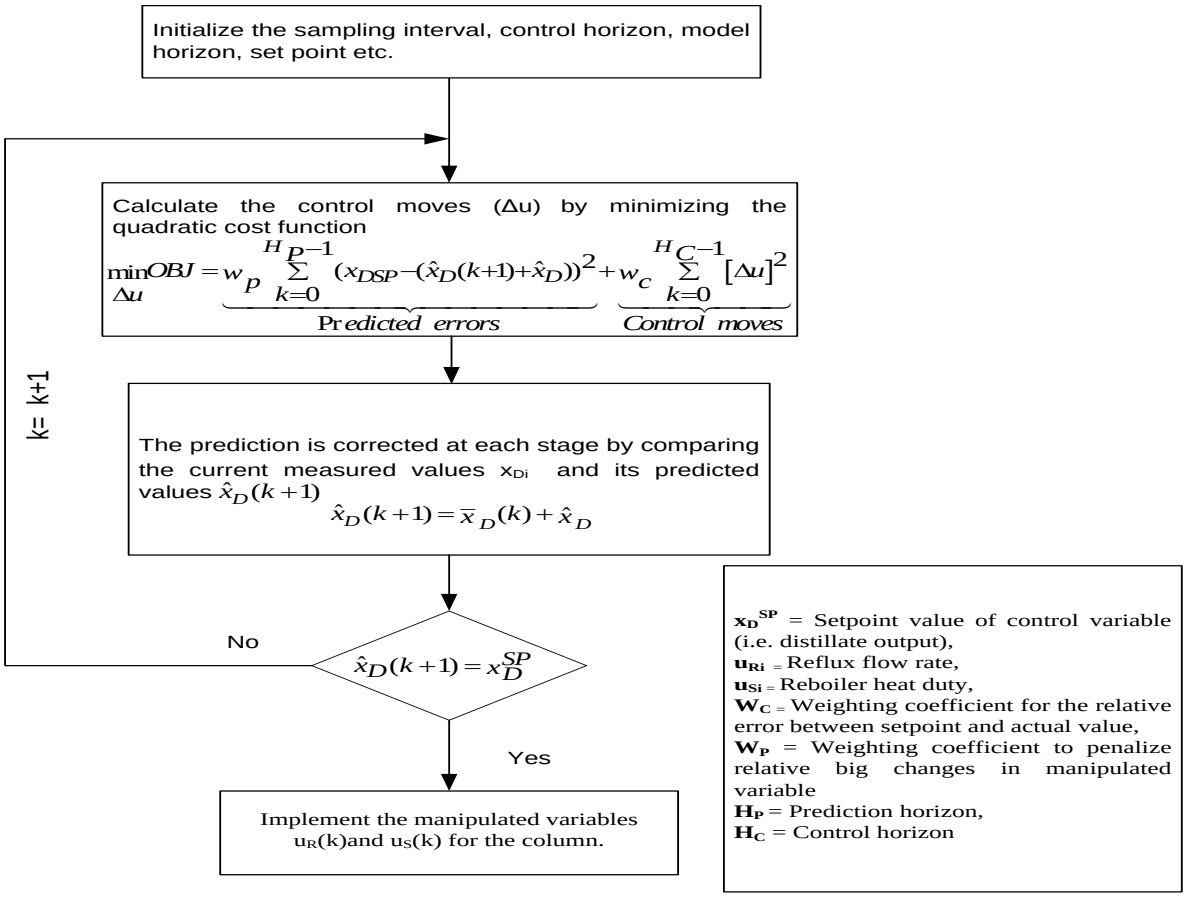


Fig. 4.3 Linear MPC algorithm

The adjustable coefficients which affect the performance of MPC scheme are $w_P$, $w_C$, $H_P$ and $H_C$. The Prediction horizon ($H_P$) is selected longer than the control horizon ($H_C$). To determine the $H_P$, the control horizon is set to 2. The response of the system is determined at different values of the prediction horizon, i.e., 10, 5 and 2. For $H_P$=10, the system gives the fastest response as shown in Fig. 4.4. To determine the best value of control horizon the value of prediction horizon is set to 10 and the system response is determined at different values of $H_C$ i.e. 1, 2 and 3 as shown in Fig. 4.5. The best response is obtained at $H_C$=2.

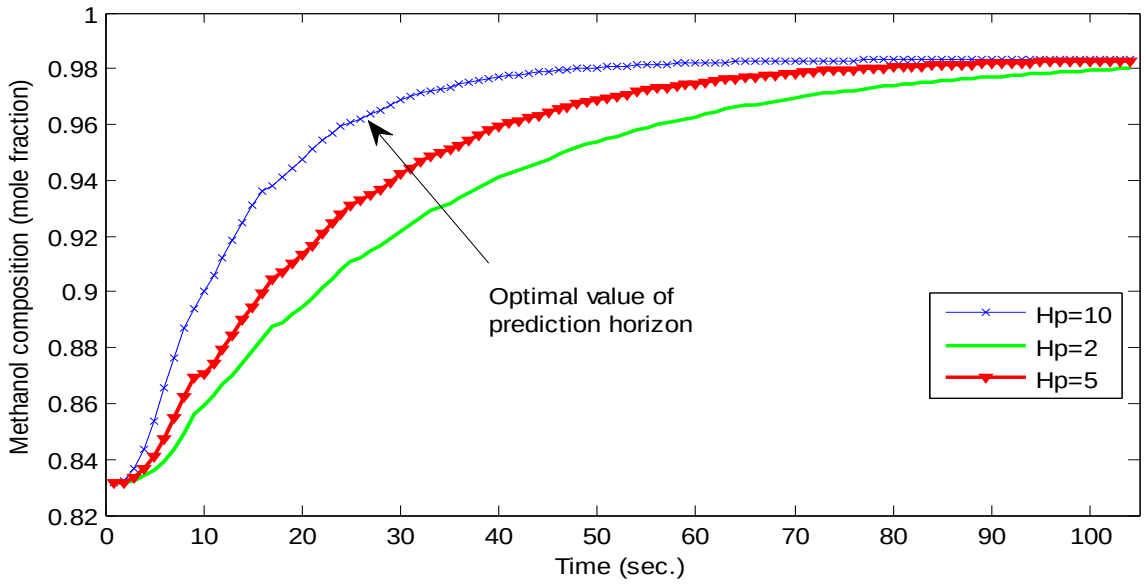


Fig. 4.4 Effect of prediction horizon on performance of MPC

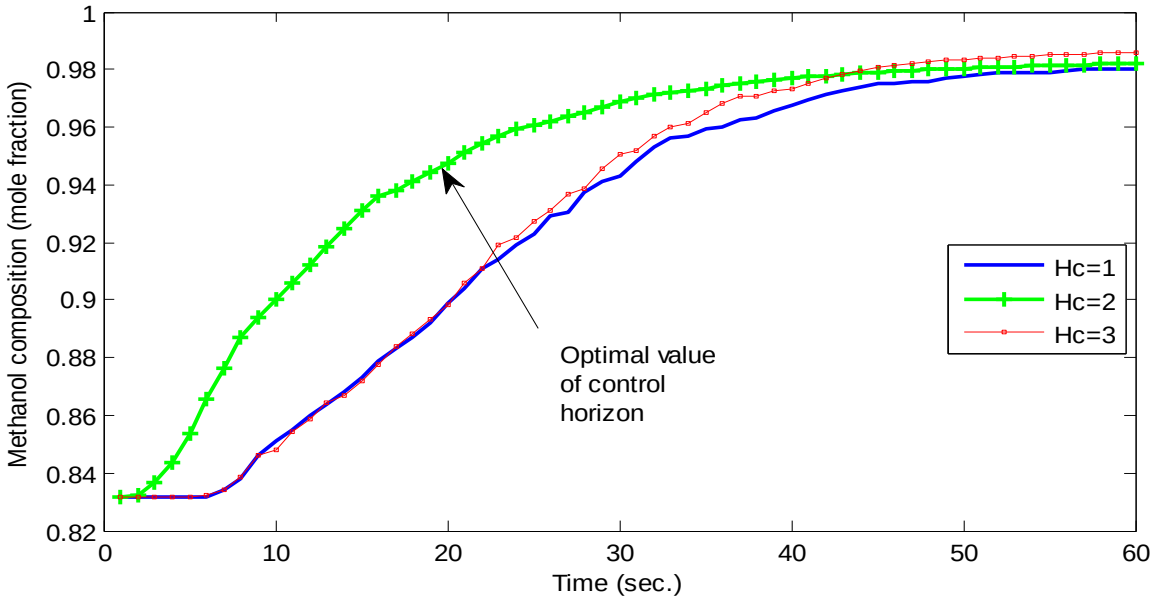


Fig. 4.5 Effect of control horizon on performance of MPC

The effect of various values of weight tuning parameter ($w_C$) is studied at constant values of prediction horizon ($H_P$=10) and control horizon ($H_C$=2). As the value of $w_C$ increases

0.5 to 0.8, system gives faster response as shown in Fig. 4.6. The effect of change in $w_P$ is negligible in the response, therefore the value of $w_P$ is considered 0.1 throughout the study.

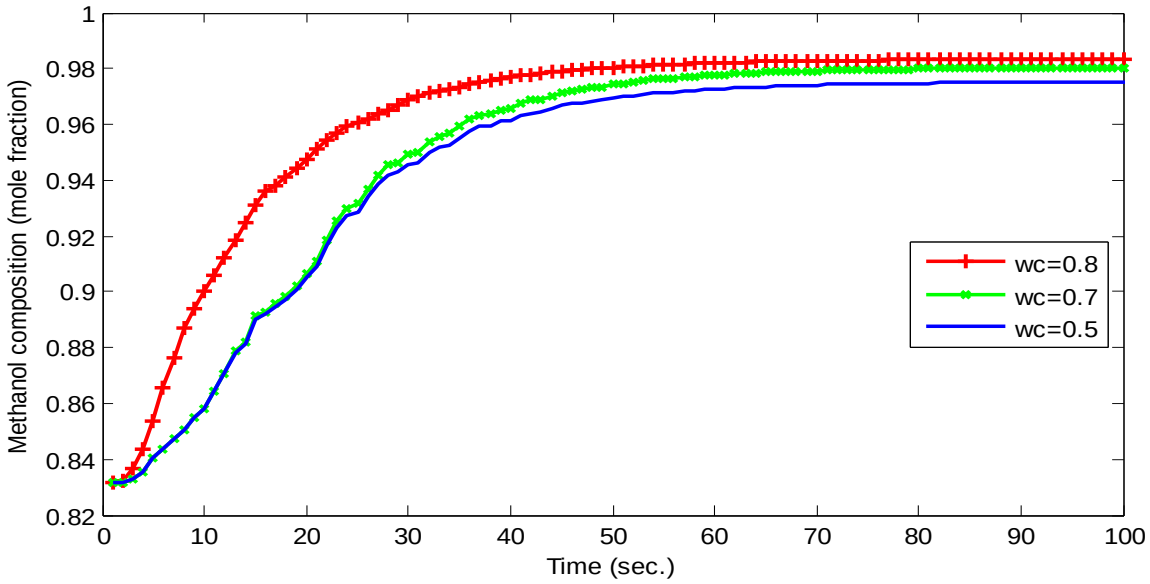


Fig. 4.6 Effect of weighting coefficient ($w_c$) on performance of MPC

The major drawback associated with Linear MPC that it does not perform uniformly well in case of wide variation in operating conditions (i.e. change in feed flow-rate and feed composition) and large disturbances. Neural network based MPC has been designed and described in the following sections to overcome the shortcomings of MPC.

### 4.3.2 Neural Network based Model Predictive Control

The need to handle difficult control problem has led to use artificial neural network (ANN) in MPC and has recently attracted more attention. ANNs have found wide applicability in modeling and control of non-linear systems because of their inherent capability of capturing the non-linear behavior of system. The advantage of the neural network approach is that an accurate representation of a process can be obtained by the training of the network. Neural networks are capable of handling complex and nonlinear problems and can reduce the engineering effort required in the model development of a controller. Following section has utilised the neural network in model predictive control algorithm to control the methanol composition in distillation column.

#### 4.3.2.1 Neural Network Modeling of BDC

In this approach, the neural network model has been used as the plant model. The relation between inputs and output for the neural network model is expressed mathematically as shown in (4.13)

$$\hat{x}_D(k+1) = f(u_R(k), u_R(k-1), u_S(k), u_S(k-1), x_D(k), x_D(k-1)) \qquad 4.13$$

Where

$\hat{x}_D(k+1)$ = Predicted value of methanol composition by neural model

$x_D(k)$ = Present value of methanol composition

$x_D(k-1)$ = Methanol composition at previous instant

$u_R(k)$ = Present value of Reflux flow-rate

$u_R(k-1)$ = value of Reflux flow-rate at previous instant

$u_S(k)$ = Present value of reboiler heat duty

$u_S(k-1)$ = value of reboiler heat duty at previous instant

The structure of neural network model for distillation column is shown in Fig. 4.7. This model has six inputs and a single output. In the neural network design, sigmoid activation function is used for hidden nodes whereas linear function is used for output. This neural network model is trained with the Levenberg-Marquardt algorithm [103]. Total 8000 sample data is used for the training and validation. The final structure of the neural network model has 6 inputs, 8 hidden neurons and 1 output layer. This neural network model is utilized as the system model in MPC structure.

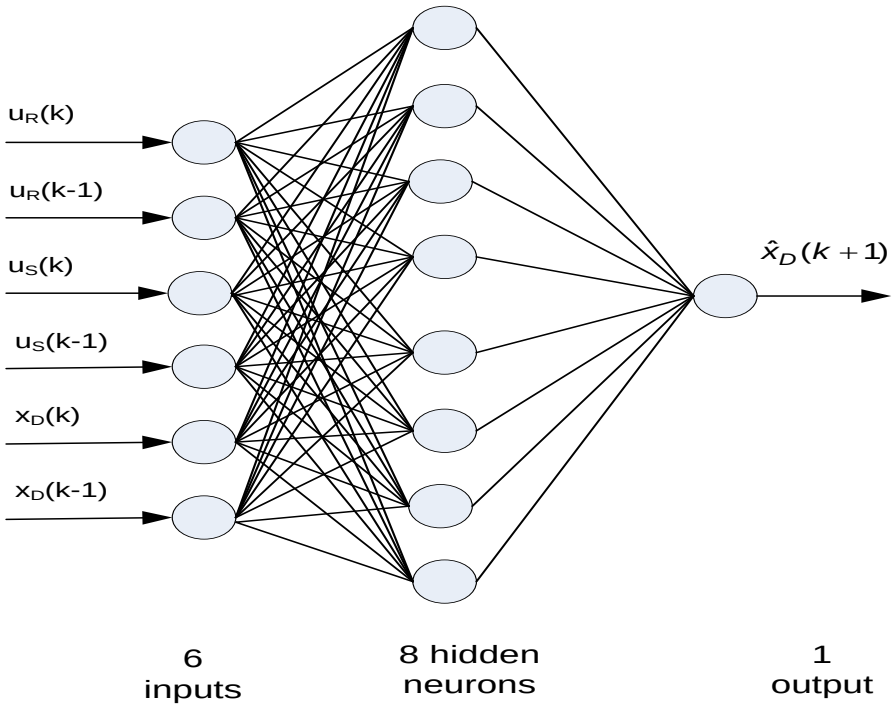


Fig. 4.7 Proposed structure of ANN model of BDC

Number of such model can be cascaded to predict the output several step ahead. Cascading of such models is shown in Fig. 4.8. The output from the first prediction $\hat{x}_D(k+1)$ is used as input for the next iteration to predict $\hat{x}_D(k+2)$. With this iterative procedure, multiple outputs can be predicted p steps ahead. Other inputs to the neural model are the direct measurements of reflux flow-rate and reboiler heat duty at the current and previous steps.

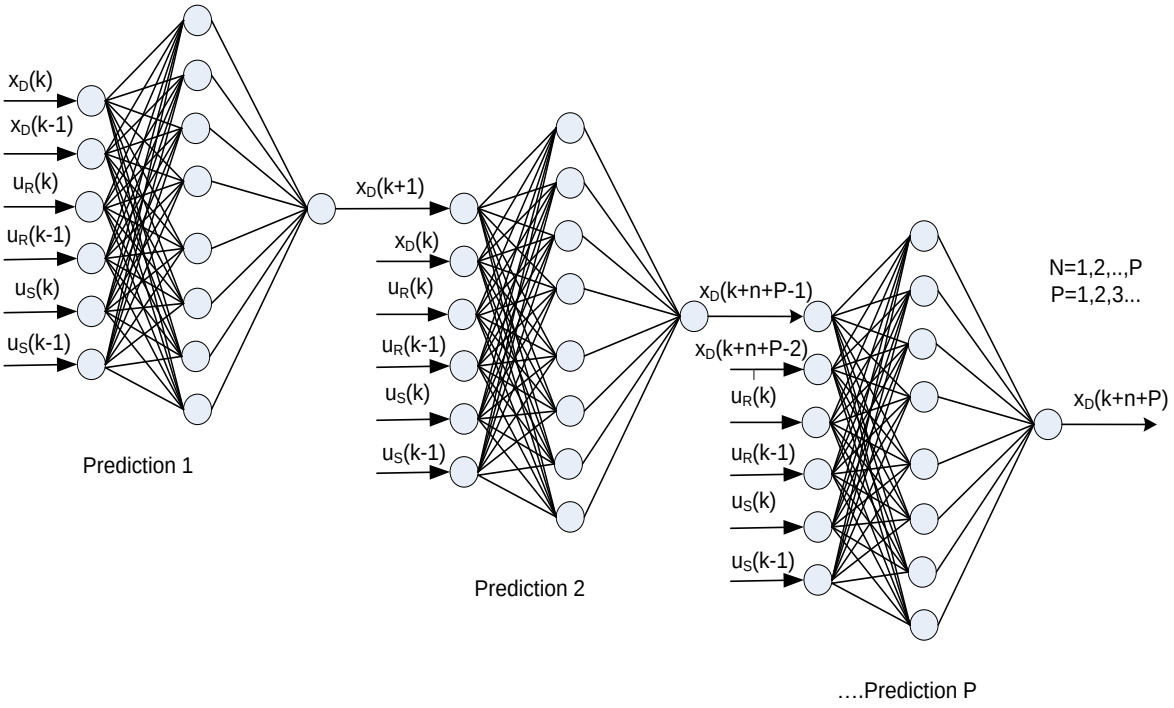


Fig. 4.8 Neural network based iterative method

### 4.3.3 Control Scheme

The MPC structure shown in Fig. 4.2 has been modified to incorporate NN model of BDC as shown in Fig. 4.9. The optimization block in this figure optimises the objective function (4.9) to get the optimum values of manipulated variables. The error between the predicted output and set point is passed to an optimization routine which produces the future control outputs.

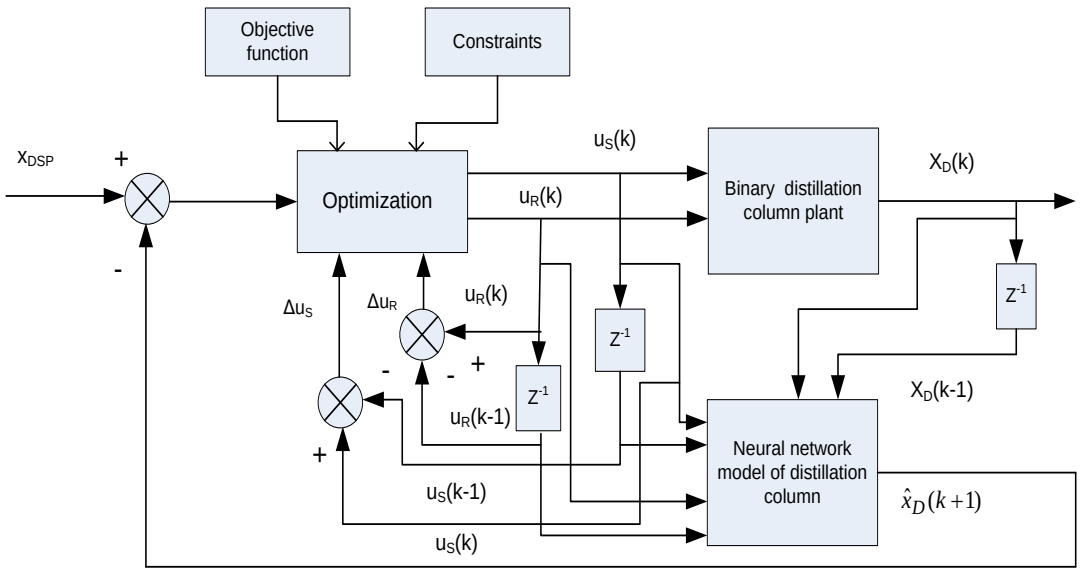


Fig. 4.9 NN-MPC scheme for BDC

The optimization problem is formulated as:

Minimize the objective function given by (4.9).

Subjected to:

- Constraint on manipulated variables:

$$\left.\begin{matrix} u_{R_{\min}} \le u_{R_i} \le u_{R_{\max}} \\ u_{S_{\min}} \le u_{S_i} \le u_{S_{\max}} \end{matrix}\right\}, \text{(i=0,…,}H_C\text{-1)}$$

- Constraint on control moves:

$$\left.\begin{matrix} \Delta u_{R_{\min}} \le \Delta u_{R_i} \le \Delta u_{R_{\max}} \\ \Delta u_{S_{\min}} \le \Delta u_{S_i} \le \Delta u_{S_{\max}} \end{matrix}\right\}, \text{(i=0,…,}H_C\text{-1)}$$

- Constraint on process variable:

$$x_{D_{\min}} \le x_{D_i} \le x_{D_{\max}}, \text{ (i=1,…,}H_P\text{-1).}$$

Sequential Quadratic Programming (SQP) is utilized to solve this optimization problem. The steps involved in SQP procedure are described in Appendix-D [11]. The adjustable parameters ($H_P$, $H_C$, $w_P$ and $w_C$) are obtained in the similar manner as explained in section 4.4.2. The best values obtained for NN-MPC approach are $H_P$=8, $H_C$=2, $w_C$=1 and $w_P$=0.1. The operation of the NNMPC algorithm is summarized in the form of flow chart and shown in Fig. 4.10.

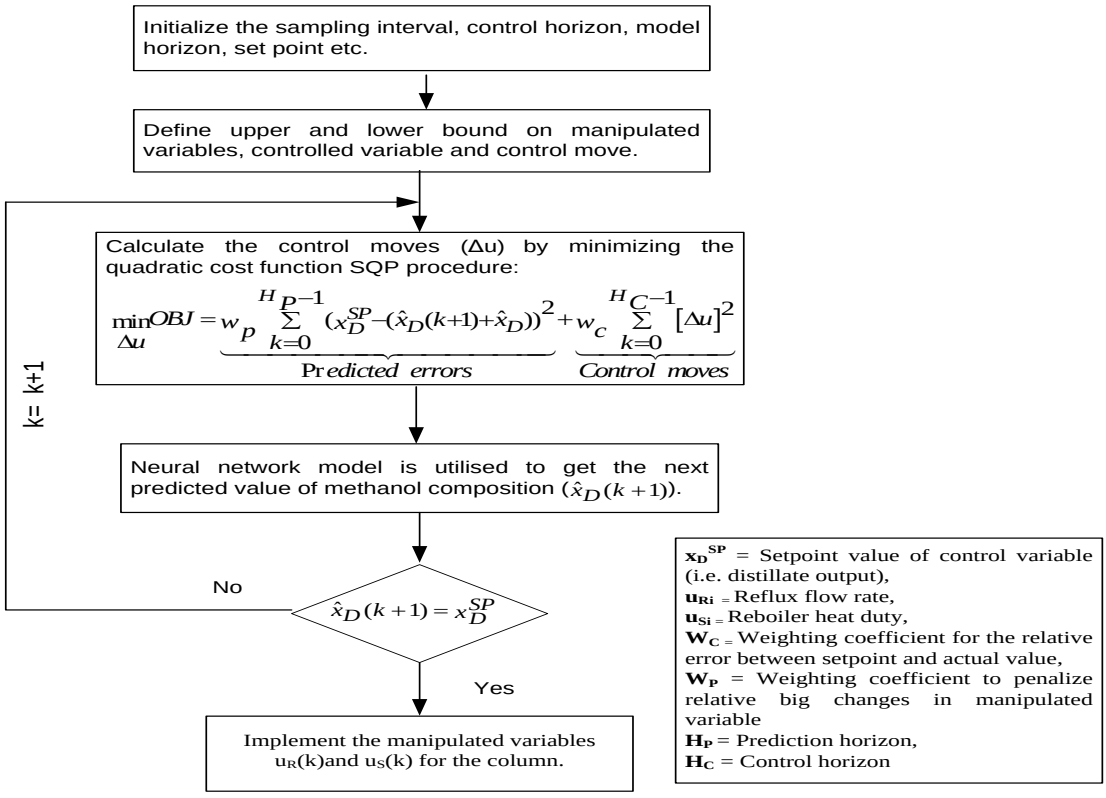


Fig. 4.10 Flow chart for NN-MPC algorithm

## 4.4 Simulation Results

The performance of linear and nonlinear MPC has been determined for the two cases: Case a: Reference Tracking and Case b: Disturbance Rejection. The simulation study has

been carried out in MATLAB®/SIMULINK environment. The results of LMPC and NN-MPC schemes are also compared with the conventional PID control scheme. The optimal parameters of PID ($K_P$, $K_I$ and $K_D$) determined using Ziegler-Nicholas approach is given in Appendix-C.

### 4.4.1 Case a: Reference Tracking

Initially the feed flow-rate has been kept at 2.5 kg-mol/hr. At this flow-rate and without any control on BDC the final composition was 0.83 mol fraction. Now methanol purity has been set to 0.98 mol fractions and the response of PID, LMPC and NN-MPC schemes have been simulated. Fig. 4.11 illustrates the comparative behaviour of LMPC, NN-MPC and PID control schemes with a change in methanol composition from 0.83 mol fractions to 0.98 mole fractions. Mean Squared Error (MSE) of these schemes are shown in Fig. 4.12. Performance parameters i.e. rise time, settling time and overshoot for all the three schemes are given in Table 4-1.

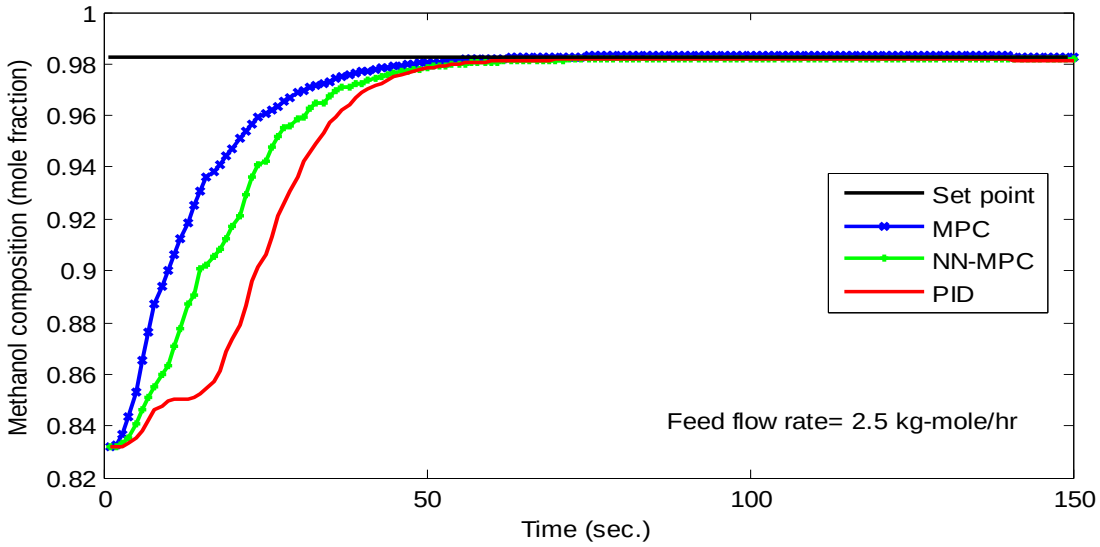


Fig. 4.11 Output of PID, LMPC and NN-MPC schemes for reference tracking

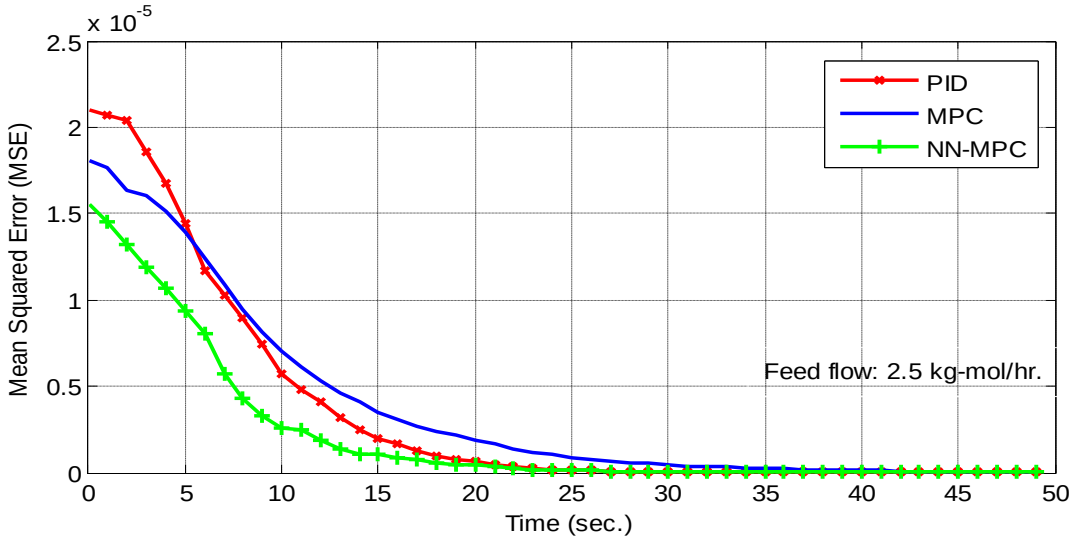


Fig. 4.12 MSE of PID, LMPC and NN-MPC schemes for reference tracking

### 4.4.2 Case b: Disturbance Rejection

In this case, the performances of NN-MPC, LMPC and PID control schemes are compared when a disturbance is created in the feed flow-rate. To simulate this change of +10% (2.5 kg-mole/hr to 2.75 kg-mole/hr) in feed flow-rate has been considered along with the set point of 0.98 mol fraction. The output and MSE for all the control schemes is shown in Fig. 4.13 and Fig. 4.14 respectively.

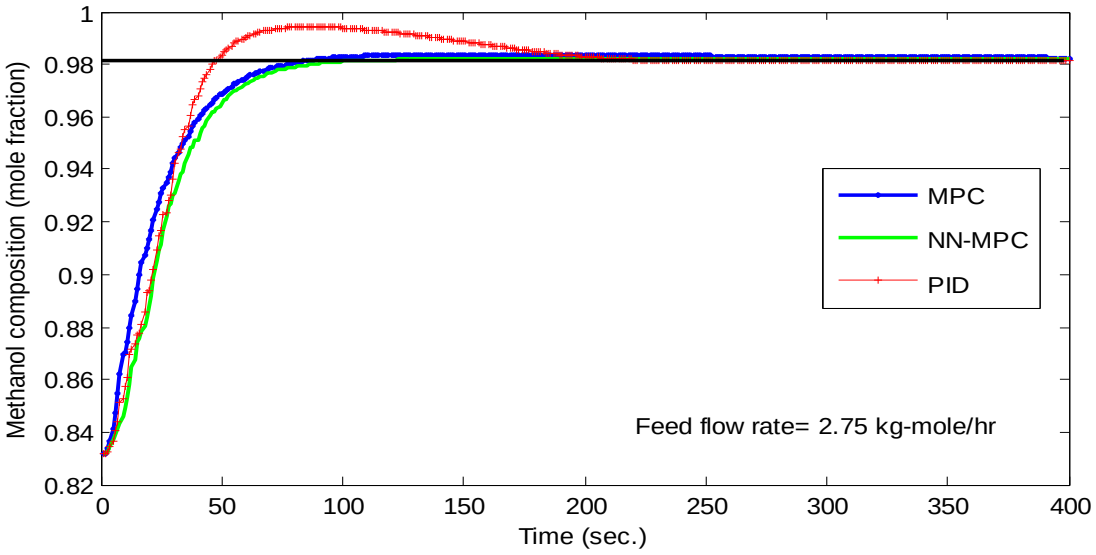


Fig. 4.13 Output of PID, LMPC and NN-MPC schemes at +10% change in feed flow-rate

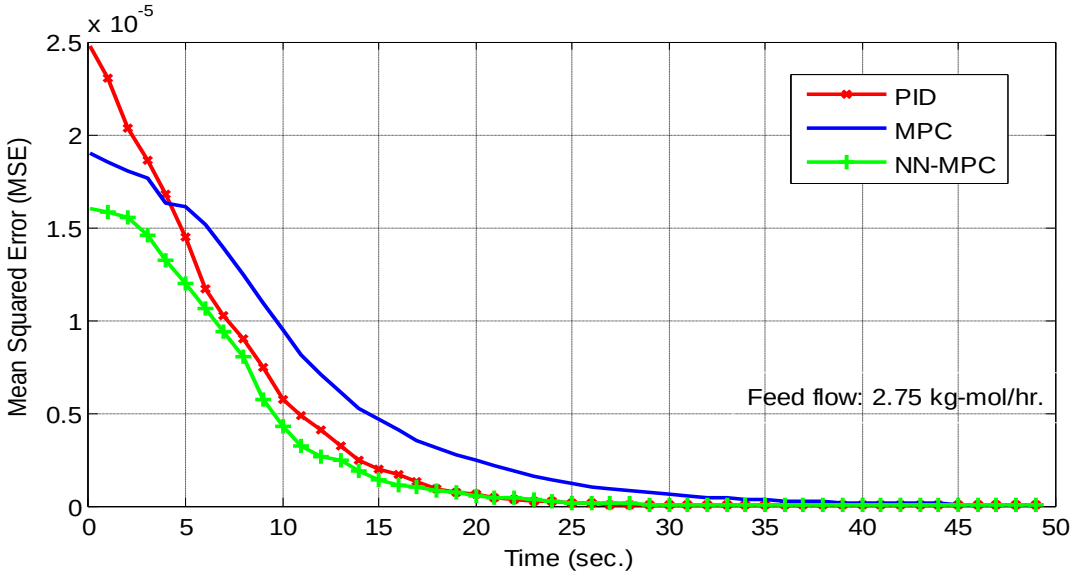


Fig. 4.14 MSE of PID, LMPC and NN-MPC schemes at +10% change in feed flow-rate

All the results obtained have been compared after achieving initial equilibrium state in distillation process. It is observed from the result that in case-a, when feed flow-rate is 2.5 kg-mole/hr, the rise time is minimum for LMPC scheme while, associated settling time is maximum. The associated settling time with LMPC is greater than NN-MPC due to its heavy dependence on the accuracy of the process model used. In case-b, when 10% increment in

the feed flow-rate is considered, the distillation process takes more time to get the desired methanol composition. For this case NN-MPC takes minimum time to achieve the desired composition with minimum associated MSE. It is observed from the results that NN-MPC scheme is comparatively better in all the three schemes.

Table 4-1 Performance parameters of PID, LMPC and NN-MPC schemes

| Performance Indicators | Case a | | | Case b(10% disturbance) | | |
|---|---|---|---|---|---|---|
| | At Feed flow (2.5 kg-mole/hr) | | | At Feed flow (2.75 kg-mole/hr) | | |
| | PID | LMPC | NN-MPC | PID | LMPC | NN-MPC |
| Rise time(sec.) | 36 | 25 | 31 | 41 | 37 | 45 |
| Settling time(sec.) | 70 | 100 | 70 | 240 | 280 | 110 |
| MSE | $2.1x10^{-5}$ | $1.8x10^{-5}$ | $1.55x10^{-5}$ | $2.5x10^{-5}$ | $1.9x10^{-5}$ | $1.6x10^{-5}$ |
| Overshoot (%) | 0 | 0 | 0 | 1.22 | 0.2 | 0 |

## 4.5 Conclusion

In this chapter Linear MPC and NN-MPC schemes have been developed to control the methanol composition in distillation column. In Linear MPC scheme, equation based model of BDC is utilized to develop the scheme. This scheme does not perform well when large changes in operating condition (change in feed flow-rate and feed composition) are considered, because BDC model is inherently nonlinear. To overcome this, a nonlinear MPC based on neural network process model is developed. Performance of these controllers has also been compared with PID controller. It can be concluded from the results that NN-MPC performs better than the other schemes on the basis of rise time, settling time, MSE and percentage overshoot.

# Chapter 5: NEURAL NETWORK BASED DIRECT INVERSE CONTROL AND INTERNAL MODEL CONTROL FOR BDC

*In this chapter, two neural network based control schemes namely; NN-DIC and NN-IMC are introduced to control the methanol composition in a binary distillation column. The proposed schemes are also compared with NN-MPC control scheme and on the basis of performance parameters it is observed that the NN-IMC scheme is better than the other schemes.*

## 5.1 Introduction

Model predictive control scheme proposed in the last chapter has some shortcomings [79]:

- Need of fast computation as online optimization involved in MPC.
- MPC models are limited to stable processes and require a large number of model coefficients to describe a response.
- MPC requires exact formulation of prediction horizon otherwise the performance gets affected.
- MPC is not suitable for the systems having a wide range of operating conditions.

Artificial Neural Network (ANN) is utilized in the different control methods to overcome the above shortcomings of MPC controller. ANN has shown an excellent ability to model any nonlinear, unstable process and not require a large number of model coefficients. ANN is suitable for the processes having wide range of operating conditions. Computation speed is not a big issue in ANN as online optimization is not involved [59], [62], [104].

In this work, neural networks have been incorporated in the inverse-model control scheme. This scheme has been used in two different ways i.e. direct inverse control (DIC) and the internal model control (IMC). In the direct inverse control approach, neural networks are used as the inverse model of the plant. In this approach, the neural network acting as the controller has to learn to supply at its output, the appropriate control parameters for the desired targets at its input.

The other approach is the internal model control (IMC) technique. In this method both the forward and inverse ANN models of the plant are used directly as elements within the feedback loop. Except for two additions, the IMC approach is similar to the direct inverse approach above. In the first addition the forward model of the plant is placed in parallel with the plant, to cater for plant or model mismatches and second is that the error between the plant output and the neural network forward model is subtracted from the set-point before being fed into the inverse model. The other inputs to the inverse model are similar to the direct method.

The forward and inverse neural network models of the BDC are required to design the NN-DIC and NN-IMC control schemes for BDC. These models are explained in the following sections.

## 5.2 Development of Forward and Inverse Models

For the development of forward and inverse models, Input/output data of plant acquired from experimental set-up of BDC has been used. The ability of ANN to represent nonlinear relations leads to the idea of using networks directly in a model-based control strategy. The development of forward and inverse models involves selection of the input and output variables, collection of input-output patterns, selection of network structure and training of the neural network.

### 5.2.1 Forward Models

The procedure of training a neural network to represent the forward dynamics of a system (i.e. the outputs for the given inputs) is referred as forward modelling. The past inputs and past output data samples of the model have been utilized to predict the output in the next instant. Neural Network based forward model is designed similarly as explained in chapter 2. The only difference in this model is that it has two inputs with their past two values and one step ahead output. BDC has two inputs namely: reflux flow-rate (*R(k)*) and reboiler heat duty (*S(k)*) whereas; the output is methanol composition ($x_D(k)$). For the forward model, two past values for inputs {*R(k-1), R(k-2), S(k-1), S(k-2)*} and one step ahead output $\{\hat{x}_D(k+1)\}$ are considered as shown in Fig. 5.1.

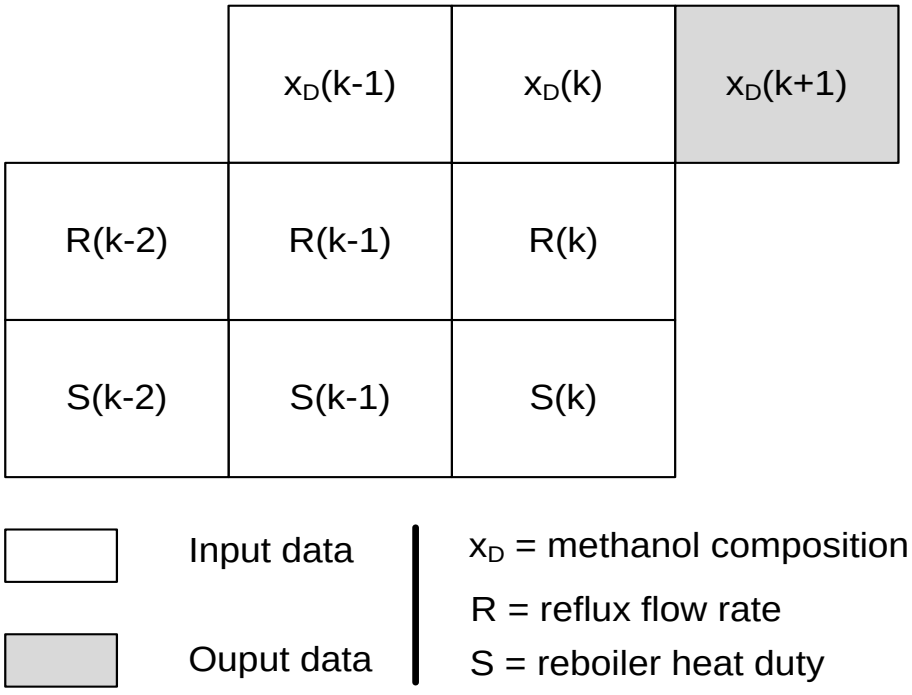


Fig. 5.1 Input and output data node assignment for BDC forward model

The schematic for learning of ANN based forward model is shown in Fig. 5.2. In this procedure, the network is fed with the present input, past inputs as well as the past outputs to predict the output. Various important steps to be followed for performing this procedure includes: proper selection of model structure and size, selection of data set, selection of suitable inputs and proper training method. The training Input-output pairs containing output (methanol composition) w.r.t. both the inputs (i.e. reflux flow-rate and reboiler heat duty) have been acquired from the experimental set-up of BDC for the complete operating range. The maximum and minimum values of inputs and outputs are given in Table 5-1.

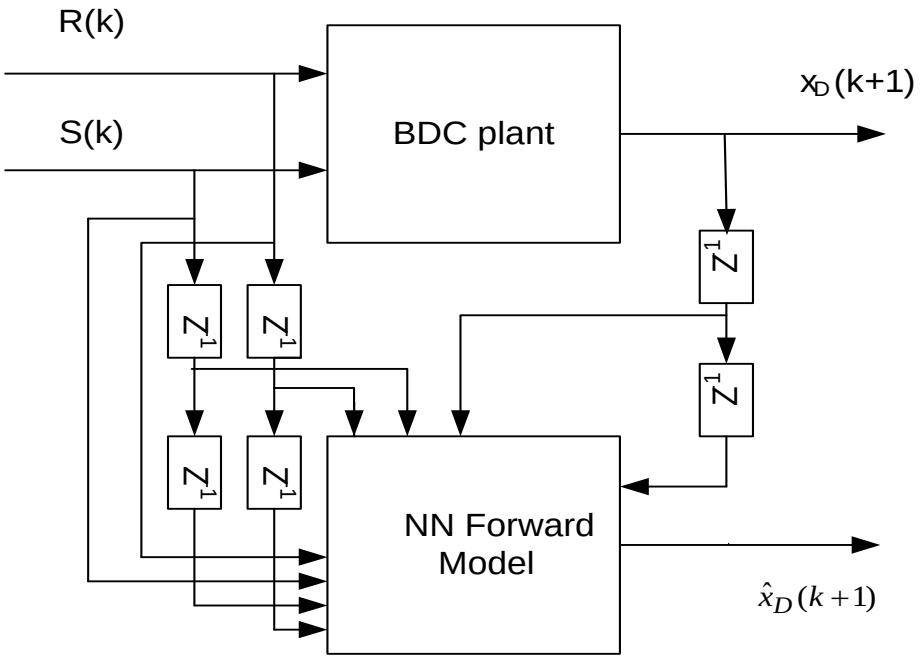


Fig. 5.2 Learning of forward model

Table 5-1 Range of I/O Variables

| I/O | Process Variable | Minimum value | Maximum value |
|---|---|---|---|
| Inputs | Reflux flow-rate (kg-mole/hr) | 2.9 | 3.1 |
| | Reboiler heat duty (kW) | 5.5 | 8.0 |
| Output | Distillate Composition (mole fraction) | 0.83 | 0.99 |

Total 1800 patterns have been acquired out of which 70% and 30% patterns have been used for training and testing respectively. The training is performed using Levenberg-Marquardt algorithm (explained in Appendix-E) until a reasonable reduction in the error is achieved. Then training is repeated using the test data set until the error decreases again to another reasonable minimum. Once a reasonable reduction in the error is achieved for both sets of data, the training is stopped. The details of ANN based forward model is given in Table 5-2. The predicted output of forward model is compared with actual output in Fig. 5.3.

Table 5-2 Network for forward model

| | |
|---|---|
| Number of inputs | 8 {R(k), R(k-1), R(k-2), S(k), S(k-1), S(k-2),$X_D$(k), $X_D$(k-1)} |
| Number of outputs | 1{$X_D$(k+1)} |
| Number of training patterns | 120 |
| Network type | Feed-forward back-propagation |
| Training method | Levenberg-Marquardt method |
| Number of hidden layers | 1 |
| Number of hidden layer neurons | 20 |
| Transfer function of hidden layer | Tangent sigmoid |
| Number of epochs | 150 |
| Learning rate | 0.001 |
| MSE | $8x10^{-8}$ |

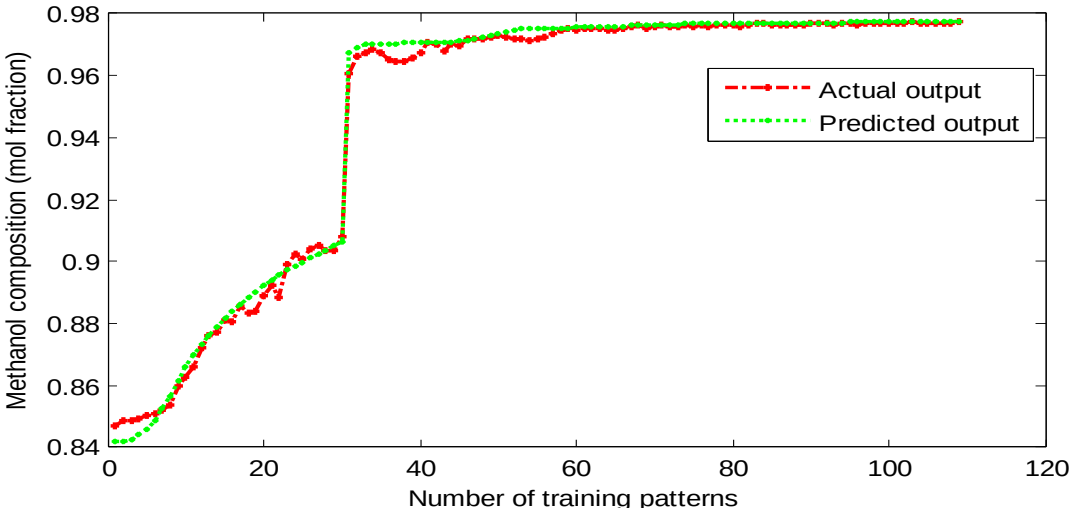


Fig. 5.3 Training performance of forward model

The MSE between the predicted output and the actual output is shown in Fig. 5.4. The results shows that the value of MSE is very low therefore estimated output matches the actual output.

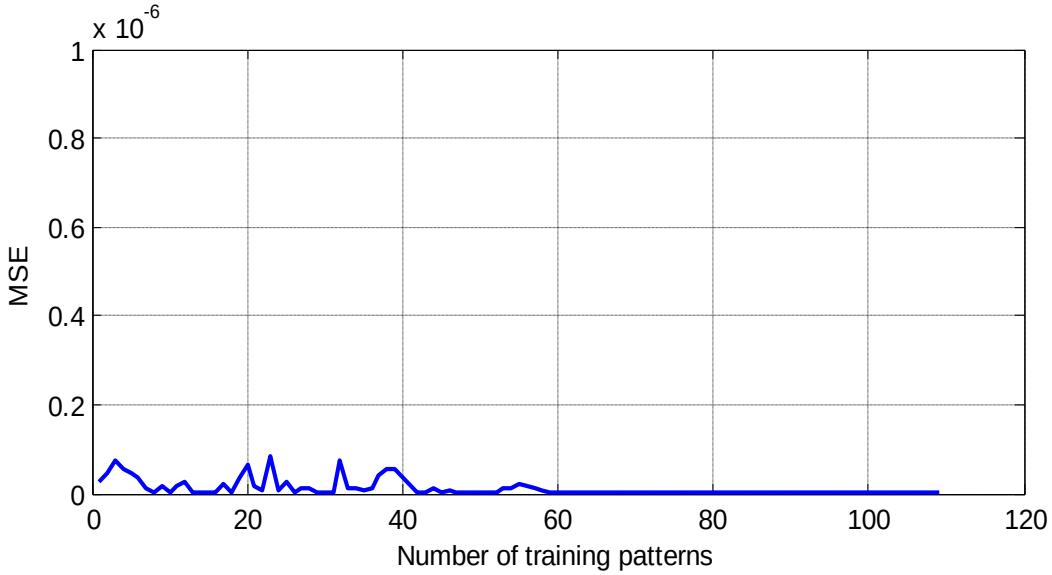


Fig. 5.4 Training MSE of forward model

### 5.2.2 Inverse Models

Inverse models are the neural network structure representing the inverse of the system dynamics. The inputs and outputs of the inverse model are shown in Fig. 5.5. In this work, reflux flow-rate (*R(k)*) and reboiler heat duty (*S(k)*) are the control actions. e(k) is the error between the desired output($x_{DSP}$) and the plant output ($x_D$(k+1)). The training, test and validation data set generated for the networks are similar to that used for forward modelling but with the different configuration as shown in Fig. 5.5. The structure to train the inverse model is shown in Fig. 5.6. Input and output of the NN inverse model are taken as give in Fig. 5.5. Levenberg-Marquardt algorithm is used for the training and given in Appendix-E.

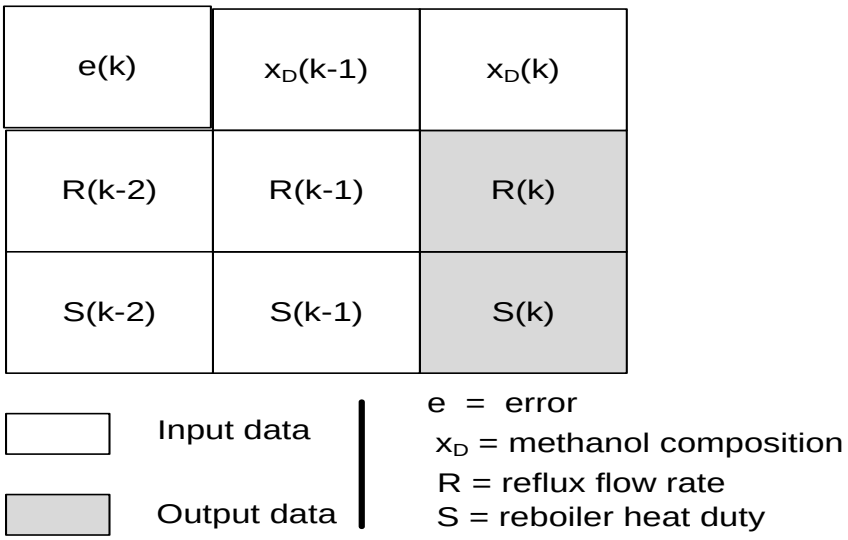


Fig. 5.5 Input and output data node assignment for BDC inverse model

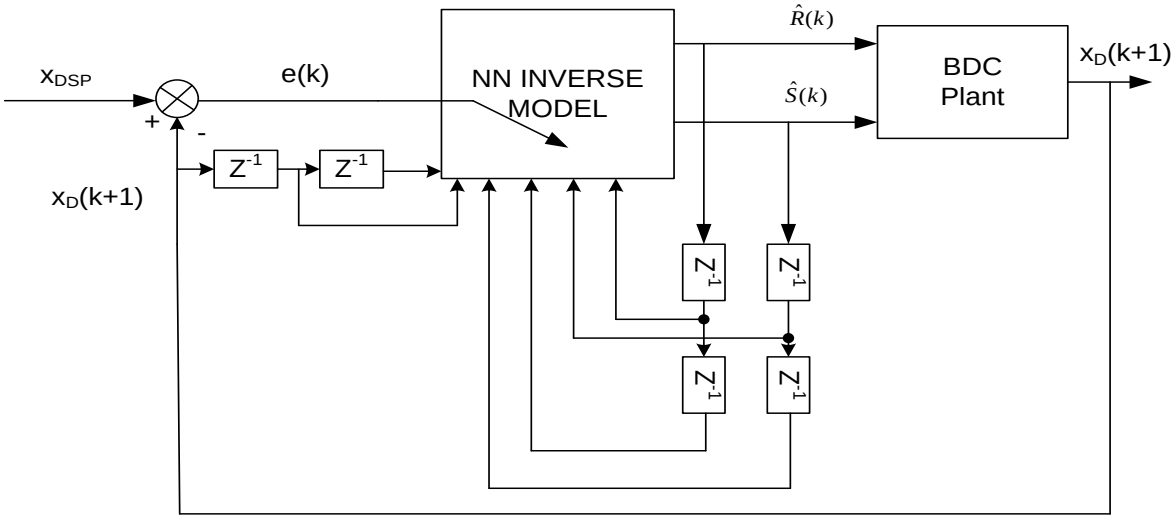


Fig. 5.6 Learning of inverse model

The details of ANN based inverse model is given in Table 5-3. Output of the NN-inverse model are reflux flow-rate and reboiler heat duty. These outputs are compared with the actual outputs as shown in Fig. 5.7 and Fig. 5.8 respectively.

Table 5-3 Network for inverse model

| | |
|---|---|
| Number of inputs | 7{e(k), R(k-1), R(k-2), S(k-1), S(k-2), $X_D$(k), $X_D$(k-1)} |
| Number of outputs | 2{ R(k), S(k)} |
| Number of training patterns | 120 |
| Network type | Feed-forward back-propagation |
| Training method | Levenberg-Marquardt method |
| Number of hidden layers | 1 |
| Number of hidden layer neurons | 14 |
| Transfer function of hidden layer | Tangent sigmoid |
| Number of epochs | 110 |
| Learning rate | 0.01 |
| MSE | $2x10^{-7}$(for reflux flow-rate),$1x10^{-7}$(for reboiler heat duty) |

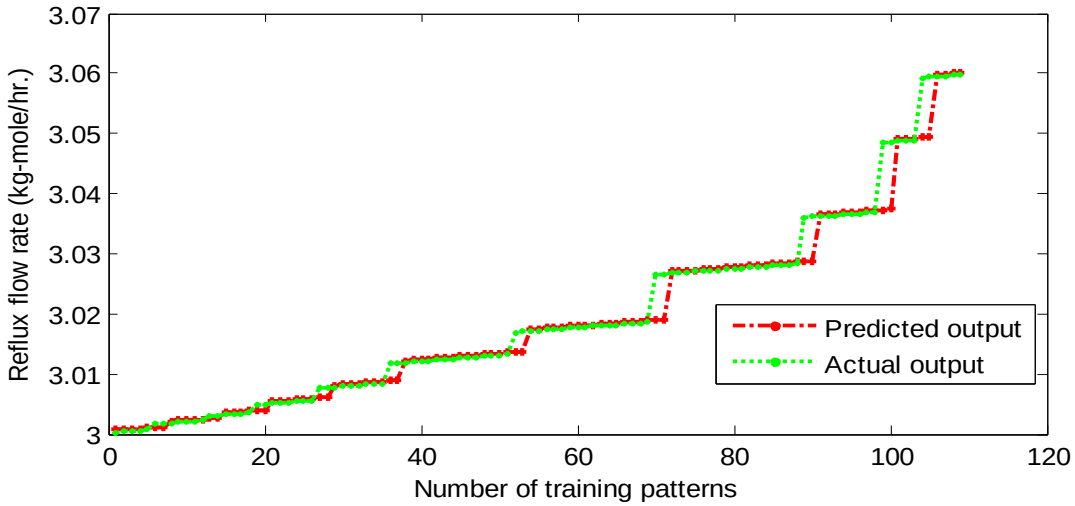


Fig. 5.7 Training performance of inverse model for reflux flow-rate

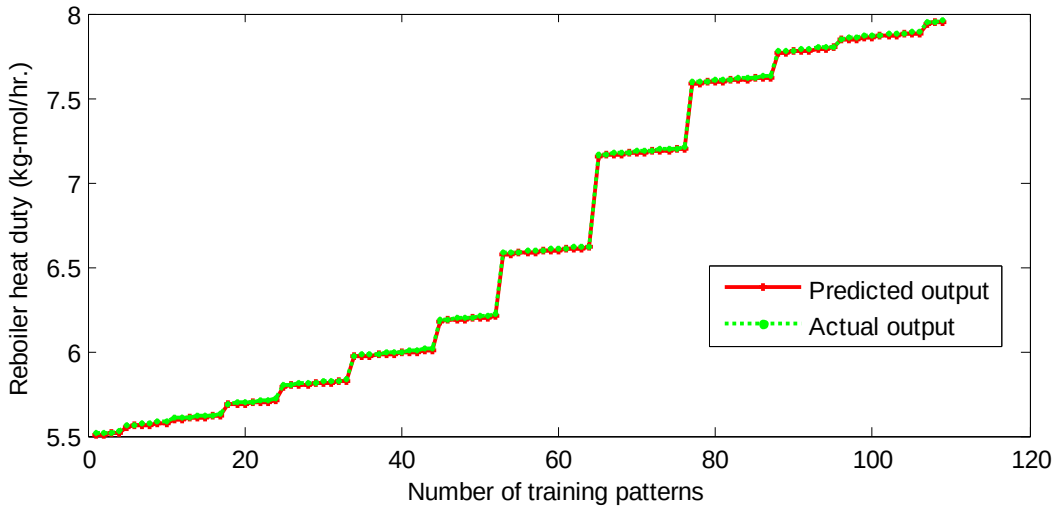


Fig. 5.8 Training performance of inverse model for reboiler heat duty

The MSE between the predicted output and actual output is shown in Fig. 5.9. The value of MSE is $2x10^{-7}$ and $1x10^{-7}$ for reflux flow-rate and reboiler heat duty respectively. It signifies that inverse model has been trained properly.

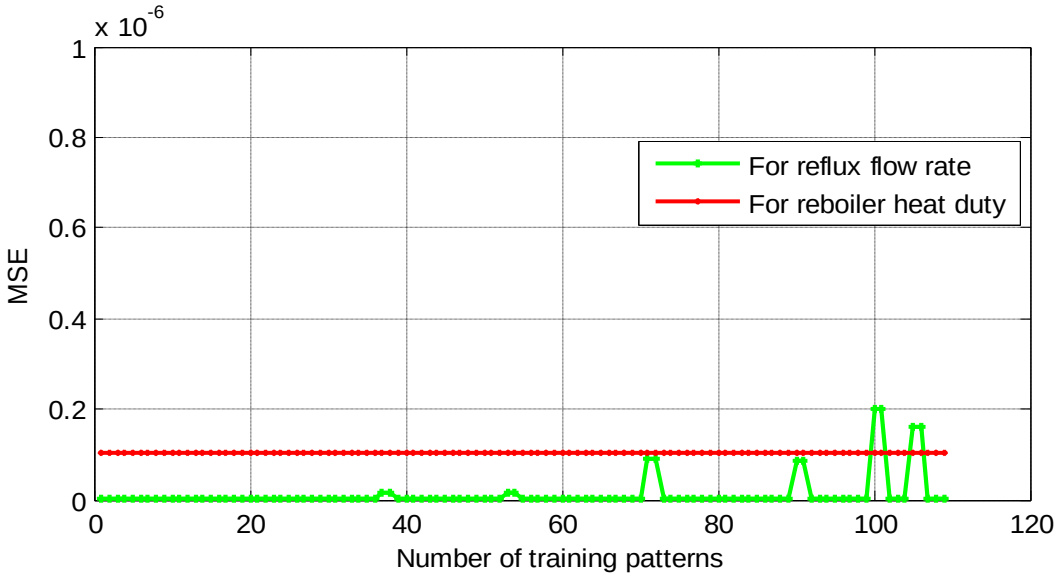


Fig. 5.9 Training MSE of inverse model

The forward and inverse models are utilized in the designing of ANN based Direct Inverse Control (NN-DIC) and ANN based Internal Model Control (NN-IMC) schemes as described in the following section.

### 5.3 ANN based Direct Inverse Control (NN-DIC)

Consider a system shown in the diagram below:

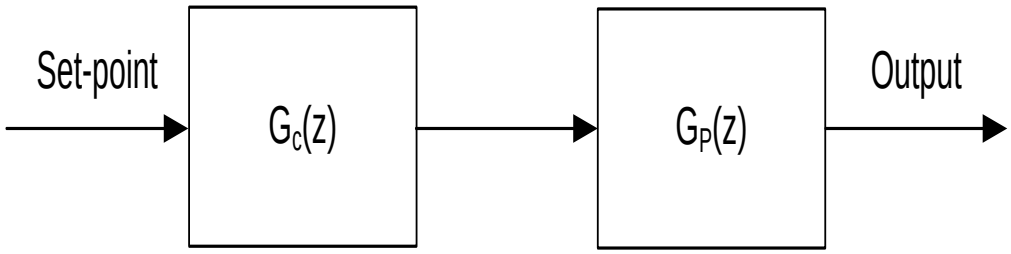


Fig. 5.10 Open loop control strategy

$G_C(z)$ is a controller used to control the process $G_P(z)$. Suppose $\tilde{G}_P(z)$ is a neural network model of $G_P(z)$. By setting $G_C(z)$ to be the inverse of the model of the process,

$$G_c(z) = \tilde{G}_P(z)^{-1}, \qquad 5.1$$

and if $G_P(z) = \tilde{G}_P(z)$, (the model is an exact representation of the process), then it is clear that the output will always be equal to the set-point. This ideal control performance is achieved without feedback. It shows that if the complete knowledge of the process is known then the perfect control can be achieved. The ANN based inverse model of the BDC has been used as the controller to determine the controlled input (reflux flow-rate and reboiler heat duty) to the actual plant. The complete scheme of NN-DIC is shown in Fig. 5.11.

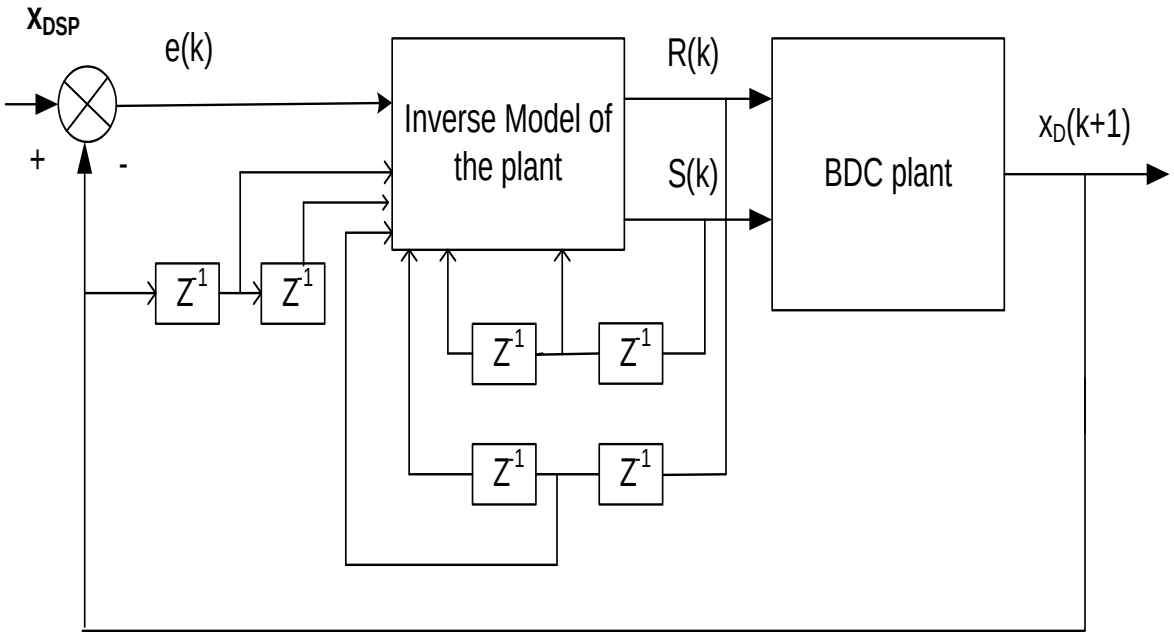


Fig. 5.11 Schematic diagram of NN-DIC scheme

The main limitations of the DIC scheme are:

(1) DIC does not work for systems with unstable inverse.

(2) DIC does not work when inverse models are not well-damped.

(3) DIC does not work when there is a lack of tuning options.

(4) DIC scheme has high sensitivity to disturbance & noise.

### 5.4 ANN based Internal Model Control (NN-IMC)

The problems of DIC approach can be eliminated using the Internal Model Control (IMC) approach. IMC is an extension of DIC scheme. IMC scheme has the general structure depicted in Fig. 5.12.

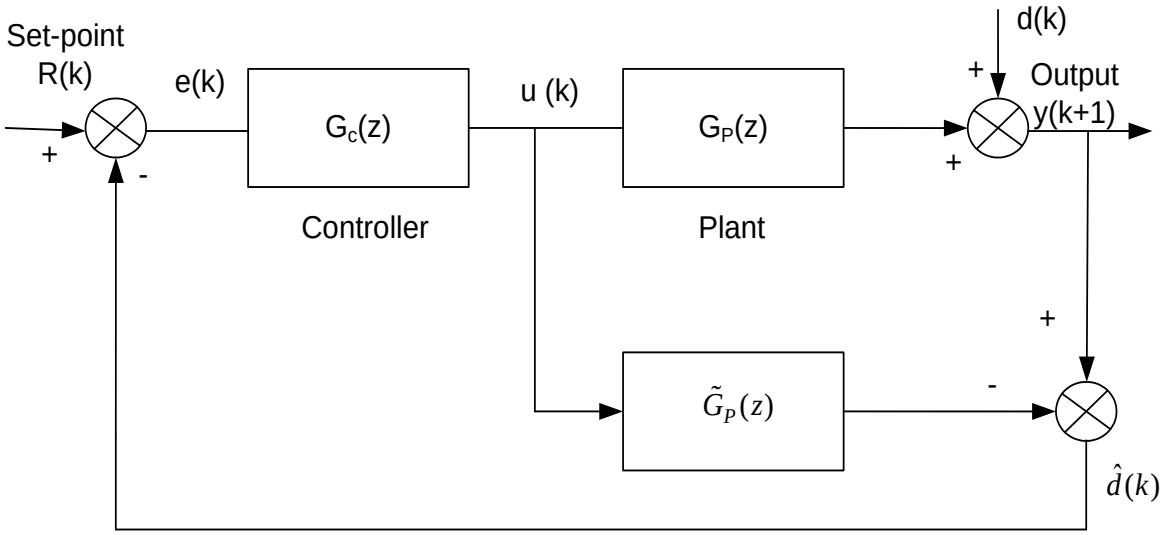


Fig. 5.12 The basic structure of IMC scheme

Where, d(k) is an unknown disturbance affecting the system. u(k) is the manipulated input to both the process and its model. The process output, y(k+1), is compared with the output of the model, resulting in a signal $\hat{d}(k)$. That is,

$$\hat{d}(k) = [G_P(z) - \tilde{G}_P(z)]U(k) + d(k) \qquad 5.2$$

- If d(k) is zero for example, then $\hat{d}(k)$ is a measure of the difference in behaviour between the process and its model.
- If $G_P(z) = \tilde{G}_P(z)$, then $\hat{d}(k)$ is equal to the unknown disturbance.

Thus $\hat{d}(k)$ may be regarded as the information that is missing in the model, $\tilde{G}_P(z)$, and can therefore be used to improve control. This is done by subtracting $\hat{d}(k)$ from the set-point *R(k),* which is very similar to affecting a set-point trim. The resulting control signal is given by,

$$U(k) = [R(k) - \hat{d}(k)]G_C(z) = \left\{R(k) - \left[G_P(z) - \tilde{G}_P(z)\right]U(k) - d(k)\right\}G_C(z) \qquad 5.3$$

Thus, $$U(k) = \frac{\left[R(k) - d(k)\right]G_C(z)}{1 + \left[G_P(z) - \tilde{G}_P(z)\right]G_C(z)} \qquad 5.4$$

Since

$$Y(k) = G_P(z)U(k) + d(k) \qquad 5.5$$

The closed loop transfer function for the IMC scheme is therefore

$$Y(k) = \frac{\left[R(k) - d(k)\right]G_C(z)G_P(z)}{1 + \left[G_P(z) - \tilde{G}_P(z)\right]G_C(z)} + d(k) \qquad 5.6$$

or, $$Y(k) = \frac{G_C(z)G_P(z)R(k) + \left[1 - G_C(z)\tilde{G}_P(z)\right]d(k)}{1 + \left[G_P(z) - \tilde{G}_P(z)\right]G_C(z)} \qquad 5.7$$

From this closed loop expression, it can be evident that if $G_C(z) = \tilde{G}_P(z)^{-1}$, and if $G_P(z) = \tilde{G}_P(z)$, then the perfect set-point tracking and disturbance rejection can be achieved. Notice that, theoretically, even if $G_P(z) \neq \tilde{G}_P(z)$, (Forward model), perfect disturbance rejection can still be realised provided $G_C(z) \neq \tilde{G}_P(z)^{-1}$, (Inverse model). In this work, $\tilde{G}_P(z)$ is the ANN based forward model of the BDC and $G_C(z)$ is the ANN based inverse model of the BDC. The complete scheme of NN-IMC for BDC is shown in Fig. 5.13.

The successful implementation of the NN-IMC approach relies on the accuracy of the forward and inverse models [62, 105]. NN-IMC scheme is capable to suppress the noisy measurements and high frequency disturbances whereas NN-DIC scheme can not handle such situations.

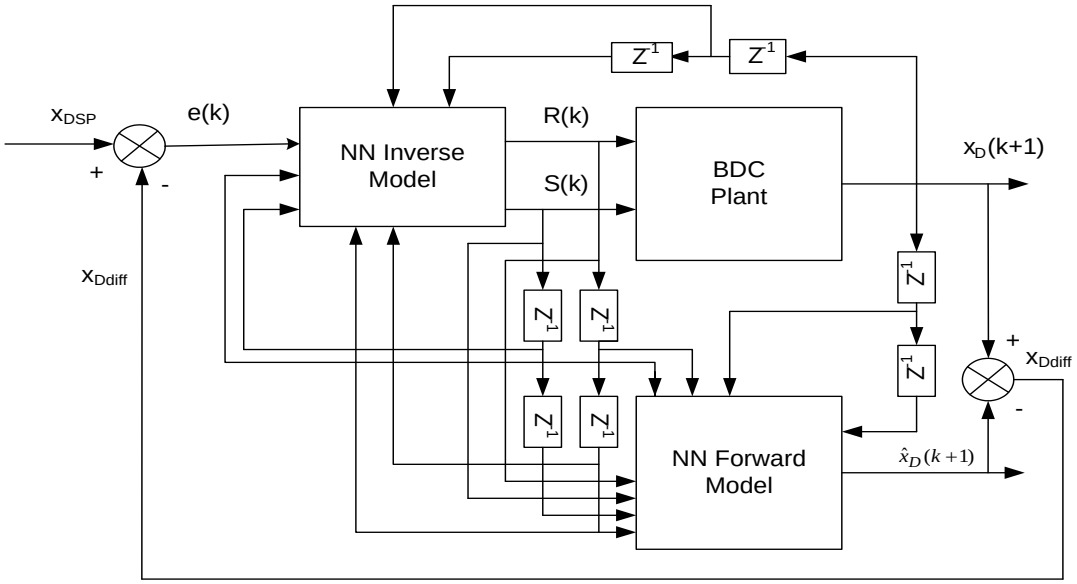


Fig. 5.13 Schematic of NN-IMC scheme

## 5.5 Simulation Results

The simulation studies have been carried out for two cases:

1. Reference tracking,
2. Disturbance rejection

### 5.5.1 Case a: Reference Tracking

Initially without any control of reflux flow and reboiler heat duty the output (methanol composition) of the BDC was 0.83 mole fraction. Now, the desired output has been set to 0.98 mole fraction and NN-DIC and NN-IMC schemes have been applied on BDC plant. The NN-DIC and NN-IMC schemes developed in the previous section are utilized in both the cases. The simulation studies have been carried out in MATLAB®/SIMULINK environment. Fig. 5.14 and 5.15 shows the output response of NN-DIC and NN-IMC schemes respectively.

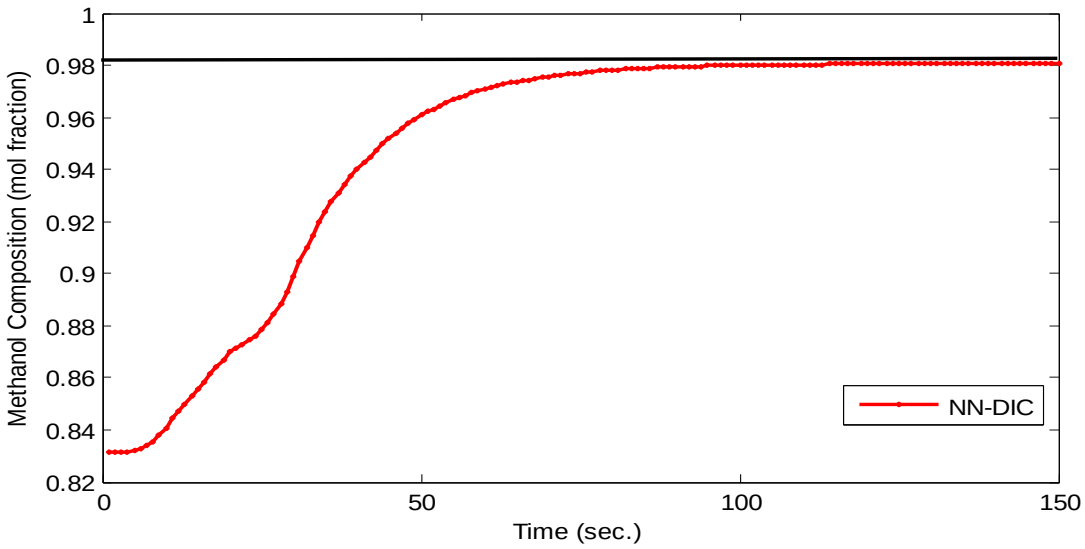


Fig. 5.14 Output of NN-DIC scheme

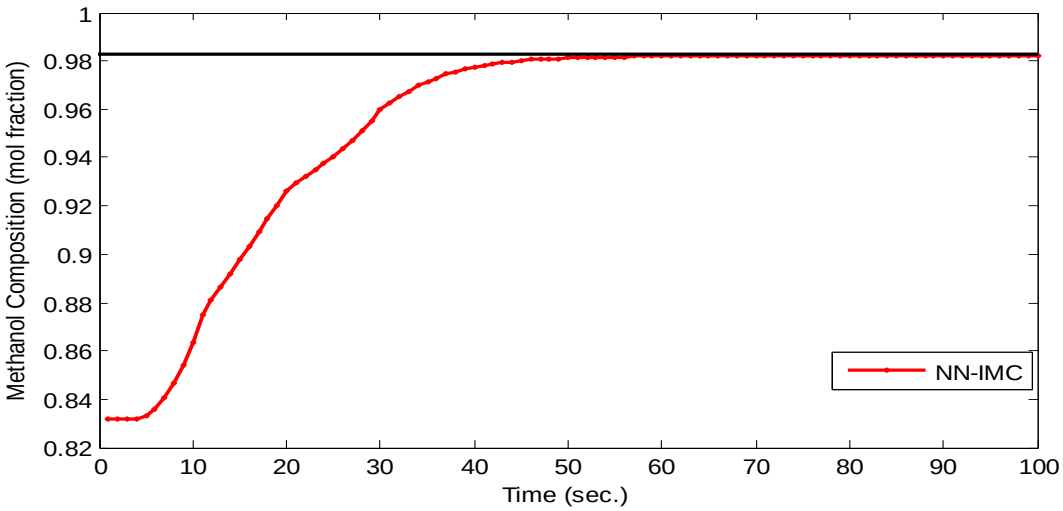


Fig. 5.15 Output of NN-IMC scheme

Outputs of these schemes have also been compared with the output of NN-MPC scheme (discussed in chapter 4) and shown in Fig. 5.16. Mean square error (MSE) obtained in all the schemes are compared in Fig. 5.17.

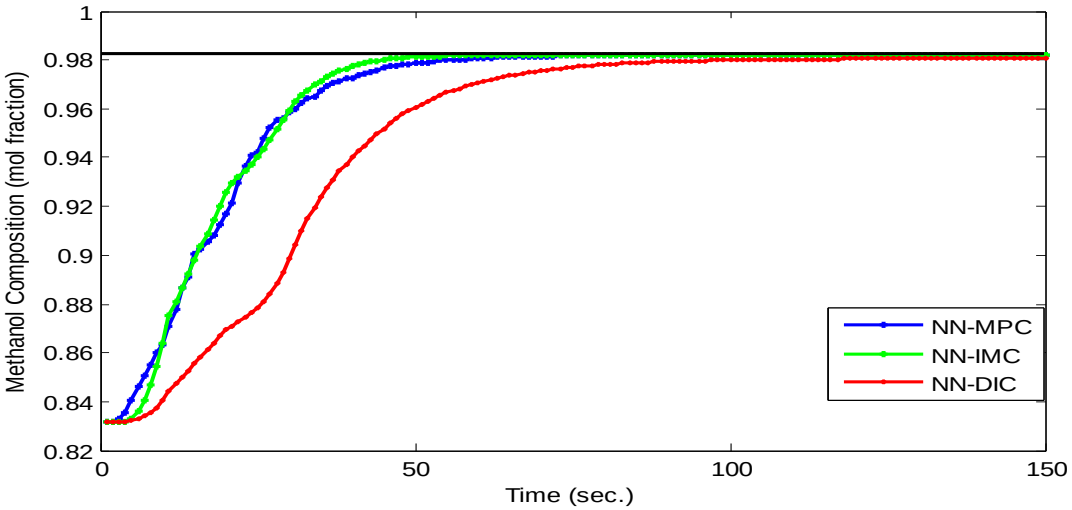


Fig. 5.16 Output of NN-DIC, NN-IMC and NN-MPC scheme for reference tracking

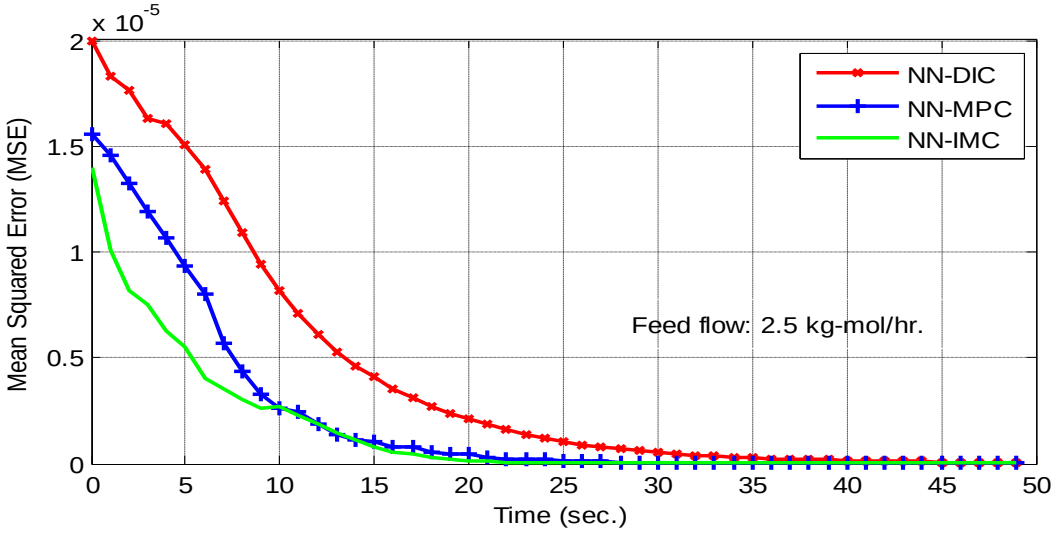


Fig. 5.17 MSE of control schemes for reference tracking

The performance parameters, rise time, settling time and MSE are given in Table 5-4. It is observed from the result that rise time, settling time and MSE reduces in NN-IMC scheme compared to other schemes.

### 5.5.2 Case b: Disturbance Rejection

To simulate this case, feed flow-rate has been increased by 10% (from 2.5 kg-mol/hr. to 2.75 kg-mole/hr.). This change is considered as a disturbance in the feed flow. The responses of NN-DIC and NN-IMC schemes have been obtained at set-point of 0.98 mole fraction and at given disturbance Fig. 5.18 shows the response of NN-DIC and NN-IMC scheme.

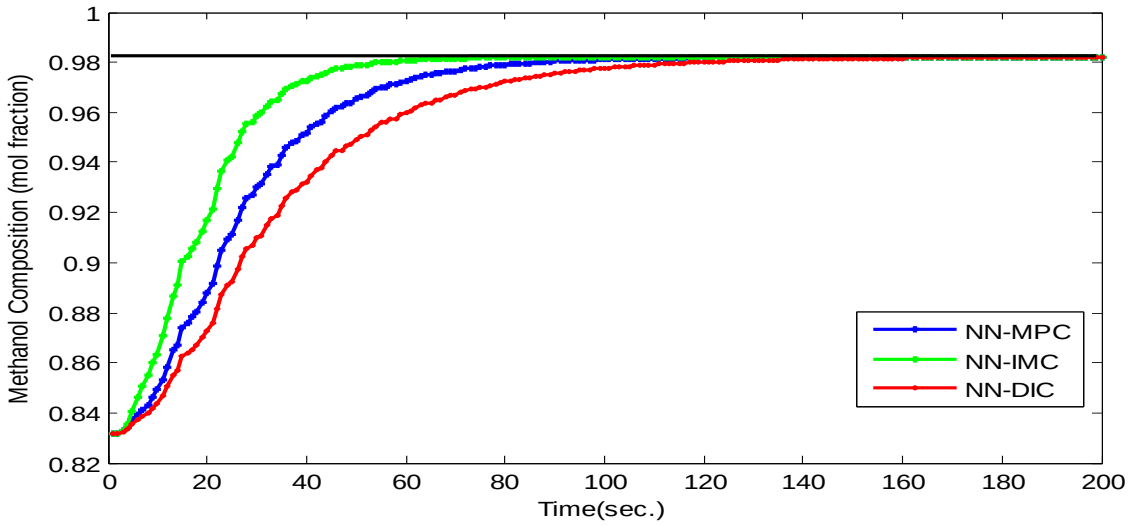


Fig. 5.18 Output of NN-DIC, NN-IMC and NN-MPC scheme for disturbance rejection

The outputs of these schemes are also compared with the output of NN-MPC scheme. Fig. 5.19 compares the MSE of all the three schemes. Table 5-4 compares the performance parameters (rise time, settling time and MSE) of all the three schemes.

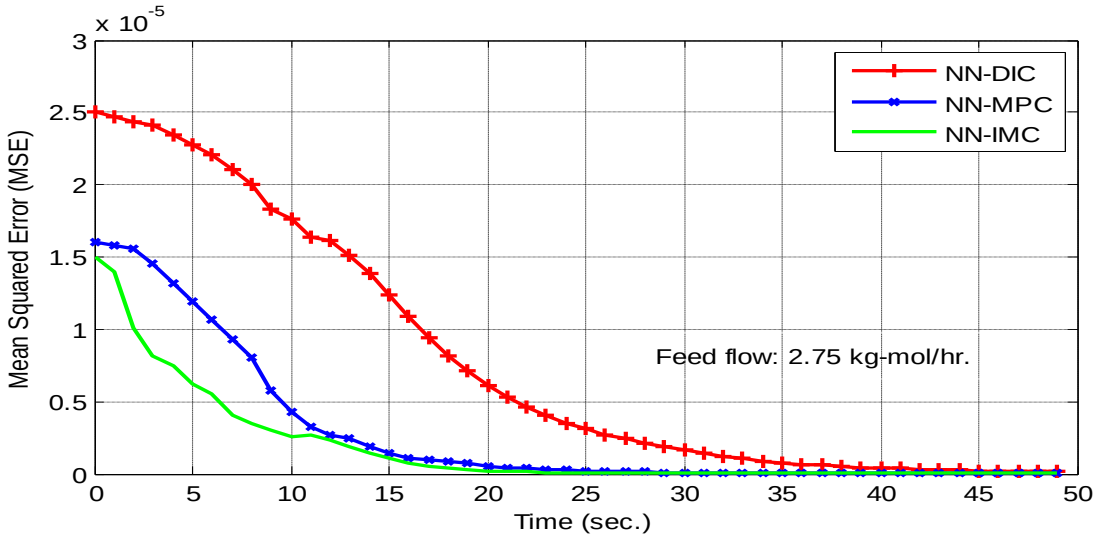


Fig. 5.19 MSE of control schemes for disturbance rejection

The superiority of the NN-IMC scheme over the NN-DIC scheme becomes evident in the disturbance rejection case. In both case studies, the NN-IMC works effectively compared to the other schemes as given in Table 5-4.

Table 5-4 Performance parameters of proposed schemes

| Performance parameters | Control schemes | | | | | |
|---|---|---|---|---|---|---|
| | Case 1: At Feed flow-rate= 2.5 kg-mol/hr | | | Case 2: At Feed flow-rate= 2.75 kg-mol/hr | | |
| | NN-DIC | NN-MPC | NN-IMC | NN-DIC | NN-MPC | NN-IMC |
| Rise time(sec.) | 50 | 31 | 30 | 60 | 45 | 35 |
| Settling time(sec.) | 105 | 70 | 52 | 150 | 110 | 85 |
| MSE | $2x10^{-5}$ | $1.55x10^{-5}$ | $1.4x10^{-5}$ | $2.5x10^{-5}$ | $1.6x10^{-5}$ | $1.5x10^{-5}$ |

## 5.6 Conclusion

In this chapter, ANN has been incorporated in the inverse-model control scheme in two different ways i.e. NN-DIC and NN-IMC methods. In NN-DIC scheme, ANN is used as the inverse model of the plant whereas; in NN-IMC approach, both the forward and inverse ANN models of the plant are used. These schemes are used to control the methanol composition in BDC. The two schemes are also compared with NN-MPC scheme on the basis of performance parameters (rise time, settling time and MSE). The performance of the schemes has been carried out for two cases (a) reference tracking (b) disturbance rejection. It is concluded by the results that in both case studies, the NN-IMC approach is more capable compared to other schemes to reject the disturbance.

# Chapter 6: ANFIS BASED CONTROL SCHEME FOR BINARY DISTILLATION COLUMN

*In this work, two ANFIS based controllers are designed to control the methanol composition in BDC by controlling the reflux flow-rate and reboiler heat duty. The performance of the proposed controller is compared with NN-IMC control scheme. The results obtained show the improvement in the settling time and MSE with ANFIS scheme as compared to the other schemes.*

## 6.1 Introduction

As described in the previous chapter, distillation is one of the most frequently used separation technique in the chemical and petroleum industries. Considering the complexity of nonlinear control problems, it is necessary to evaluate the performance of advance control techniques to overcome the shortcomings of conventional control schemes. In chapter 5, different Neural Network (NN) schemes have been evaluated to control the methanol composition in BDC. Among various kinds of industrial process control techniques, Adaptive Neuro-Fuzzy Inference System (ANFIS) is proposed in this work to control the methanol composition in BDC [87]. In ANFIS, ANN is incorporated in Fuzzy Inference System (FIS), which can use knowledge by learning algorithms of ANN. The learning capability is an advantage from the viewpoint of FIS and the formation of linguistic rule base is advantageous from the viewpoint of ANN. The literature review of ANFIS controller has been discussed in chapter 1.

The ANN based model of BDC (described in chapter 2) is utilized as the plant in ANFIS control scheme. Two separate ANFIS controllers have been designed to control the reflux flow and reboiler heat duty respectively.

## 6.2 Adaptive Neuro-Fuzzy Inference System

An intelligent system is a system that is able to make decisions by its own. Intelligent systems adapt themselves using some example situations (inputs of a system) and correct decisions for future situations [106]. Neural networks and Fuzzy systems are the examples of the artificial intelligent systems. Fuzzy systems provide a unified framework to represent incomplete information by taking into account the gradual or flexible nature of variables [107]. This is an alternative approach to classical method that is based on the observations that, humans think using linguistic terms such as “small” or “large” rather than crisp numerical values. Fuzzy systems work on conditional if-then rules. These fuzzy if then rules use fuzzy sets as linguistic terms in antecedent and conclusion parts and can be determined from human experts or can be generated from observed data. The fuzzy systems are advantageous in a way that it is easy to interpret knowledge in the rule base [89]. ANFIS constructs an input-output mapping based both on human knowledge (in the form of fuzzy rules) and on generated input-output data pairs (in the form of ANN). Neuro-Fuzzy systems have advantages over fuzzy systems because acquired knowledge is easy to understand.

ANFIS is one of the examples of Neuro-Fuzzy systems in which a FIS is implemented in the framework of adaptive neural networks. The basic structure of a FIS consists of three conceptual components: a *rule base,* which contains a selection of fuzzy rules, a *database,* which defines the membership functions used in the fuzzy rules, and a *reasoning mechanism,* which performs the inference procedure upon the rules and a given condition to derive a reasonable output or conclusion. ANFIS is based on Takagi–Sugeno FIS [108]. In Takagi-Sugeno FIS, the output of each rule is a linear combination of input variables plus a constant term. The final output is the weighted average of each rule's output. These weights can be determined utilizing the ANN training algorithm.

In distillation process, composition control is very important. A continuous column has to be operated as precisely as possible to meet the purity specifications. In this work, ANFIS controllers are designed to control the methanol composition in BDC.

### 6.3 Design of ANFIS control scheme for BDC

In a fuzzy control system selection of the range for each fuzzy set is a difficult task. For the best performance of a fuzzy controller, this range has to be tuned effectively. There is not an effective method in FIS for tuning Membership Functions (MF's) to minimize the output error and it is totally depends on human knowledge or experience. In ANFIS, using a given I/O data set, the ANFIS constructs a FIS whose MF's parameters are tuned to create the best IF-THEN rules. ANFIS architecture contains five layers. The first layer is 'fuzzification' layer and adapts the parameters for the chosen MF's. The second layer represents the IF conditions to set the rules. The output of the second layer is normalized in the third layer. In the fourth layer, premise and consequent parameters (explained later) are determined using ANN approach. Weighted sum output of rules is obtained in the fifth layer. In this work, ANFIS based controller is designed and used in an adaptive way in the distillation column control scheme as shown in Fig. 6.1. ANN based model for BDC is used as a real plant to design the ANFIS based controller.

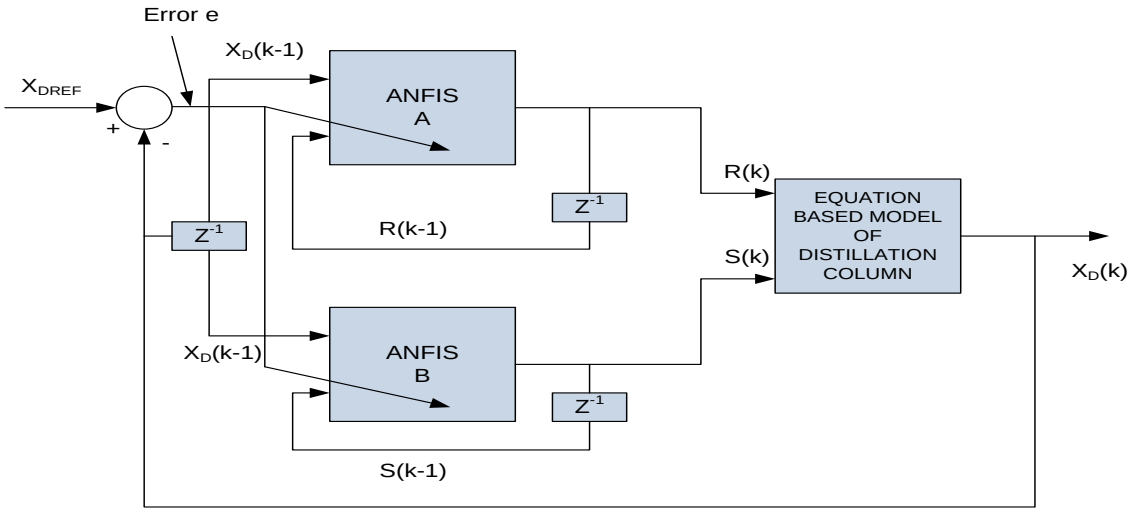


Fig. 6.1 ANFIS control scheme for BDC

Two separate ANFIS controllers namely: ANFIS A and ANFIS B are designed for the reflux flow-rate and the reboiler heat duty respectively. Each ANFIS controller has three inputs. The inputs to ANFIS A are plant output, $x_D(k-1)$, error (between the desired process output and measured process output), e(k-1); and; reflux flow-rate, R(k-1). All inputs are measured at previous sampling instant. The inputs to the controller ANFIS B are plant output, error (between the desired process output and measured process output), e(k-1); $x_D(k-1)$; and; reboiler heat duty, S(k-1).

ANFIS is a kind of neural network that is based on Takagi-Sugeno FIS. Since it integrates both neural networks and fuzzy logic principles, it has potential to capture the benefits of both in a single framework. The working and design of an ANFIS controller is explained in the following section.

### 6.3.1 Structure of ANFIS

To understand the ANFIS architecture, consider three fuzzy if-then rules based on first order Sugeno model:

Rule 1: If ($I_1$ is $A_1$) and ($I_2$ is $B_1$) and ($I_3$ is $C_1$) then ($f_1=p_1I_1+q_1I_2+r_1I_3+s_1$),

Rule 2: If ($I_1$ is $A_2$) and ($I_2$ is $B_2$) and ($I_3$ is $C_2$) then ($f_2=p_2I_1+q_2I_2+r_2I_3+s_2$),

Rule 3: If ($I_1$ is $A_3$) and ($I_2$ is $B_3$) and ($I_3$ is $C_3$) then ($f_3=p_3I_1+q_3I_2+r_3I_3+s_3$).

Where $I_1$, $I_2$ and $I_3$ are the inputs, $A_i$, $B_i$ and $C_i$ (i=1, 2, 3) are the fuzzy sets, $f_i$ are the outputs within the fuzzy region specified by the fuzzy rule. $p_i$, $q_i$, $r_i$ and $s_i$ are the design parameters or weights, called consequent parameters which are determined during the training process. In the proposed scheme, $I_1$, $I_2$ and $I_3$ inputs corresponds to $x_D(k-1)$, e(k-1) and R(k-1) which are fed to ANFIS A. For ANFIS B, $I_1$, $I_2$ and $I_3$ inputs corresponds to $x_D(k-1)$, e(k-1) and S(k-1). The control output is R(k) and S(k) for the proposed controllers ANFIS A and ANFIS B respectively.

The structure of ANFIS is shown in Fig. 6.2. In this figure $A_1$, $A_2$, $A_3$, $B_1$, $B_2$, $B_3$, $C_1$, $C_2$, $C_3$, Π, N and Z are called the nodes. A node is either, a fixed node, or an adaptive node. In Fig. 6.2, square node represents the adaptive node and circle node represents the fixed node. Symbol $Y_1^1$ means output signal of first node of first layer, where superscript corresponds to layer number and subscript to node number. Similarly other output signals are defined.

First layer of ANFIS have adaptive nodes. The outputs of layer 1 are the fuzzy membership grade of the inputs which are given by:

$Y_i^1 = \mu_{A_i}(I_1)$, for i={1,2,3}, $Y_j^1 = \mu_{B_j}(I_2)$, for j={1,2,3}, $Y_k^1 = \mu_{C_k}(I_3)$, for k={1,2,3}

Where $I_1$, $I_2$ and $I_3$ are inputs and $Y_i^1$, $Y_j^1$ and $Y_k^1$ are the Membership Functions of $A_i$, $B_j$, and $C_k$ respectively.

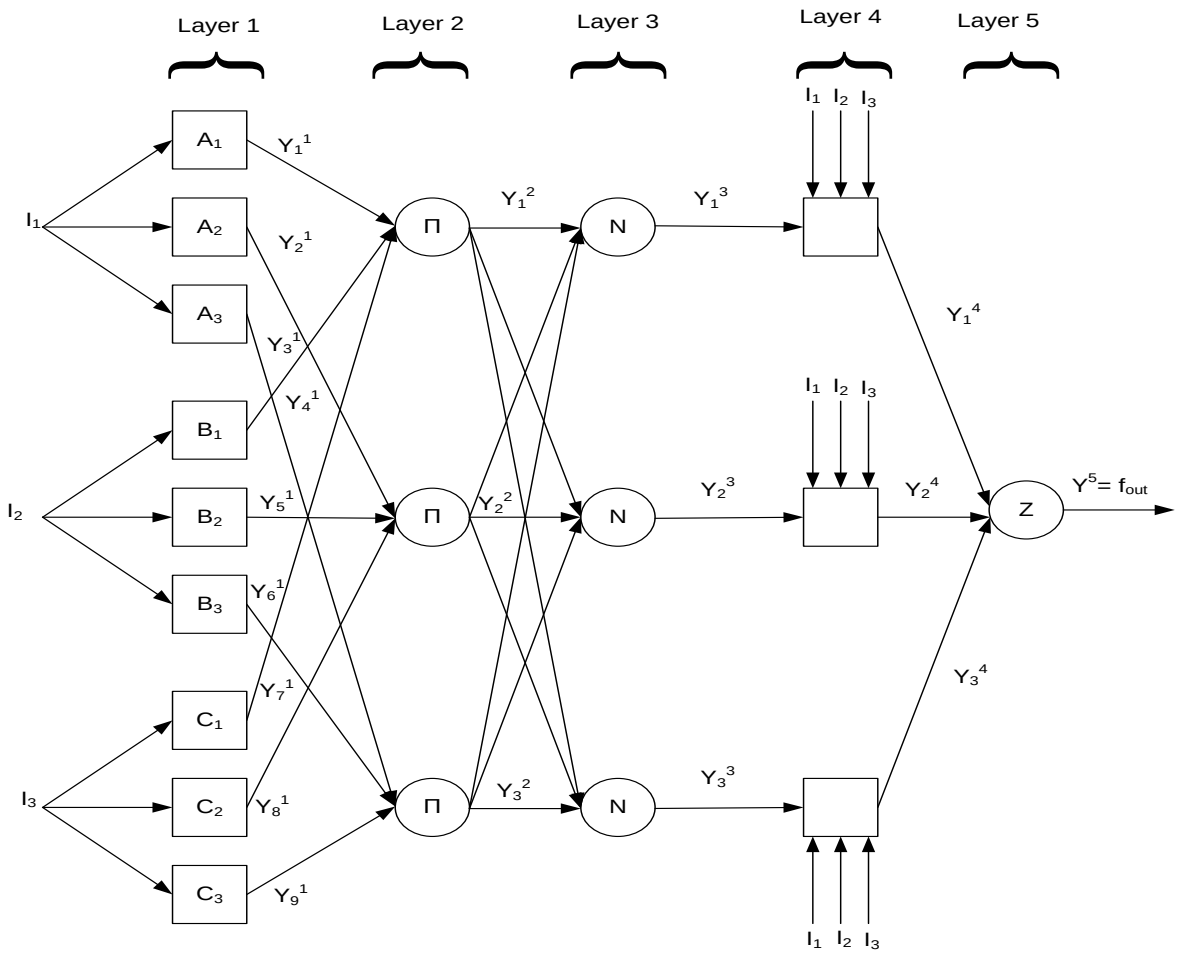


Fig. 6.2 Architecture of ANFIS

In this work, for each input, three Gaussian fuzzy sets (named 'small', 'medium' and 'large') have been considered as shown in Fig. 6.3. Where c is the centre of the corresponding fuzzy set; and σ is the half-width.

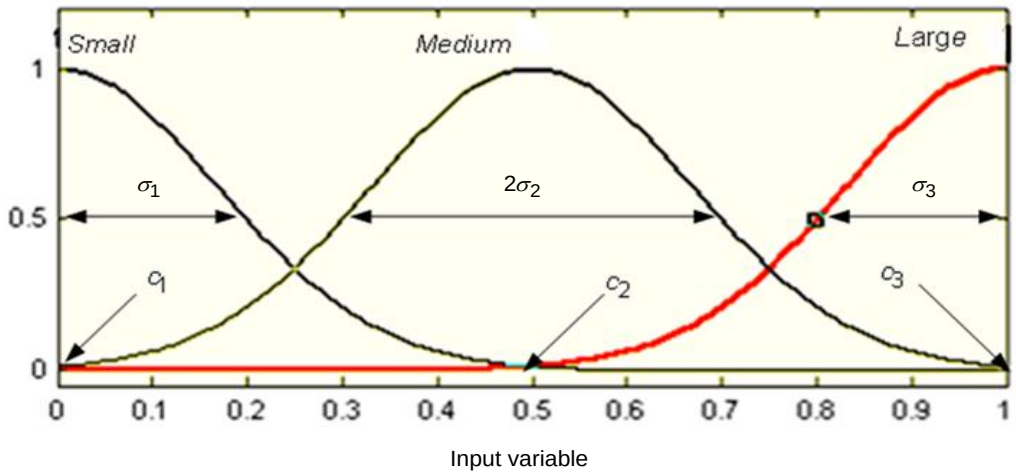


Fig. 6.3 Gaussian Membership Function

For each input, membership grade can be determined in the following manner. $\mu_{A_i}(I_1)$ , $\mu_{A_i}(I_2)$ and $\mu_{A_i}(I_3)$ are the membership grades for inputs $I_1$, $I_2$ and $I_3$ respectively.

$$\mu_{A_i}(I_1) = e^{-\frac{(I_1 - c_i)^2}{2\sigma_i{}^2}} \quad 6.1$$

$$\mu_{B_j}(I_2) = e^{-\frac{(I_2 - c_j)^2}{2\sigma_j{}^2}} \quad 6.2$$

$$\mu_{C_k}(I_3) = e^{-\frac{(I_3 - c_k)^2}{2\sigma_k{}^2}} \quad 6.3$$

Where $c_i, c_j, c_k, \sigma_i, \sigma_j$ and $\sigma_k$ are called as premise parameters. These parameters are depending on the shape of membership function.

Second layer has fixed nodes Π, indicating that they are simple multiplier nodes. Outputs of this layer are also called the firing strength, and represented as:

$$Y_1^2 = \mu_{A_i}(I_1) \bullet \mu_{B_j}(I_2) \bullet \mu_{C_k}(I_3), \text{ i=1 \& j=4 \& k=7} \quad 6.4$$

$$Y_2^2 = \mu_{A_i}(I_1) \bullet \mu_{B_j}(I_2) \bullet \mu_{C_k}(I_3), \text{ i=2 \& j=5 \& k=8} \quad 6.5$$

$$Y_3^2 = \mu_{A_i}(I_1) \bullet \mu_{B_j}(I_2) \bullet \mu_{C_k}(I_3), \text{ i=3 \& j=6 \& k=9} \quad 6.6$$

In third layer, nodes are also fixed nodes lebeled with N. This layer normalizes the output of previous layer. Outputs of third layer are called the normalized firing strengths, and represented as:

$$Y_l^3 = \frac{Y_l^2}{Y_l^2 + Y_2^2 + Y_3^2}, l = 1,2,3 \quad 6.7$$

The fourth layer nodes are adaptive nodes. The output of each node in this layer is simply the product of the normalized firing strength and a first order polynomial (for a first order Sugeno model). The outputs of this layer are given by:

$$\begin{aligned} Y_l^4 &= Y_l^3 f_l \\ &= Y_l^3 (p_l 1_1 + q_l I_2 + r_l I_3 + s_l), l = 1,2,3 \end{aligned} \quad 6.8$$

Where, $p_l$, $q_l$, $r_l$ and $s_l$ are the consequent parameters. The fifth layer node is a single fixed node labelled 'Z'. This node performs the summation of all incoming signals. The output of this node is given by:

$$\begin{aligned} Y^5 &= \sum_l^3 Y_l^3 f_l \\ &= \frac{\sum_l^3 Y_l^2 (p_l I_1 + q_l I_2 + r_l I_3 + s_l)}{Y_l^2 + Y_2^2 + Y_3^2} \\ &= f_{out} \end{aligned} \quad 6.9$$

In ANFIS architecture first layer has two variables $\{c_i, \sigma_i; c_j, \sigma_j; c_k, \sigma_k\}$ for each input, which are related to the input membership functions and called premise parameters. Fourth

layer has four variables $\{p_i, q_i, r_i, s_i; p_j, q_j, r_j, s_j; p_k, q_k, r_k, s_k\}$ for each normalized input, pertaining to the first order polynomial, which are known as consequent parameters. The learning algorithm determines the premise and consequent parameters and discussed in the following section.

### 6.3.2 Learning Algorithm of ANFIS

The objective of the learning algorithm for ANFIS architecture is to determine the best value for premise and consequent parameters to make the ANFIS output match the training data. When the premise parameters $\{c_i, \sigma_i; c_j, \sigma_j; c_k, \sigma_k\}$ of the membership functions are fixed, the output of the ANFIS controller can be written as:

$$\begin{aligned} f_{out} &= Y_1^3 f_1 + Y_2^3 f_2 + Y_3^3 f_3 \\ &= Y_1^3 (p_1 I_1 + q_1 I_2 + r_1 I_3 + s_1) \\ &+ Y_2^3 (p_2 I_1 + q_2 I_2 + r_2 I_3 + s_2) \\ &+ Y_3^3 (p_3 I_1 + q_3 I_2 + r_3 I_3 + s_3) \end{aligned} \quad 6.10$$

$$\begin{aligned} f_{out} = &(Y_1^3 I_1) p_1 + (Y_1^3 I_2) q_1 + (Y_1^3 I_3) r_1 + (Y_1^3) s_1 \\ &+ (Y_2^3 I_1) p_2 + (Y_2^3 I_2) q_2 + (Y_2^3 I_3) r_2 + (Y_2^3) s_2 \\ &+ (Y_3^3 I_1) p_3 + (Y_3^3 I_2) q_3 + (Y_3^3 I_3) r_3 + (Y_3^3) s_3 \end{aligned} \quad 6.11$$

This is a linear combination of the consequent parameters $\{p_1, q_1, r_1, s_1; p_2, q_2, r_2, s_2; p_3, q_3, r_3, s_3\}$. The optimal value of these parameters can be obtained by using any optimal approach. The hybrid learning algorithm is used to determine the ANFIS parameters. Hybrid learning algorithm combines the gradient method and the least square estimation (LSE) to determine these parameters. The output of ANFIS can be written as the following matrix format for $n$ number of training samples.

$$[f] = [B][X] \quad 6.12$$

Where

$$[f] = \begin{bmatrix} f_{out1} \\ f_{out2} \\ . \\ . \\ f_{outn} \end{bmatrix}, [X] = \begin{bmatrix} p_1 & q_1 & r_1 & s_1 & p_2 & q_2 & r_2 & s_2 & p_3 & q_3 & r_3 & s_3 \end{bmatrix}^T \text{ and,}$$

$$[B] = \begin{bmatrix} \left(Y_1^3 I_1\right)_1 & \left(Y_1^3 I_2\right)_1 & \left(Y_1^3 I_3\right)_1 & Y_1^3 & \left(Y_2^3 I_1\right)_1 & \left(Y_2^3 I_2\right)_1 & \left(Y_2^3 I_3\right)_1 & Y_2^3 & \left(Y_3^3 I_1\right)_1 & \left(Y_3^3 I_2\right)_1 & \left(Y_3^3 I_3\right)_1 & Y_3^3 \\ \left(Y_1^3 I_1\right)_2 & \left(Y_1^3 I_2\right)_2 & \left(Y_1^3 I_3\right)_2 & Y_1^3 & \left(Y_2^3 I_1\right)_2 & \left(Y_2^3 I_2\right)_2 & \left(Y_2^3 I_3\right)_2 & Y_2^3 & \left(Y_3^3 I_1\right)_2 & \left(Y_3^3 I_2\right)_2 & \left(Y_3^3 I_3\right)_2 & Y_3^3 \\ \vdots & \vdots & \vdots & \vdots & \vdots & \vdots & \vdots & \vdots & \vdots & \vdots & \vdots & \vdots \\ \left(Y_1^3 I_1\right)_n & \left(Y_1^3 I_2\right)_n & \left(Y_1^3 I_3\right)_n & Y_1^3 & \left(Y_2^3 I_1\right)_n & \left(Y_2^3 I_2\right)_n & \left(Y_2^3 I_3\right)_n & Y_2^3 & \left(Y_3^3 I_1\right)_n & \left(Y_3^3 I_2\right)_n & \left(Y_3^3 I_3\right)_n & Y_3^3 \end{bmatrix} \quad 6.13$$

Where $[X]$ is an unknown matrix, whose elements come from the consequent parameters set. This is a standard linear least squares problem, so The LSE of *X,* X*, is the best solution which minimizes the squared error $|f - BX|^2$

$$X^* = (B^T B)^{-1} B^T f \qquad 6.14$$

Where $B^T$ is the transpose of *B* and $B^{-1}$ is the inverse of *B.* Now the Gradient method and the LSE method are combined to update the parameters in an adaptive network. For hybrid learning, each epoch is composed of a forward pass and a backward pass. In the forward pass, after an input vector is presented, the node outputs in the network are determined layer by layer until a corresponding row in the matrices $[f]$ and $[B]$ in (6.12) are obtained. This process is repeated for all the training data entries to form the complete $[f]$ and $[B]$ *;* then consequent parameters are determined by using Equ. 6.14. After the consequent parameters are identified, the measured error (between the desired methanol composition and measured methanol composition) is computed for each training data entry. In the backward pass, the error signals are propagated from the output end to the input end; the gradient vector is accumulated for each training data entry. At the end of the backward pass for all training data, the premise parameters are updated by the gradient method. In the gradient method, the error between the desired target and measured output is utilized. The error in the output of distillation column is $e = x_{Dref} - x_D$.

The error function, to be optimized is

$$E = \frac{1}{2} e^2 = \frac{1}{2} (x_{Dref} - x_D)^2 = E(\alpha) \qquad 6.15$$

Where 'α' can take any value from the premise parameters set i.e. α may be either $c_i$ or $\sigma_i$ , Cost function gradient δE/δα is determined by applying the chain rule to find the value of the parameter 'α' as

$$\frac{\partial E}{\partial \alpha} = \frac{\partial E}{\partial e} . \frac{\partial e}{\partial x_D} . \frac{\partial x_D}{\partial u} . \frac{\partial u}{\partial \alpha} \qquad 6.16$$

$$\frac{\partial E}{\partial \alpha} = -(x_{Dref} - x_D) . \frac{\partial x_D}{\partial u} . \frac{\partial u}{\partial \alpha} \qquad 6.17$$

Where $\frac{\partial x_D}{\partial u}$ is the plant Jacobian; u(k) is controller output; Reflux flow (R(k)) and reboiler heat duty (S(k)) are the controller outputs for ANFIS A and ANFIS B respectively. To minimize the error, the parameter change should be in the negative direction. Therefore,

$$\Delta \alpha = -\eta \frac{\partial E}{\partial \alpha} \qquad 6.18$$

Adaptation formula for the parameter $\alpha$ is calculated as

$$\alpha(k) = \alpha(k-1) + \Delta\alpha \qquad 6.19$$

From (6.18) and (6.19)

$$\alpha(k) = \alpha(k-1) - \eta \frac{\partial E}{\partial \alpha} \qquad 6.20$$

Where, η is the learning rate. Learning rate is the training parameter that controls the size of weight and bias changes during learning. All parameters in the controller are adapted according to (6.20). Table 6-1 summarizes the activities in each pass.

Table 6-1 Hybrid learning procedure in ANFIS

| - | Forward Pass | Backward Pass |
|---|---|---|
| Premise Parameters | Fixed | Gradient Descent |
| Consequent Parameters | Least Square Estimate | Fixed |
| Signals | Node Outputs | Error Signals |

### 6.3.3 Training and Testing of ANFIS Controller

In this work, the training data set is acquired from the experimental set-up of BDC. The training data set should include data for each process variable ($x_D$(k-1), e(k-1), R(k-1) and S(k-1)), evenly distributed throughout the operational range including the maximum and minimum values of input-output variables. The range of inputs and output is given in Table 5-1 in chapter 5. The data for the training of the ANFIS are sampled at interval of 5 seconds and 2508 data sets have been collected. This frequency is fast enough to capture the system dynamics for training of the ANFIS controllers. Out of total 2508 data samples, 2048 data samples are used for the training purpose (each input and output containing 512 samples). Remaining 460 data samples are used for testing (each input and output containing 115 samples). Gaussian membership functions are used for all the input variables. Each input is labelled with three linguistic variables Small (S), Medium (M) and Large (L). Table 6-2 lists the linguistic labels and the corresponding premise parameters.

Table 6-2 Initial Premise parameters

| ANFIS | Inputs | Linguistic label | c | σ | ANFIS | Inputs | Linguistic label | c | σ |
|---|---|---|---|---|---|---|---|---|---|
| ANFIS A | $I_1$ | Small | 0.83 | 0.08 | ANFIS B | $I_1$ | Small | 0.83 | 0.08 |
| | | Medium | 0.91 | 0.08 | | | Medium | 0.91 | 0.08 |
| | | Large | 0.99 | 0.08 | | | Large | 0.99 | 0.08 |
| | $I_2$ | Small | -0.40 | 0.50 | | $I_2$ | Small | -0.40 | 0.50 |
| | | Medium | 0.15 | 0.55 | | | Medium | 0.10 | 0.50 |
| | | Large | 0.70 | 0.60 | | | Large | 0.70 | 0.50 |
| | $I_3$ | Small | 3.00 | 0.03 | | $I_3$ | Small | 5.50 | 1.25 |
| | | Medium | 3.03 | 0.02 | | | Medium | 6.75 | 1.05 |
| | | Large | 3.06 | 0.03 | | | Large | 8.00 | 1.25 |

With these values the training and the testing of ANFIS controllers have been performed. Fig. 6.4 shows the performance of ANFIS A for training data. The output of

ANFIS A with testing data is shown in Fig. 6.5. The root mean square error (RMSE) of ANFIS A for testing data is shown in Fig. 6.6.

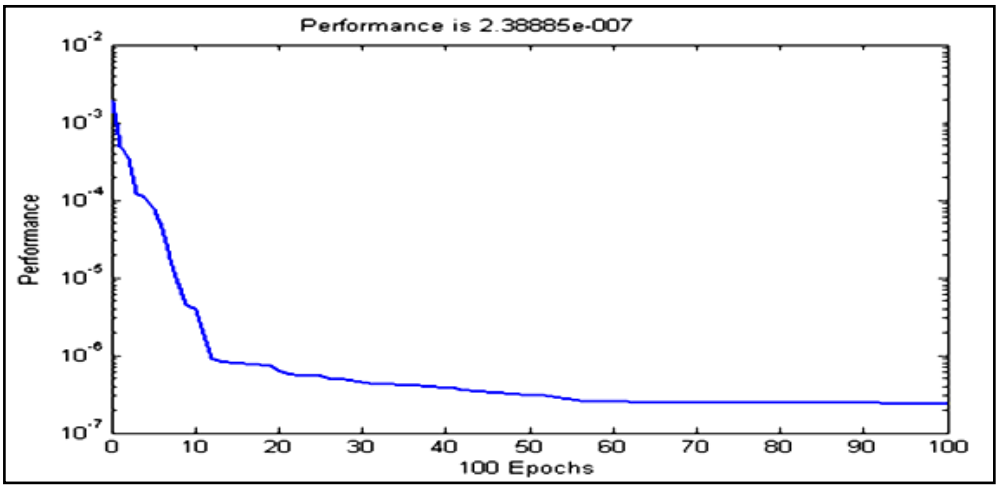


Fig. 6.4 Training performance of ANFIS A

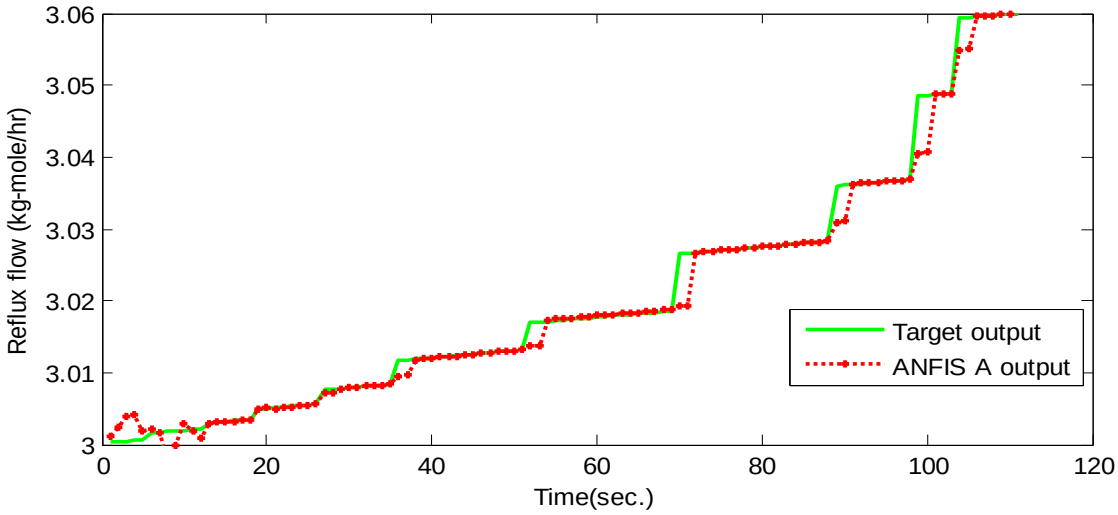


Fig. 6.5 Output of ANFIS A for testing data

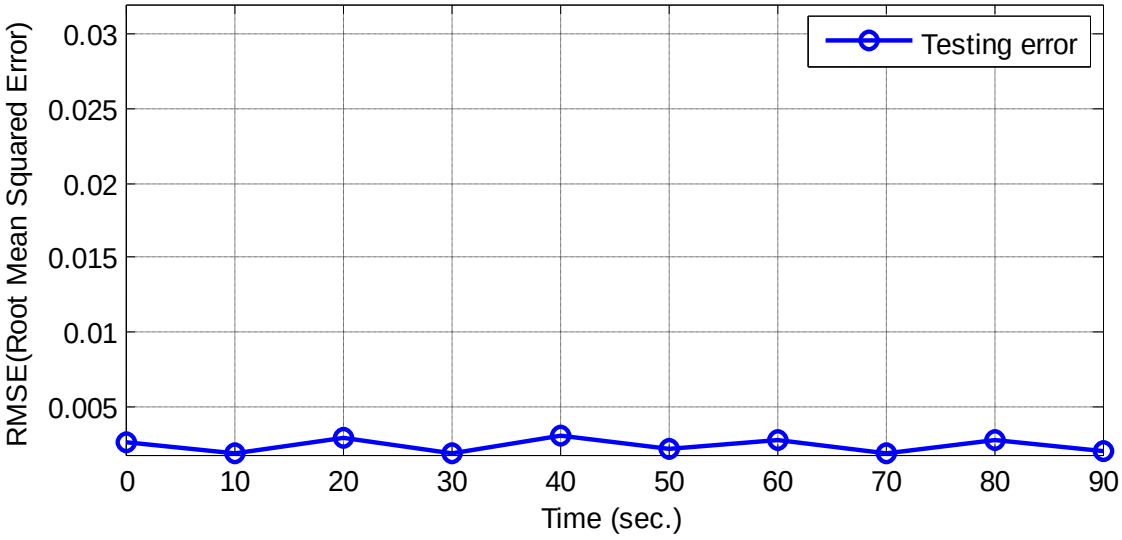


Fig. 6.6 RMSE of ANFIS A for testing data

Similarly the training and testing for ANFIS B is performed. The training performance for ANFIS B is shown in Fig. 6.7. The output of ANFIS B with testing data is shown in Fig. 6.8. The root mean square error (RMSE) of ANFIS B for testing data is shown in Fig. 6.9.

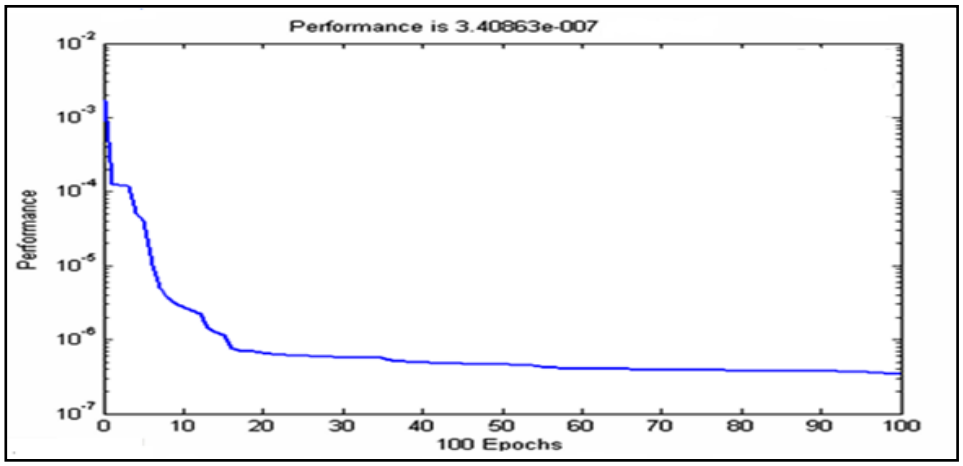


Fig. 6.7 The training performance of ANFIS B

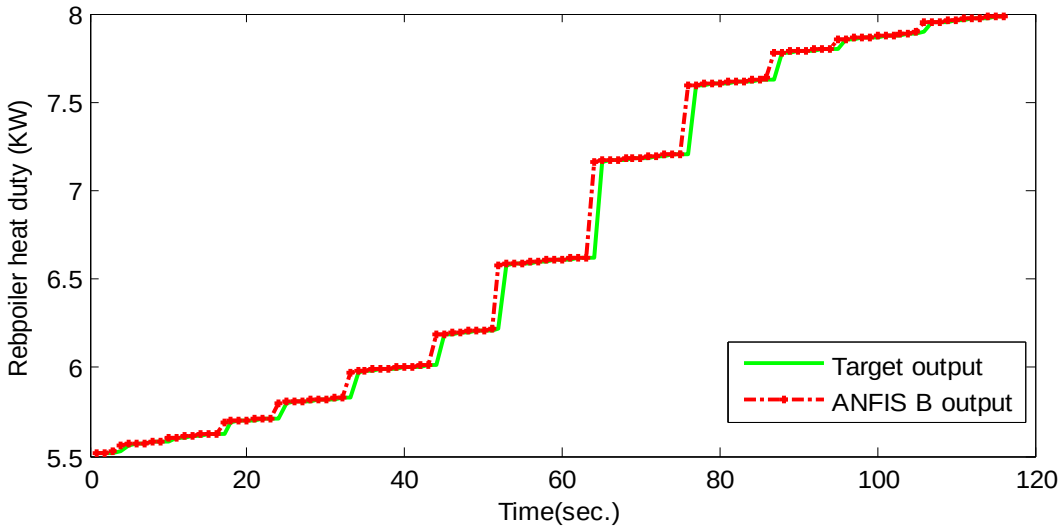


Fig. 6.8 Output of ANFIS B for testing data

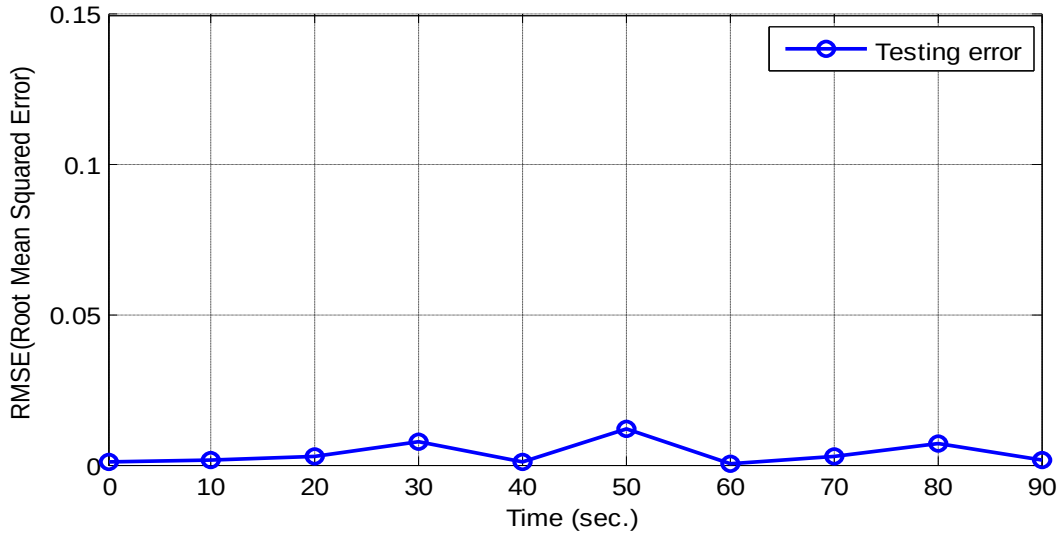


Fig. 6.9 RMSE of ANFIS B for testing data

Hybrid learning algorithm described in section 6.3.2 has been used to determine the best value of premise and consequent parameters. The initial premise parameters given in Table 6-2 has been modified after learning and given in Table 6-3.

Table 6-3 Premise Parameters after Learning

| ANFIS | Inputs | Linguistic label | c | σ | ANFIS | Inputs | Linguistic label | c | σ |
|---|---|---|---|---|---|---|---|---|---|
| ANFIS A | $I_1$ | Small | 0.818 | 0.04 | ANFIS B | $I_1$ | Small | 0.83 | 0.08 |
| | | Medium | 0.90 | 0.06 | | | Medium | 0.91 | 0.08 |
| | | Large | 0.95 | 0.08 | | | Large | 0.99 | 0.08 |
| | $I_2$ | Small | -0.40 | 0.55 | | $I_2$ | Small | -0.40 | 0.50 |
| | | Medium | 0.10 | 0.50 | | | Medium | 0.15 | 0.60 |
| | | Large | 0.43 | 0.40 | | | Large | 0.70 | 0.55 |
| | $I_3$ | Small | 3.00 | 0.03 | | $I_3$ | Small | 5.50 | 1.25 |
| | | Medium | 3.035 | 0.01 | | | Medium | 6.75 | 1.25 |
| | | Large | 3.06 | 0.03 | | | Large | 8.00 | 1.25 |

The shape of the fuzzy sets considered initially has also been modified due to change in premise parameters. Initial and final shape of fuzzy sets for each input of ANFIS A is shown in Fig. 6.10.

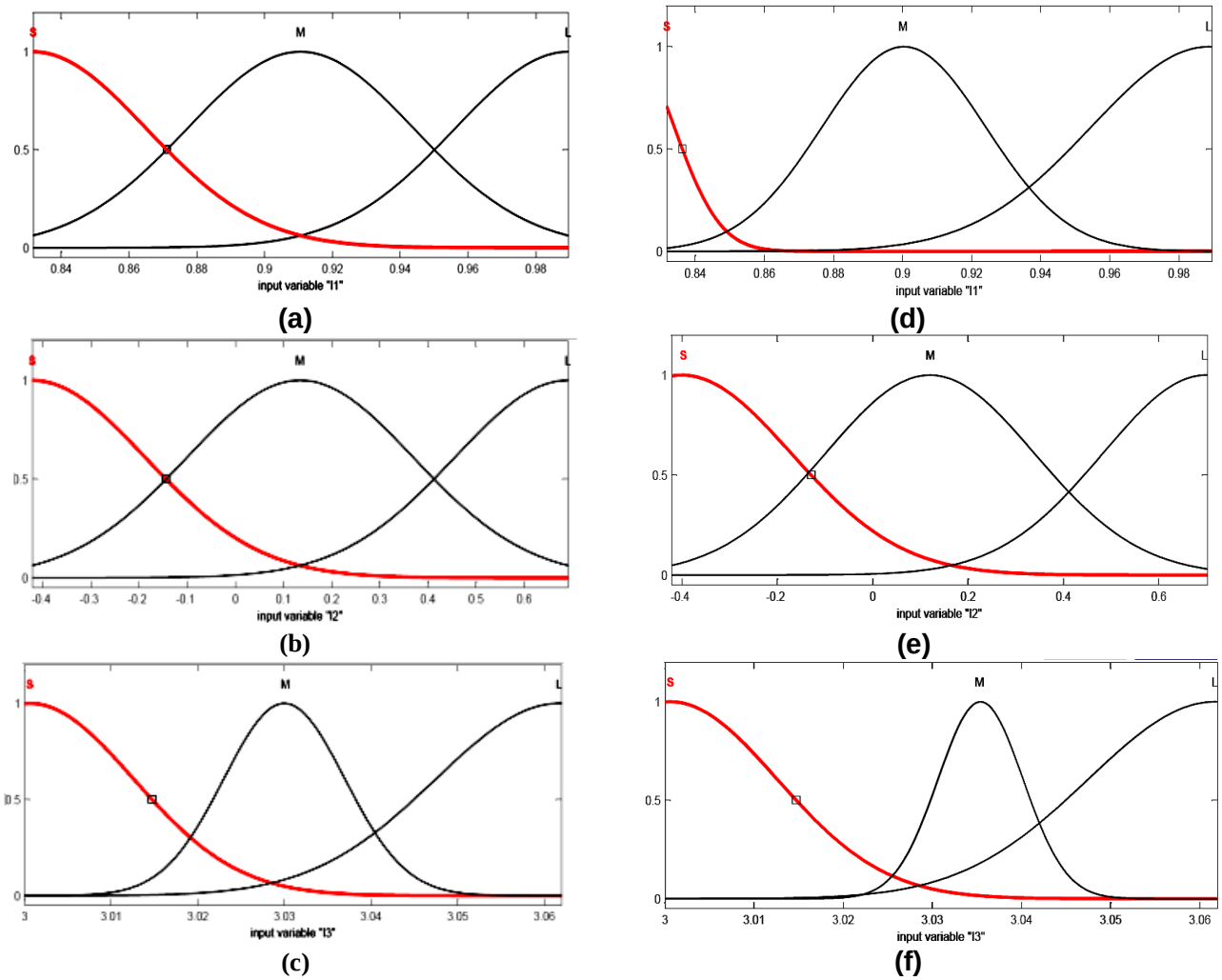


Fig. 6.10 Initial and final MFs for ANFIS A (a) Initial MF's for $I_1$ (b) Initial MF's for $I_2$ (c) Initial MF's for $I_3$ (d) Final MF's for $I_1$ (e) Final MF's for $I_2$ (f) Final MF's for $I_3$

For ANFIS B, the initial and final shape of fuzzy sets is shown in Fig. 6.11.

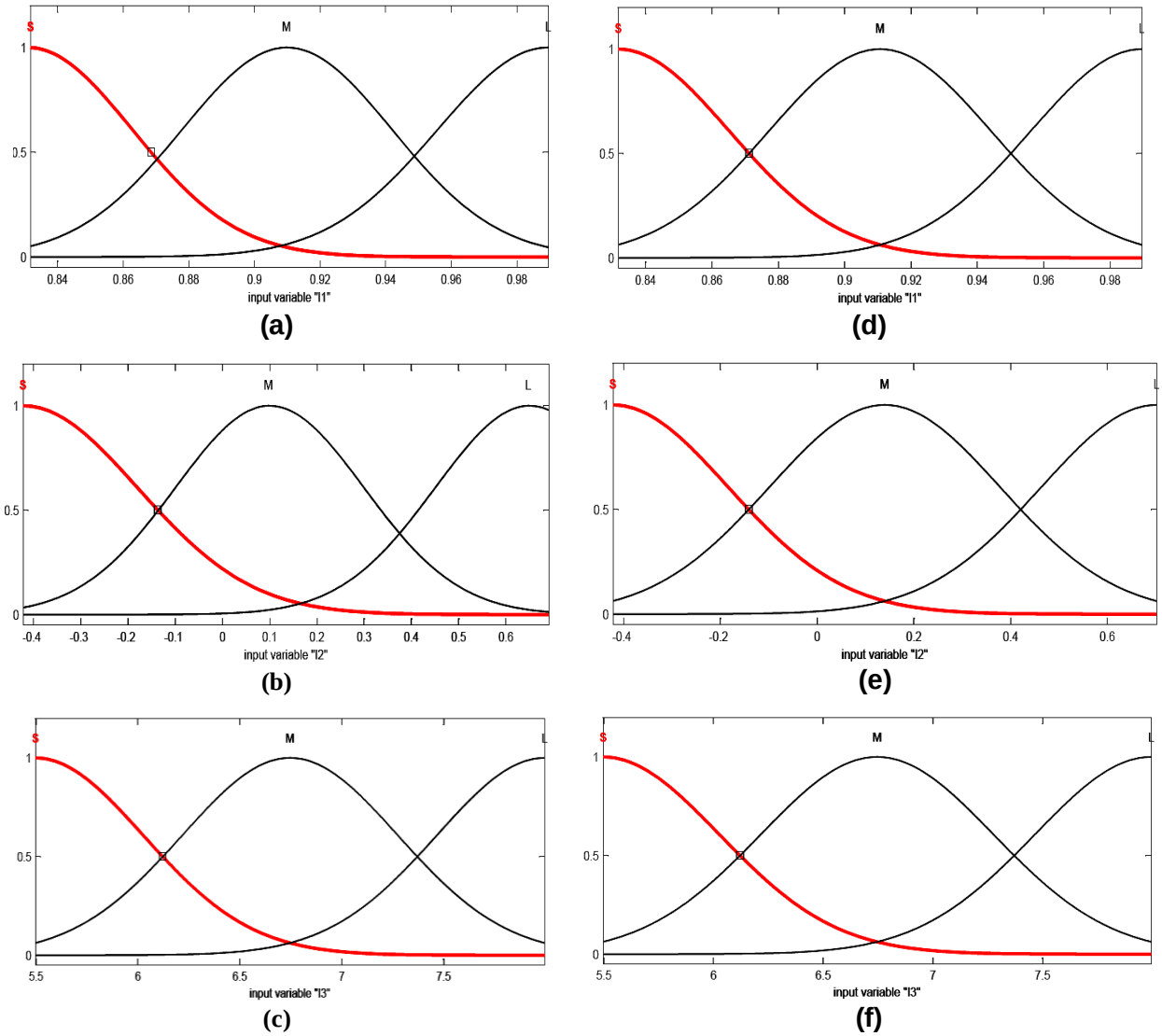


Fig. 6.11 Initial and final MFs for ANFIS B(a) Initial MF's for $I_1$ (b) Initial MF's for $I_2$ (c) Initial MF's for $I_3$ (d) Final MF's for $I_1$ (e) Final MF's for $I_2$ (f) Final MF's for $I_3$

## 6.4 Simulation Results

In this section, the performance of the ANFIS controllers is evaluated for reference tracking and disturbance rejection cases. The objective of the controller is to get the desired purity of methanol composition by manipulating the reflux flow and reboiler heat duty. The performance of ANFIS controller has also been compared with NN-IMC controller for both the cases.

### 6.4.1 Case a: Reference Tracking

For reference tracking case, a step change from 0.83 to 0.98 mol fraction in methanol composition is considered. The output with ANFIS control scheme is shown in Fig. 6.12. The change in feed flow-rate affects the thermal equilibrium of the BDC; therefore, the value of feed flow-rate has been kept constant at 2.5 kg-mole/hr. The MSE with ANFIS control scheme is given in Fig. 6.13. These figures also compare the performance of ANFIS with NN-IMC control scheme.

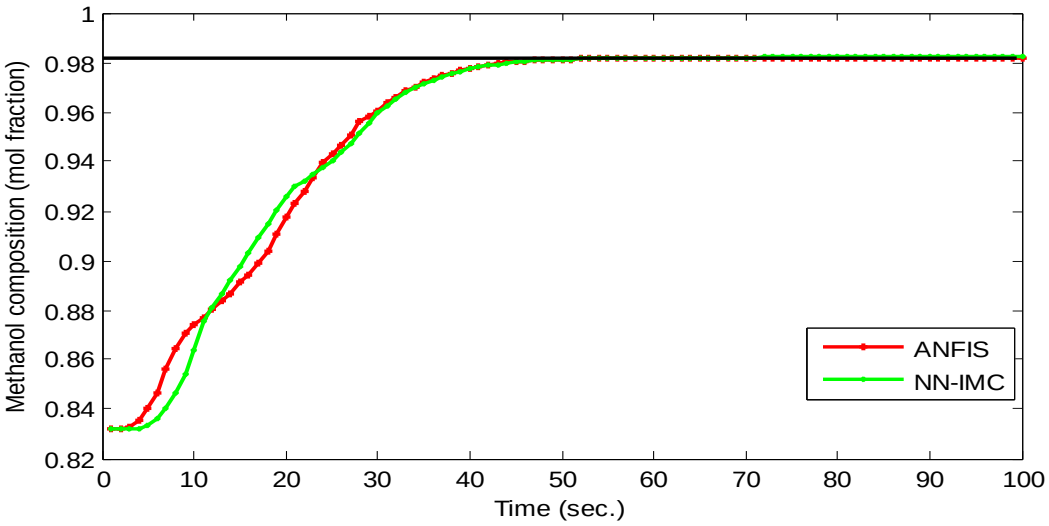


Fig. 6.12 Output of ANFIS and NN-IMC controller at feed flow-rate 2.5 kg-mole/hr.

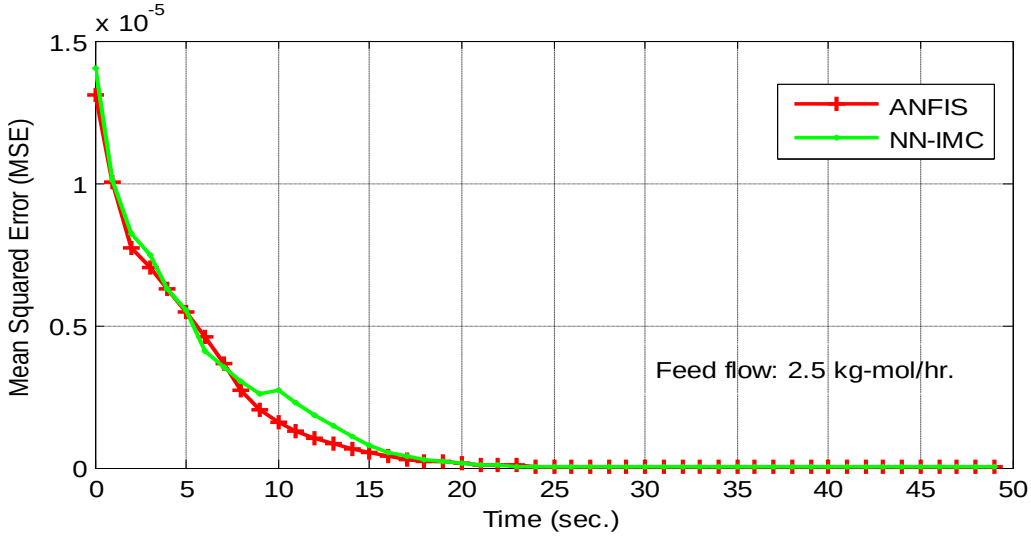


Fig. 6.13 MSE of ANFIS and NN-IMC controller at feed flow-rate 2.5 kg-mole/hr

The performance of the proposed ANFIS controller is evaluated on the basis of rise time, settling time and MSE. The values of these performance parameters with ANFIS scheme are given in Table 6-4. In this table the performance parameters (rise time, settling time and MSE) of all the schemes proposed in this thesis have also been compared. It is observed from these results that for reference tracking all the schemes give the satisfactory results. Amongst all the schemes best performance is obtained from ANFIS scheme.

### 6.4.2 Case b: Disturbance Rejection

Fig. 6.14 illustrates the comparative performance of ANFIS scheme at the +10% and change in feed flow-rate. The MSE at output with ANFIS control scheme is shown in Fig. 6.15. These figures also compare the performance of ANFIS controller with NN-IMC controller for disturbance rejection case.

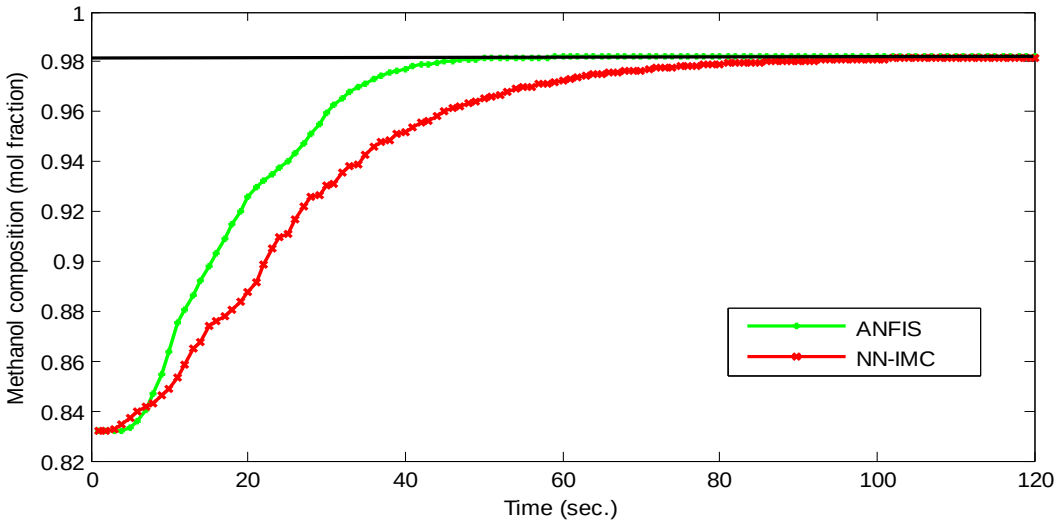


Fig. 6.14 Output of ANFIS and NN-IMC controller at +10% change in feed flow-rate

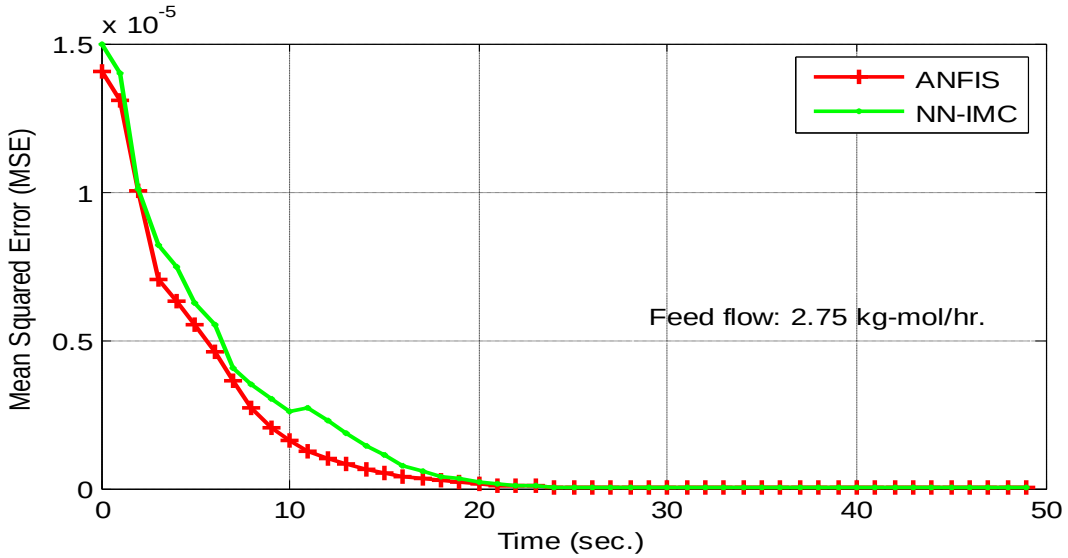


Fig. 6.15 MSE of ANFIS and NN-IMC controller at +10% change in feed flow-rate

In Table 6-5, the performance parameters (rise time, settling time and MSE) of all the schemes proposed in this thesis has also been compared for disturbance rejection case. The results obtained show that ANFIS controller works effectively for this case. It is observed from the results that BDC with ANFIS controller is faster and reaches the steady state values earlier as compared to the other controllers discussed in this thesis.

Table 6-4 Performance parameters with different proposed control schemes for reference tracking case

| Performance Indicators | Control Schemes | | | | | |
|---|---|---|---|---|---|---|
| | PID | LMPC | NN-MPC | NN-DIC | NN-IMC | ANFIS |
| Rise time(sec.) | 36 | 25 | 31 | 50 | 30 | 30 |
| Settling time(sec.) | 70 | 100 | 70 | 105 | 52 | 45 |
| MSE | $2.1\times10^{-5}$ | $1.8\times10^{-5}$ | $1.55\times10^{-5}$ | $2\times10^{-5}$ | $1.4\times10^{-5}$ | $1.3\times10^{-5}$ |

Table 6-5 Performance parameters with different proposed control schemes for disturbance rejection case

| Performance Indicators | Control Schemes | | | | | |
|---|---|---|---|---|---|---|
| | PID | LMPC | NN-MPC | NN-DIC | NN-IMC | ANFIS |
| Rise time(sec.) | 41 | 37 | 45 | 60 | 35 | 30 |
| Settling time(sec.) | 240 | 280 | 110 | 150 | 85 | 50 |
| MSE | $2.5x10^{-5}$ | $1.9x10^{-5}$ | $1.6x10^{-5}$ | $2.5x10^{-5}$ | $1.5x10^{-5}$ | $1.4x10^{-5}$ |

## 6.5 Conclusion

In this work, ANFIS control scheme is proposed and its performance is evaluated to control the methanol composition in BDC. The nonlinear ANN model of BDC is used to implement the ANFIS control scheme. Two separate ANFIS controllers have been designed for the control of reflux flow-rate and reboiler heat duty. Performance of the ANFIS control scheme is evaluated for reference tracking and disturbance rejection cases. A perturbation of +10% is incorporated in feed flow-rate for disturbance rejection case. The performance of this ANFIS control scheme is compared with NN-IMC control scheme on the basis of considered performance indicators (rise time, settling time, MSE). For both of the cases, it is concluded that the settling time and MSE with ANFIS control scheme have been improved as compare to other control schemes.

# Chapter 7: CONCLUSIONS AND FUTURE SCOPE

## 7.1 Conclusion

In this thesis, different control schemes for BDC have been developed. Laboratory set-up of BDC has been utilized to generate the input data (reflux flow-rate and reboiler heat duty) and output data (methanol composition) for the development of accurate model of the column. The work carried out in this thesis has been summarized and concluded in the following paragraphs.

In the first chapter, detailed description of the laboratory set-up has been given. A detailed literature survey about the BDC and its control schemes has also been carried out in this chapter.

In second chapter, an equation based model of the existing set-up of BDC has been developed. The concept of mass balance and constant relative volatility has been utilized to develop the equation based model. This equation based model has been validated with the experimental set-up results. The result shows that the developed equation based model is in good agreement with the experimental set-up. To develop the equation based model many assumptions have been considered, which give errors if large disturbances are considered. Therefore; an ANN based model is also developed for the BDC based upon the knowledge of the six inputs and single output acquired from the real BDC laboratory set-up. The inputs are tray temperature, reflux flow-rate, feed flow-rate, reboiler duty, reflux drum top pressure and reboiler bottom pressure. The output of the neural network model is methanol composition. Two neural network topologies namely: FFNN and RNN have been used for the modeling. The training of the ANN based model of BDC has been carried out by the data acquired from experiments performed on the laboratory set-up of BDC. Performance of the developed ANN models are also compared with the equation based model of BDC. The results obtained show that the ANN model more closely represents the existing set-up.

In third chapter, inferential control scheme is developed to control the output methanol composition and implemented on the laboratory set-up of BDC. Inferential control scheme is the technique in which secondary variable is controlled to get the desired output. In the present work, tray temperature is used as the secondary variable. For the laboratory set-up, it is found by the sensitivity analysis that the temperature of fourth tray is an exact indicator of the corresponding output methanol composition. A relation between the controller current and the tray-4 temperature has been established and used to control the temperature of the tray with a PID controller. The optimal parameters of the PID controller have been determined using Genetic Algorithm. These parameters have been used to set the PID parameters of existing PID controller with laboratory BDC set-up. With these parameter settings, experiments have been performed for two cases. In first case, set-point is varied and output is observed at steady-state. In second case, feed flow-rate is increased by 10% and again the output is observed. It is observed in the first case that the output is following

the set-point. In second case, feed flow disturbance is rejected and final output is obtained as per the set-point.

In fourth chapter, Linear Model Predictive Control (LMPC) and Neural Network based Model Predictive Control (NN-MPC) schemes have been developed to control the methanol composition in BDC. In linear MPC scheme, equation based model of BDC is utilized to develop the scheme. This scheme does not perform well when large changes in operating condition (change in feed flow-rate and feed composition) are considered, because BDC model is inherently nonlinear. To overcome this, a nonlinear MPC based on ANN model is developed. This model is utilized to predict the process future response in the MPC algorithm to get the desired methanol composition. Performance of these controllers has also been compared with PID controller. The performance of linear and nonlinear MPC has been evaluated for two cases: Case A: reference tracking and Case B: disturbance rejection. It can be concluded from the results that NN-MPC scheme performs better than the LMPC and PID schemes on the basis of rise time, settling time, MSE and percentage overshoot.

In chapter five, direct inverse control (DIC) and internal model control (IMC) schemes have been developed to control the final composition of methanol. In this chapter forward model and inverse model of BDC have been developed utilizing the ANN approach. In developing the NN-DIC scheme, inverse model is utilized whereas, in NN-IMC scheme, both forward and inverse models are used. Both the schemes have been simulated for reference tracking and disturbance rejection cases. Results of both the schemes have also been compared with NN-MPC scheme. It is observed from the results that on the basis of rise time, settling time and MSE, the performance of the NN-IMC scheme is better than the NN-DIC and NN-MPC schemes.

In sixth chapter, Adaptive Neuro Fuzzy Inference System (ANFIS) based control scheme is proposed and its performance is evaluated to control the methanol composition in BDC. In ANFIS, ANN is incorporated with Fuzzy Inference System, which can use knowledge by learning algorithms. The learning capability is an additional advantage for FIS while the formation of linguistic rule base is useful for the training of ANN. The ANN based model of BDC is used to implement the ANFIS control scheme. Two separate ANFIS controllers have been designed for the control of reflux flow-rate and reboiler heat duty. ANFIS control scheme is evaluated for reference tracking and disturbance rejection cases. A perturbation of +10% is incorporated in feed flow-rate for disturbance rejection case. The performance of the proposed ANFIS control scheme is also compared with NN-IMC control scheme on the basis of performance indicators (rise time, settling time, MSE). It is concluded that the settling time and MSE with ANFIS control scheme have been improved as compare to other control schemes for both of the cases.

## 7.2 Future Scope

In the present research work, the experimentation is performed for binary mixture of methanol and water. The equation based model and ANN based model is developed and validated with the experimental set-up. Various control schemes are developed for these models. The following suggestions are made for future work:

1. The mathematical model (described in chapter-2) is developed for binary mixture. A mathematical model may be developed for multi-component mixture.
2. A hybrid model for BDC may be developed by utilizing the advantages of both mathematical modeling and ANN based modelling.
3. In the present work, only temperature closed loop control is existing therefore; tray temperature is utilized as a secondary measurement variable in inferential control scheme. There is a scope to add more closed loops (reflux flow, steam flow etc.) for the better inferential control of BDC.
4. The inferential control of distillation process is carried out on the basis of single tray temperature control for the laboratory set-up of BDC. As the set-up is of small capacity, the single tray temperature control was enough for controlling temperature profile of distillation process; however for large distillation columns, single tray temperature control may not be sufficient and it may become necessary to control two or more tray temperatures for smooth control of the temperature profile of distillation process that produces desired concentration of the distillate.
5. The existing refractometer, which is connected with the output distillate flow path, produces its output in the form of 4-20mA signal. This signal may be utilized as one of the manipulated variable to get the desired purity of output distillate with some modifications in the existing set-up of BDC.
6. Field-programmable gate arrays (FPGAs) have become an alternative solution for fast realization of digital control systems. Various control schemes developed in the present work (ANN schemes, MPC based scheme, ANFIS scheme) may be implemented on FPGA platform.

## BIBLIOGRAPHY


[1] **A. Bonsfills and L. Puigjaner**, "Batch distillation: simulation and experimental validation," Chemical Engineering and Processing: Process Intensification, vol. 43, no. 10, pp. 1239-1252, 2004.

[2] **A. Mehlhorn, A. Espuña, A. Bonsfills, A. Górak, and L. Puigjaner**, "Modeling and experimental validation of both mass transfer and tray hydraulics in batch distillation," Computers & Chemical Engineering, vol. 20, Supplement 1, no. 0, pp. S575-S580, 1996.

[3] **B. V. Babu, V. Ramakrishna**, "Extended studies on mathematical modeling of site sensitive indices in the site selection criteria for hazardous waste treatment ,storage and disposal facility," journal of the institution of public health Engineers india, vol. 2, pp. 11-17, 2003.

[4] **E. Darnon, E. Morin, M. P. Belleville, and G. M. Rios**, "Ultrafiltration within downstream processing: some process design considerations," Chemical Engineering and Processing: Process Intensification, vol. 42, no. 4, pp. 299-309, 2003.

[5] **E. Sørensen and S. Skogestad**, "Optimal startup procedures for batch distillation," Computers & Chemical Engineering, vol. 20, Supplement 2, no. 0, pp. S1257-S1262, 1996.

[6] **M. Gupta, J. Yang, and C. Roy**, "Modelling the Effective Thermal Conductivity in Polydispersed Bed Systems: A Unified Approach using the Linear Packing Theory and Unit Cell Model," The Canadian Journal of Chemical Engineering, vol. 80, no. 5, pp. 830-839, 2002.

[7] **H. B. Bacha, T. Damak, M. Bouzguenda, and A. Y. Maalej**, "Experimental validation of the distillation module of a desalination station using the SMCEC principle," Renewable Energy, vol. 28, no. 15, pp. 2335-2354, 2003.

[8] **H. G. Schoenmakers and B. Bessling**, "Reactive and catalytic distillation from an industrial perspective," Chemical Engineering and Processing: Process Intensification, vol. 42, no. 3, pp. 145-155, 2003.

[9] **K. Sundmacher, G. Uhde, and U. Hoffmann**, "Multiple reactions in catalytic distillation processes for the production of the fuel oxygenates MTBE and TAME: Analysis by rigorous model and experimental validation," Chemical Engineering Science, vol. 54, no. 13–14, pp. 2839-2847, 1999.

[10] **Z. Wang, B. C. Y. Lu, D. Y. Peng, and C. Q. Lan**, "Liebermann-fried model parameters for calculating vapour-liquid equlibria of oxygenate and hydrocarbon mixtures," Journal of the Chinese Institute of Engineers, vol. 28, no. 7, pp. 1089-1105, 2005/10/01 2005.

[11] **K. Sundmacher and Z. Qi**, "Conceptual design aspects of reactive distillation processes for ideal binary mixtures," Chemical Engineering and Processing: Process Intensification, vol. 42, no. 3, pp. 191-200, 2003.

[12] **L. U. Kreul, A. Górak, C. Dittrich, and P. I. Barton**, "Dynamic catalytic distillation: Advanced simulation and experimental validation," Computers & Chemical Engineering, vol. 22, Supplement 1, no. 0, pp. S371-S378, 1998.

[13] **L. Zullo**, "Validation and verification of continuous plants operating modes using multivariate statistical methods," Computers & Chemical Engineering, vol. 20, Supplement 1, no. 0, pp. S683-S688, 1996.

[14] **M. Tapp, S. Kauchali, B. Hausberger, C. McGregor, D. Hildebrandt, and D. Glasser**, "An experimental simulation of distillation column concentration profiles using a batch apparatus," Chemical Engineering Science, vol. 58, no. 2, pp. 479-486, 2003.

[15] **M. J. Doma, P. A. Taylor, and P. J. Vermeer**, "Closed loop identification of MPC models for MIMO processes using genetic algorithms and dithering one variable at a time: Application to an industrial distillation tower," Computers & Chemical Engineering, vol. 20, Supplement 2, no. 0, pp. S1035-S1040, 1996.

[16] **P. F. Lith van, B. H. L. Betlem, and B. Roffel**, "Combining prior knowledge with data driven modeling of a batch distillation column including start-up," Computers & Chemical Engineering, vol. 27, no. 7, pp. 1021-1030, 2003.

[17] **P. B. Deshpande and C. A. Plank**, *Distillation dynamics and control*: Instrument Society of America, 1985.

[18] **R. Henrion and A. Möller**, "Optimization of a continuous distillation process under random inflow-rate," Computers & Mathematics with Applications, vol. 45, no. 1–3, pp. 247-262, 2003.

[19] **R. Schneider, G. Wozny, and G. Fieg**, "Optimization of an industrial three phase distillation column train with experimental verification," Computers & Chemical Engineering, vol. 21, Supplement, no. 0, pp. S1131-S1136, 1997.

[20] **W. L. Luyben**, "Simple method for tuning SISO controllers in multivariable systems," Industrial & Engineering Chemistry Process Design and Development, vol. 25, no. 3, pp. 654-660, 1986/07/01 1986.

[21] **Y. H. Jhon and T.-h. Lee**, "Dynamic simulation for reactive distillation with ETBE synthesis," Separation and Purification Technology, vol. 31, no. 3, pp. 301-317, 2003.

[22] **Akanksha, K. K. Pant, and V. K. Srivastava**, "Modeling of sulphonation of tridecylbenzene in a falling film reactor," Mathematical and Computer Modelling, vol. 46, no. 9–10, pp. 1332-1344, 2007.

[23] **Ü. Can, M. Jimoh, J. Steinbach, and G. Wozny**, "Simulation and experimental analysis of operational failures in a distillation column," Separation and Purification Technology, vol. 29, no. 2, pp. 163-170, 2002.

[24] **V. Bansal, J. D. Perkins, E. N. Pistikopoulos, R. Ross, and J. M. G. van Schijndel**, "Simultaneous design and control optimisation under uncertainty," Computers & Chemical Engineering, vol. 24, no. 2–7, pp. 261-266, 2000.

[25] **M. Diehl, R. Findeisen, S. Schwarzkopf, I. Uslu, F. Allgöwer, H. G. Bock, E.-D. Gilles, and J. P. Schlöder**, "An Efficient Algorithm for Nonlinear Model Predictive Control of Large-Scale Systems Part II: Experimental Evaluation for a Distillation Column," at - Automatisierungstechnik, vol. 51, no. 1-2003, pp. 22-29, 2003/01/01 2003.

[26] **D. R. Yang and K. S. Lee**, "Monitoring of a distillation column using modified extended Kalman filter and a reduced order model," Computers & Chemical Engineering, vol. 21, Supplement, no. 0, pp. S565-S570, 1997.

[27] **A. Kienle**, "Low-order dynamic models for ideal multicomponent distillation processes using nonlinear wave propagation theory," Chemical Engineering Science, vol. 55, no. 10, pp. 1817-1828, 2000.

[28] **A. Higler, R. Chande, R. Taylor, R. Baur, and R. Krishna**, "Nonequilibrium modeling of three-phase distillation," Computers & Chemical Engineering, vol. 28, no. 10, pp. 2021-2036, 2004.

[29] **S. Bian and M. A. Henson**, "Measurement selection for on-line estimation of nonlinear wave models for high purity distillation columns," Chemical Engineering Science, vol. 61, no. 10, pp. 3210-3222, 2006.

[30] **W. Li and J. H. Lee**, "Control relevant identification of ill-conditioned systems: Estimation of gain directionalyty," Computers & Chemical Engineering, vol. 20, no. 8, pp. 1023-1042, 1996.

[31] **I. Muntean, M. Stuckert, and M. Abrudean**, "A general distillation modeling framework applied to an isotopic distillation column," in *Control & Automation (MED), 2011 19th Mediterranean Conference on*, 2011, pp. 1150-1154.

[32] **E. Quintero-Marmol, W. L. Luyben, and C. Georgakis**, "Application of an extended Luenberger observer to the control of multicomponent batch distillation," Industrial & Engineering Chemistry Research, vol. 30, no. 8, pp. 1870-1880, 1991/08/01 1991.

[33] **E. Quintero-Marmol and W. L. Luyben**, "Inferential model-based control of multicomponent batch distillation," Chemical Engineering Science, vol. 47, no. 4, pp. 887-898, 1992.

[34] **P. M. Bhagat**, "An introduction to neural nets," Chem. Eng. Prog., pp. 55–60, 1990.

[35] **A. J. Morris, G. A. Montague, and M. J. Willis**, "Artificial Neural Networks - Studies in-Process Modeling and Control," Chemical Engineering Research & Design, vol. 72, no. 1, pp. 3-19, 1994.

[36] **J. C. Macmurray and D. M. Himmelblau**, "Modeling and control of a packed distillation column using artificial neural networks," Computers & Chemical Engineering, vol. 19, no. 10, pp. 1077-1088, 1995.

[37] **J. Ou and R. R. Rhinehart**, "Grouped-neural network modeling for model predictive control," ISA Transactions, vol. 41, no. 2, pp. 195-202, 2002.

[38] **S. Jagannathan and F. L. Lewis**, "Identification of nonlinear dynamical systems using multilayered neural networks," Automatica, vol. 32, no. 12, pp. 1707-1712, 1996.

[39] **J. I. Canelon, L. S. Shieh, and N. B. Karayiannis**, "A new approach for neural control of nonlinear discrete dynamic systems," Information Sciences, vol. 174, no. 3–4, pp. 177-196, 2005.

[40] **W. Yu**, "Nonlinear system identification using discrete-time recurrent neural networks with stable learning algorithms," Information Sciences, vol. 158, no. 0, pp. 131-147, 2004.

[41] **G. Gupta, R. N. Yadav, P. K. Kalra, and J. John**, "Modeling with Recurrent Neural Networks using Compensatory Neuron Model," Neural Information Processing- Letters and Reviews, vol. 6, no. 1, pp. 69-78, March 2005.

[42] **V. Singh, I. Gupta, and H. O. Gupta**, "ANN based estimator for distillation—inferential control," Chemical Engineering and Processing: Process Intensification, vol. 44, no. 7, pp. 785-795, 2005.

[43] **V. Singh, I. Gupta, and H. O. Gupta**, "ANN-based estimator for distillation using Levenberg–Marquardt approach," Engineering Applications of Artificial Intelligence, vol. 20, no. 2, pp. 249-259, 2007.

[44] **K. J. Åström and T. Hägglund**, "PID Controllers - Theory, Design, and Tuning (2nd Edition)," ISA, 1995.

[45] **J. G. Ziegler and N. B. Nichols**, "Optimum Settings for Automatic Controllers," Journal of Dynamic Systems, Measurement, and Control, vol. 115, no. 2B, pp. 220-222, 1993.

[46] **Z. Zhen-Yu**, "Fuzzy gain scheduling of PID controllers," Systems, Man and Cybernetics, IEEE Transactions on, vol. 23, no. 5, pp. 1392-1398, 1993.

[47] **L. Hsie and T. J. McAvoy**, "Comparison of single loop and QDMC-based control of crude oil distillation towers," Journal of Process Control, vol. 1, no. 1, pp. 15-21, 1991.

[48] **S. K. Nagar, J. Pal, and J. D. Sharma**, "A computer-aided method for digital controller design via optimization," Computers & Electrical Engineering, vol. 16, no. 2, pp. 79-85, 1990.

[49] **B. Porter and A. H. Jones**, "Genetic tuning of digital PID controllers," in *Electronics Letters*. vol. 28: Institution of Engineering and Technology, 1992, pp. 843-844.

[50] **S. Skogestad**, "Probably The Best Simple PID Tuning Rules In The World," in *AIChE annual meeting*, Reno,NV ,USA, 2001.

[51] **S. R. Upreti**, "A new robust technique for optimal control of chemical engineering processes," Computers & Chemical Engineering, vol. 28, no. 8, pp. 1325-1336, 2004.

[52] **S. K. Gupta and S. Garg**, "Chapter Four - Multiobjective Optimization Using Genetic Algorithm," in *Advances in Chemical Engineering*. vol. Volume 43, S. Pushpavanam, Ed.: Academic Press, 2013, pp. 205-245.

[53] **Y. Chen, U. Northwest Normal, Y.-j. Ma, and W.-x. Yun**, "Application of Improved Genetic Algorithm in PID Controller Parameters Optimization," TELKOMNIKA Indonesian Journal of Electrical Engineering, vol. 11, no. 3, pp. 1524-1530, 2013.

[54] **B. Joseph and C. B. Brosilow**, "Inferential control of processes: Part I. Steady state analysis and design," AIChE Journal, vol. 24, no. 3, pp. 485-492, 1978.

[55] **N. R. Amundson and A. J. Pontinen**, "Multicomponent Distillation Calculations on a Large Digital Computer," Industrial & Engineering Chemistry, vol. 50, no. 5, pp. 730-736, 1958/05/01 1958.

[56] **M. J. Piovoso, K. A. Kosanovich, V. Rokhlenko, and A. Guez**, "A Comparison of Three Nonlinear Controller Designs Applied to a Non-Adiabatic First-Order Exothermic Reaction in a CSTR," in *American Control Conference, 1992*, 1992, pp. 490-494.

[57] **E. P. Nahas, M. A. Henson, and D. E. Seborg**, "Nonlinear internal model control strategy for neural network models," Computers & Chemical Engineering, vol. 16, no. 12, pp. 1039-1057, 1992.

[58] **M. Pottmann and D. E. Seborg**, "A nonlinear predictive control strategy based on radial basis function models," Computers & Chemical Engineering, vol. 21, no. 9, pp. 965-980, 1997.

[59] **K. Hornik, M. Stinchcombe, and H. White**, "Multilayer feedforward networks are universal approximators," Neural Networks, vol. 2, no. 5, pp. 359-366, 1989.

[60] **K. Andersen, G. E. Cook, G. Karsai, and K. Ramaswamy**, "Artificial neural networks applied to arc welding process modeling and control," Industry Applications, IEEE Transactions on, vol. 26, no. 5, pp. 824-830, 1990.

[61] **T. H. Lee, C. C. Hang, L. L. Lian, and B. C. Lim**, "An approach to inverse nonlinear control using neural networks," Mechatronics, vol. 2, no. 6, pp. 595-611, 1992.

[62] **K. J. Hunt, D. Sbarbaro, R. Żbikowski, and P. J. Gawthrop**, "Neural networks for control systems—A survey," Automatica, vol. 28, no. 6, pp. 1083-1112, 1992.

[63] **K. S. Narendra and K. Parthasarathy**, "Identification and control of dynamical systems using neural networks," IEEE Trans Neural Netw, vol. 1, no. 1, pp. 4-27, 1990.

[64] **N. Bhat and T. J. M. Avoy**, "Use of Neural Nets For Dynamic Modeling and Control of Chemical Process Systems," in *American Control Conference, 1989*, 1989, pp. 1342-1348.

[65] **M. J. Willis, C. Di Massimo, G. A. Montague, M. T. Tham, and A. J. Morris**, "Artificial neural networks in process engineering," Control Theory and Applications, IEE Proceedings D, vol. 138, no. 3, pp. 256-266, 1991.

[66] **D. H. Nguyen and B. Widrow**, "Neural networks for self-learning control systems," Control Systems Magazine, IEEE, vol. 10, no. 3, pp. 18-23, 1990.

[67] **J. R. Noriega and W. Hong**, "A direct adaptive neural-network control for unknown nonlinear systems and its application," Neural Networks, IEEE Transactions on, vol. 9, no. 1, pp. 27-34, 1998.

[68] **C.-w. Chen, D.-z. Chen, and G.-z. Cao**, "An improved differential evolution algorithm in training and encoding prior knowledge into feedforward networks with application in chemistry," Chemometrics and Intelligent Laboratory Systems, vol. 64, no. 1, pp. 27-43, 2002.

[69] **M. T. Hagan, H. B. Demuth, and O. D. Jesús**, "An introduction to the use of neural networks in control systems," International Journal of Robust and Nonlinear Control, vol. 12, no. 11, pp. 959-985, 2002.

[70] **F. N. Chowdhury, P. Wahi, R. Raina, and S. Kaminedi**, "A survey of neural networks applications in automatic control," in *System Theory, 2001. Proceedings of the 33rd Southeastern Symposium on*, 2001, pp. 349-353.

[71] **M. J. Willis, G. A. Montague, C. Di Massimo, M. T. Tham, and A. J. Morris**, "Artificial neural networks in process estimation and control," Automatica, vol. 28, no. 6, pp. 1181-1187, 1992.

[72] **R. Carotenuto**, "An iterative system inversion technique," International Journal of Adaptive Control and Signal Processing, vol. 15, no. 1, pp. 85-91, 2001.

[73] **P. Kuttisupakorn, M. A. Hussain, and J. Petcherdask**, "Studies on the use of neural networks in nonlinear control strategies," Journal of Chemical Engineering of Japan, vol. 34, no. 4, pp. 453-465, 2001.

[74] **J. Q. Gong and B. Yao**, "Neural network adaptive robust control of nonlinear systems in semi-strict feedback form," Automatica, vol. 37, no. 8, pp. 1149-1160, 2001.

[75] **M. Morari and E. Zafiriou**, *Robust Process Control*: Prentice Hall, 1989.

[76] **A. K. Singh, B. Tyagi, and V. Kumar**, "Application of Neural Network based Control Strategies to Binary Distillation Column," Control engineering and applied informatics, vol. 15, no. 4, pp. 47-57, 2013.

[77] **M. Mohammadzaheri and L. Chen**, "Intelligent predictive control of a model helicopter's yaw angle," Asian Journal of Control, vol. 12, no. 6, pp. 667-679, 2010.

[78] **W. Yu, G. Chen, and J. Cao**, "Adaptive synchronization of uncertain coupled stochastic complex networks," Asian Journal of Control, vol. 13, no. 3, pp. 418-429, 2011.

[79] **C. E. García, D. M. Prett, and M. Morari**, "Model predictive control: Theory and practice—A survey," Automatica, vol. 25, no. 3, pp. 335-348, 1989.

[80] **M. Azlan Hussain**, "Review of the applications of neural networks in chemical process control — simulation and online implementation," Artificial Intelligence in Engineering, vol. 13, no. 1, pp. 55-68, 1999.

[81] **S. J. Qin and T. A. Badgwell**, "A survey of industrial model predictive control technology," Control Engineering Practice, vol. 11, no. 7, pp. 733-764, 2003.

[82] **S. Nugroho, Y. Y. Nazaruddin, and H. A. Tjokronegoro**, "Non-linear identification of aqueous ammonia binary distillation column based on simple Hammerstein model," in *Control Conference, 2004. 5th Asian*, 2004, pp. 118-123 Vol.1.

[83] **S. K. Doherty, J. B. Gomm, and D. Williams**, "Experiment design considerations for non-linear system identification using neural networks," Computers & Chemical Engineering, vol. 21, no. 3, pp. 327-346, 1996.

[84] **D. Himmelblau**, "Applications of artificial neural networks in chemical engineering," Korean Journal of Chemical Engineering, vol. 17, no. 4, pp. 373-392, 2000/07/01 2000.

[85] **K. Konakom, P. Kittisupakorn, and I. M. Mujtaba**, "Neural network-based controller design of a batch reactive distillation column under uncertainty," Asia-Pacific Journal of Chemical Engineering, vol. 7, no. 3, pp. 361-377, 2012.

[86] **S. K. Arumugasamy and Z. Ahmad**, "Elevating Model Predictive Control Using Feedforward Artificial Neural Networks: A Review," Chemical Product and Process Modeling, vol. 4, no. 1, 2009.

[87] **J. S. R. Jang**, "ANFIS: adaptive-network-based fuzzy inference system," Systems, Man and Cybernetics, IEEE Transactions on, vol. 23, no. 3, pp. 665-685, 1993.

[88] **K. Belarbi, K. Bettou, and A. Mezaache**, "Fuzzy neural networks for estimation and fuzzy controller design: simulation study for a pulp batch digester," Journal of Process Control, vol. 10, no. 1, pp. 35-41, 2000.

[89] **K. Leiviska**, *Industrial Applications of Soft Computing*. New York: Physica-Verlag Heidelberg, 2001.

[90] **S.-K. Oh, W. Pedrycz, and H.-S. Park**, "Hybrid identification in fuzzy-neural networks," Fuzzy Sets and Systems, vol. 138, no. 2, pp. 399-426, 2003.

[91] **M. Buragohain and C. Mahanta**, "A novel approach for ANFIS modelling based on full factorial design," Applied Soft Computing, vol. 8, no. 1, pp. 609-625, 2008.

[92] **J. Fernandez de Canete, A. Garcia-Cerezo, I. Garcia-Moral, P. Del Saz, and E. Ochoa**, "Object-oriented approach applied to ANFIS modeling and control of a distillation column," Expert Systems with Applications, vol. 40, no. 14, pp. 5648-5660, 2013.

[93] **J. F. de Canete, P. del Saz-Orozco, and S. Gonzalez-Perez**, "Application of adaptive neurofuzzy control using soft sensors to continuous distillation," in *Computer Aided*

*Chemical Engineering*. vol. Volume 25, B. Bertrand and J. Xavier, Eds.: Elsevier, 2008, pp. 465-470.

[94] **R. K. Wood and M. W. Berry**, "Terminal composition control of a binary distillation column," Chemical Engineering Science, vol. 28, no. 9, pp. 1707-1717, 1973.

[95] **W. L. Luyben**, *Process modeling, simulation, and control for chemical engineers*: McGraw-Hill, 1990.

[96] **A. K. Singh, B. Tyagi, and V. Kumar**, "Application of Feed Forward and Recurrent Neural Network Topologies for the Modeling and Identification of Binary Distillation Column," IETE Journal of Research, vol. 59, no. 2, pp. 167-175 2013

[97] **V. Singh**, "Dynamic Simulation and Control of Distillation Column." vol. PhD Thesis, 2007.

[98] **D. E. Goldberg**, *Genetic Algorithms in Search, Optimization and Machine Learning*: Addison-Wesley Longman Publishing Co., Inc., 1989.

[99] "Digital Indicating Controller, Models UT320," User Manual, **Yokogawa**

[100] **E. F. Camacho and C. Bordons**, *Model Predictive Control*: Springer-Verlag GmbH, 2004.

[101] **J. M. Maciejowski**, *Predictive Control: With Constraints*: Prentice Hall, 2002.

[102] **P. T. Boggs and J. W. Tolle**, "Sequential Quadratic Programming," Acta Numerica, vol. 4, pp. 1-51, 1995.

[103] **F. Meng-Hock and M. T. Hagan**, "Levenberg-Marquardt training for modular networks," in *Neural Networks, 1996., IEEE International Conference on*, 1996, pp. 468-473 vol.1.

[104] **R. Haber, R. H. Haber, A. Alique, S. Ros, and J. R. Alique**, "Dynamic Model of the Machining Process on the Basis of Neural Networks: from Simulation to Real Time Application," in *Computational Science — ICCS 2002*. vol. 2331, P. A. Sloot, A. Hoekstra, C. J. K. Tan, and J. Dongarra, Eds.: Springer Berlin Heidelberg, 2002, pp. 574-583.

[105] **K. J. Hunt and D. Sbarbaro**, "Neural networks for nonlinear internal model control," Control Theory and Applications, IEE Proceedings D, vol. 138, no. 5, pp. 431-438, 1991.

[106] **C. Ernest, Jacek, Łęski**, *Fuzzy and Neuro-Fuzzy Intelligent Systems*: Physica-Verlag HD, 2000.

[107] **D. Dubois and H. Prade**, "Fuzzy sets in approximate reasoning, Part 1: Inference with possibility distributions," Fuzzy Sets and Systems, vol. 100, Supplement 1, no. 0, pp. 73-132, 1999.

[108] **T. Takagi and M. Sugeno**, "Fuzzy identification of systems and its applications to modeling and control," Systems, Man and Cybernetics, IEEE Transactions on, vol. SMC-15, no. 1, pp. 116-132, 1985.

[109] **J. Nocedal and S. Wright**, *Numerical Optimization*: Springer, 2000.

[110] **K. Levenberg**, "A method for the solution of certain non-linear problems in least squares," Quarterly Journal of Applied Mathmatics, vol. II, no. 2, pp. 164-168, 1944.

[111] **D. W. Marquardt**, "An Algorithm for Least-Squares Estimation of Nonlinear Parameters," Journal of the Society for Industrial and Applied Mathematics, vol. 11, no. 2, pp. 431-441, 1963.

## PUBLICATIONS FROM THE WORK

**Journals**

[1] **Amit Kumar Singh**, **Barjeev Tyagi, and Vishal Kumar**, "Application of Feed Forward and Recurrent Neural Network Topologies for the Modeling and Identification of Binary Distillation Column" in *IETE Journal of Research,* vol. 59, no. 2, pp. 167-175, 2013.

[2] **Amit Kumar Singh, Barjeev Tyagi, and Vishal Kumar**, "First Principle Modeling and Neural Network–Based Empirical Modeling with Experimental Validation of Binary Distillation Column " *Chemical Product and Process Modeling,* vol. 8, no. 1, pp. 53-70, 2013.

[3] **Amit Kumar Singh**, **Barjeev Tyagi, and Vishal Kumar,** "Application of Neural Network based Control Strategies to Binary Distillation Column" *Control Engineering and Applied Informatics,* vol. 15, no. 4, pp. 47-57, 2013.

[4] **Amit Kumar Singh**, **Barjeev Tyagi, and Vishal Kumar, "**Classical and Neural Network–Based Approach of Model Predictive Control for Binary Continuous Distillation Column" *Chemical Product and Process Modeling,* vol. 9, no. 1, pp. 71-87, 2014.

**International conferences**

[5] **Amit Kumar Singh, Barjeev Tyagi, and Vishal Kumar,** "Fuzzy Rule-Based Controller for Binary Distillation Column" Proceedings of International Conference on Advances in Computing and Artificial Intelligence (*ACAI-2011*), pp.166-169 (2011).

[6] **Amit Kumar Singh, Barjeev Tyagi, and Vishal Kumar,** "Comparative performance analysis of Fuzzy Logic Controller for the Composition control of Binary Distillation Column" Proceedings of Recent Advances in Intelligent Computational Systems (*RAICS-2011*), 2011 IEEE, pp.515-519 (2011).

[7] **Amit Kumar Singh, Barjeev Tyagi, and Vishal Kumar,** "ANN Controller for Binary Distillation Column-A Marquardt-Levenberg approach " Proceedings of IEEE Nirma University International Conference on Engineering (*NUiCONE-2011*), pp.1-6 (2011).

[8] **Amit Kumar Singh, Barjeev Tyagi, and Vishal Kumar,** "Neural Network Modelling & Validation of Binary Distillation Column" Proceedings of International Conference on Electrical Engineering and Computer Science (*EECS-2012*), 16-19 august, 2012, Shanghai (china).

[9] **Amit Kumar Singh, Barjeev Tyagi, and Vishal Kumar,** "Design and Verification of Embedded Controller for Binary Distillation Column" IEEE International Conference on Control, Communication and Computing (*ICCC 2013*) (*accepted*).

**Communicated Papers under review**

[10] **Amit Kumar Singh, Barjeev Tyagi, and Vishal Kumar,** "Application of ANFIS Approach to Composition Control of Binary Distillation Column" *Journal of Chemical Engineering and Processing: Process Intensification.*

## EXPERIMENTAL SET UP OF DISTILLATION COLUMN

## APPENDIX-A

Table A-1 Column and mixture details for binary mixture

| | |
|---|---|
| Number of trays | 9 |
| Weir height in stripping section | 0.47 inch |
| Weir length in stripping section | 0.47 inch |
| Column diameter in stripping section | 4.80 inch |
| Weir height in rectifying section | 5.91 inch |
| Weir length in rectifying section | 5.91 inch |
| Column diameter in rectifying section | 4.80 inch |
| Volumetric hold up in column base | 0.5414 ft3 |
| Volumetric hold up in reflux drum | 0.0001 ft3 |
| Liquid feed rate | 2.5 kg-moles/hr |
| Liquid feed temperature | 34.5 deg-C |
| Pressure in the bottom | 115.21 kPa |
| Pressure in the reflux drum | 101.42 kPa |
| Reboiler heat input | 6.0 kW |
| Reflux flow-rate | 3.0 kg-moles/hr |
| Vapor distillate product flow-rate | 0.0 kg-moles/hr |
| Murphree vapor efficiency | 0.60 |

## B.1 REFLUX DIVIDER UNIT

The reflux divider controls the reflux ratio of the process and hence the reflux flow-rate. The connection diagram of reflux divider is shown in Fig. B.1.The timer controls the on-off switching time of the relay and by using a transformer for step down the voltage and AC to DC converter, the relay is operated. The output of the relay is converted to 230 V AC to energize the coil and magnetize the core. At the time of magnetization, the core attracts the upper part of metallic funnel and lower portion of funnel gets the opposite direction and the flow of liquid goes in reflux. When the timer is off the magnetic core gets discharged and the metallic funnel occupies its normal position and the liquid goes to the distillate container.

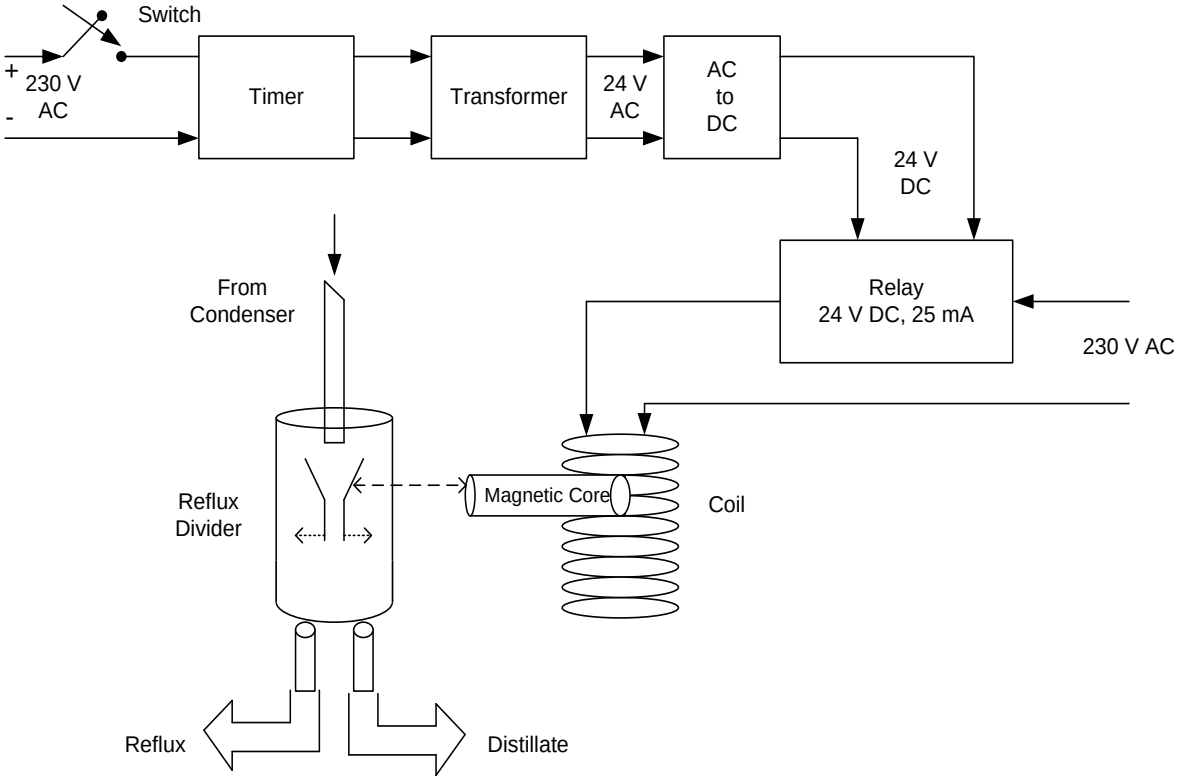


Fig. B.1 Schematic diagram of reflux divider unit

## APPENDIX-C

The parameters of PID controllers obtained by the Ziegler-Nichols method [45] are given in Table C-1.

Table C-1 PID controller parameters

| Tuning parameters | PID controller-1 (Reflux flow-rate loop) | PID controller 2 (Reboiler heat duty loop) |
|---|---|---|
| $K_P$ | 2 | 5 |
| $K_i$ | 10 | 15 |
| $K_d$ | 0.01 | 0.02 |

### D.1 Sequential Quadratic Programming (SQP)

To understand the use of SQP [109] in problems with general constraints, we begin by considering the equality-constrained problem,

Minimize *f(x)*

Subject to $\hat{c}_j(x) = 0$ , j=1,…, $\hat{m}$

The idea of SQP is to model this problem at the current point $x_k$ by a quadratic sub-problem and to use the solution of this sub-problem to find the new point $x_{k+1}$. SQP is in a way the application of Newton's method to the KKT optimality conditions.

The Lagrangian function for this problem is $L(x,\hat{\lambda}) = f(x) - \hat{\lambda}^T \hat{c}(x)$.

We define the Jacobian of the constraints by

$$A(x)^T = \nabla \hat{c}(x)^T = [\nabla \hat{c}_1(x), ..., \nabla \hat{c}_{\hat{m}}(x)] \qquad \text{D.1}$$

Which is an n x m matrix and $g(x) = \nabla f(x)$ is an n-vector as before.

Applying the first order KKT conditions to this problem we obtain

$$\begin{bmatrix} g(x) - A(x)^T \hat{\lambda} \\ \hat{c}(x) \end{bmatrix} = 0 \qquad \text{D.2}$$

This set of nonlinear equations can be solved using Newton's method,

$$\begin{bmatrix} W(x,\hat{\lambda}) & -A(x)^T \\ A(x) & 0 \end{bmatrix} \begin{bmatrix} p_k \\ p_{\hat{\lambda}} \end{bmatrix} = \begin{bmatrix} -g_k + A^T{}_k \hat{\lambda}_k \\ -c_k \end{bmatrix} \qquad \text{D.3}$$

Where the Hessian of the Lagrangian is denoted by $W(x,\hat{\lambda}) = \nabla^2_{xx} L(x,\hat{\lambda})$ and the Newton step from the current point is given by

$$\begin{bmatrix} x_{k+1} \\ \hat{\lambda}_{k+1} \end{bmatrix} = \begin{bmatrix} x_k \\ \hat{\lambda}_k \end{bmatrix} + \begin{bmatrix} p_k \\ p_{\hat{\lambda}} \end{bmatrix} \qquad \text{D.4}$$

An alternative way of looking at this formulation of the SQP is to define the following quadratic problem at $(x_k, \hat{\lambda}_k)$

minimize $\frac{1}{2} p^T W_k p + g_k^T p$

Subject to $A_k p + \hat{c}_k = 0$

This problem has a unique solution that satisfies

$W_k p + g_k - A_k^T \hat{\lambda}_k = 0$

$A_k p + \hat{c}_k = 0$

By writing this in matrix form, we see that $p_k$ and $\mu_k$ can be identified as the solution of the Newton equations we derived previously.

$$\begin{bmatrix} W_k & -A_k^T \\ A_k & 0 \end{bmatrix} \begin{bmatrix} p_k \\ \hat{\lambda}_{k+1} \end{bmatrix} = \begin{bmatrix} -g_k \\ -\hat{c}_k \end{bmatrix} \qquad \text{D.5}$$

This problem is equivalent to (D.3), but the second set of variables, is now the actual Lagrange multipliers $\hat{\lambda}_{k+1}$ instead of the Lagrange multiplier step, $p_{\hat{\lambda}}$. To obtain (D.3) simply substitute $\hat{\lambda}_k$ by $p_{\hat{\lambda}} - \lambda_k$ in (D.5).

A line search SQP algorithm:

1. Choose parameters $0<\eta<0.5$, $0<\tau<1$ and the initial point ($x_0$, $\lambda_0$).
2. Initialize the hessian estimate, say $B_0=I$.
3. Evaluate $f_0$, $g_0$, $c_0$ and $A_0$.
4. Begin major iteration loop in k:
   - 4.1 If termination criteria are met, then stop.
   - 4.2 Compute $p_k$ by solving (D.3).
   - 4.3 Choose $\mu_k$ such that $p_k$ is a descent direction for $\varphi$ at $x_k$.
   - 4.4 Set $\alpha_k=1$,
     - I. While $\phi(x_k+\alpha_k p_k,\mu_k) > \varphi(x_k,\mu_k)+\eta\alpha_k D\phi(x_k,p_k)$
     - II. Set $\alpha_k=\tau_\alpha\alpha_k$ for some $0<\tau_\alpha<\tau$.
   - 4.5 Set $x_{k+1}=x_k+\alpha_k p_k$.
   - 4.6 Evaluate $f_{k+1}$, $g_{k+1}$, $c_{k+1}$ and $A_{k+1}$.
   - 4.7 Compute $\lambda_{k+1}$ by solving $\lambda_{k+1}=-\left[A_{k+1}A_{k+1}^T\right]^{-1}A_{k+1}g_{k+1}$
   - 4.8 Set $s_k=\alpha_k p_k, y_k=\nabla_x L(x_{k+1},\lambda_{k+1})-\nabla_x L(x_k,\lambda_{k+1})$.
   - 4.9 Obtain $B_{k+1}$ by updating $B_k$ using a quasi- Newton formula.
5. End major iteration loop.

## E.1 LEVENBERG-MARQUARDT ALGORITHM

The Levenberg-Marquardt algorithm [110, 111] iteratively adjusts estimates of model parameters {β} to minimize residuals between measured dependent variable outputs {y} and predictions from a numerical model f(.) based on independent variable inputs {x} as shown in (E.1). For a given set of model parameters $\{\beta\}_k$ at iteration *k* each measured training pair $\{x\}_i$ and $\{y\}_i$ will have residuals $\{e\}_{i,k}$ as shown in (E.2). For parameter updates {Δβ} shown in (E.3), the Taylor series expansion for residuals at iteration *k+1* may be written as shown in (E.4) using the Jacobian [J] of the numerical model with respect to model parameters in (E.5).

$$\underset{\text{nout x 1}}{\{y\}} = f\left( \underset{\text{ninp x 1}}{\{x\}}, \underset{\text{npar x 1}}{\{\beta\}} \right) \tag{E.1}$$

$$\{e\}_{i,k} = \{y\}_i - f\left(\{x\}_i, \{\beta\}_k\right) \tag{E.2}$$

$$\{\beta\}_{k+1} = \{\beta\}_k + \{\Delta\beta\} \tag{E.3}$$

$$\underset{\text{nout x 1}}{\{e\}_{i,k+1}} = \underset{\text{nout x 1}}{\{e\}_{i,k}} - \underset{\text{nout x npar}}{[J]_{i,k}} \quad \underset{\text{npar x 1}}{\{\Delta\beta\}} \tag{E.4}$$

$$[J]_{i,k} = \begin{bmatrix} \frac{\partial f_1}{\partial \beta_1} & \frac{\partial f_1}{\partial \beta_2} & \cdots & \frac{\partial f_1}{\partial \beta_{npar}} \\ \frac{\partial f_2}{\partial \beta_1} & \frac{\partial f_2}{\partial \beta_2} & \cdots & \frac{\partial f_2}{\partial \beta_{npar}} \\ \vdots & \vdots & \ddots & \vdots \\ \frac{\partial f_{nout}}{\partial \beta_1} & \frac{\partial f_{nout}}{\partial \beta_2} & \cdots & \frac{\partial f_{nout}}{\partial \beta_{npar}} \end{bmatrix} \quad \text{evaluated for } \{x\}_i \tag{E.5}$$

If only one training pair is available and the number of dependent variable outputs is equal to the number of parameters (*nobs*=1 and *nout=npar*), Equation E.4 is deterministic and one can try to drive all *nout* residuals $\{e\}_{i,k+1}$ to zero using (E.6). This provides the classical Newton-Raphson root finding algorithm shown in (E.7).

$$\{\Delta\beta\} = [J]_{i,k}^{-1} \{e\}_{i,k} \tag{E.6}$$

$$\{\Delta\beta\} = -[J]_{i,k}^{-1} \; f\left(\{x\}_i, \{\beta\}_k\right) \qquad \text{for } \{y\}_i = \{0\} \tag{E.7}$$

If only one training pair is available and the number of dependent variable outputs is larger than the number of parameters (*nobs*=1 and *nout>npar*), residuals $\{e\}_{i,k+1}$ at iteration *k+1* can be minimized by the standard linear least squares solution shown in (E.8).

$$\underset{\text{npar x 1}}{\{\Delta\beta\}} = \left( \underset{\text{npar x nout}}{[J]_{i,k}^T} \quad \underset{\text{nout x npar}}{[J]_{i,k}} \right)^{-1} \left( \underset{\text{npar x nout}}{[J]_{i,k}^T} \quad \underset{\text{nout x 1}}{\{e\}_{i,k}} \right) \tag{E.8}$$

However, if the number of parameters is greater than the number of dependent variable outputs, E.8 is row insufficient and multiple training pairs are required (*nobs*>1 for

*nout<npar*). Residuals from all training pairs at iteration *k* shown in (E.2) may be concatenated as shown in (E.9) providing an aggregate sum of squares (SSQ) over all observations. Similarly all residuals predicted at iteration *k+1* for update {Δβ} in (E.4) may be concatenated as shown in (E.10). The linear least squares solution for parameter updates that will minimize the predicted aggregate SSQ after at iteration *k+1* is then shown in (E.11) and (E.12).

$$SSQ_k = \begin{Bmatrix} \{e\}_{1,k} \\ \{e\}_{2,k} \\ \vdots \\ \{e\}_{nobs,k} \end{Bmatrix}^T \begin{Bmatrix} \{e\}_{1,k} \\ \{e\}_{2,k} \\ \vdots \\ \{e\}_{nobs,k} \end{Bmatrix} = \sum_{i=1}^{nobs} \left( \{e\}_{i,k}^T \{e\}_{i,k} \right) \tag{E.9}$$

$$\begin{Bmatrix} \{e\}_{1,k+1} \\ \{e\}_{2,k+1} \\ \vdots \\ \{e\}_{nobs,k+1} \end{Bmatrix} = \begin{Bmatrix} \{e\}_{1,k} \\ \{e\}_{2,k} \\ \vdots \\ \{e\}_{nobs,k} \end{Bmatrix} - \begin{bmatrix} [J]_{1,k} \\ [J]_{2,k} \\ \vdots \\ [J]_{nobs,k} \end{bmatrix} \{\Delta\beta\} \tag{E.10}$$

$$\{\Delta\beta\} = \left( \begin{bmatrix} [J]_{1,k} \\ [J]_{2,k} \\ \vdots \\ [J]_{nobs,k} \end{bmatrix}^T \begin{bmatrix} [J]_{1,k} \\ [J]_{2,k} \\ \vdots \\ [J]_{nobs,k} \end{bmatrix} \right)^{-1} \left( \begin{bmatrix} [J]_{1,k} \\ [J]_{2,k} \\ \vdots \\ [J]_{nobs,k} \end{bmatrix}^T \begin{Bmatrix} \{e\}_{1,k} \\ \{e\}_{2,k} \\ \vdots \\ \{e\}_{nobs,k} \end{Bmatrix} \right) \tag{E.11}$$

$$\{\Delta\beta\} = \left( \sum_{i=1}^{nobs} \left( [J]_{i,k}^T [J]_{i,k} \right) \right)^{-1} \left( \sum_{i=1}^{nobs} \left( [J]_{i,k}^T \{e\}_{i,k} \right) \right) \tag{E.12}$$

Equation E.12 provides rapid second order Newtonian convergence but can become unstable if the square Jacobian summation is nearly singular. Levenberg and Marquardt showed that a positive factor λ added to the diagonal elements of the square Jacobian summation matrix as shown in Equation E.13 can provide both rapid and stable convergence. For very small values of λ, this provides Newtonian convergence similar to Equation E.12. For larger values of λ, this provides small but stable steps along the gradient shown in Equation E.14.

$$\{\Delta\beta\} = \left( \sum_{i=1}^{nobs} \left( [J]_{i,k}^T [J]_{i,k} \right) + \lambda \underset{npar\ x\ npar}{[I]} \right)^{-1} \left( \sum_{i=1}^{nobs} \left( [J]_{i,k}^T \{e\}_{i,k} \right) \right) \tag{E.13}$$

$$\{\Delta\beta\} = \frac{1}{\lambda} \left( \sum_{i=1}^{nobs} \left( [J]_{i,k}^T \{e\}_{i,k} \right) \right) \tag{E.14}$$

If parameter updates provide a stable step with smaller aggregate SSQ than prior iterations, factor λ is reduced in preparation for the next iteration. If parameter updates provide an unstable step with larger aggregate SSQ than prior iterations, those updates are

rejected, factor λ is increased and the process is repeated. Typically λ is started at a value of 0.1, is reduced by a factor of 10 for stable steps, and is increased by a factor of 10 for unstable steps.

Convergence may be assessed by observing when absolute values of parameter updates are small while the aggregate SSQ approaches the expected standard deviation of residuals. Observing the progression of factor λ can also help indicate convergence.

The algorithm may be summarized as follows.

1) Postulate initial estimates for parameters {β}
2) Evaluate aggregate SSQ over all training pairs for initial parameter estimates (E.9)
3) Set factor β = 0.1
4) Proceed through all training pairs
    a) Evaluate all residuals $\{e\}_{i,k}$ (E.2)
    b) Evaluate all Jacobians $[J]_{i.k}$ (E.5)
    c) Accumulate summations $\sum_{i=1}^{nobs}\left( [J]_{i,k}^{T} [J]_{i,k} \right)$ and $\sum_{i=1}^{nobs}\left( [J]_{i,k}^{T} \{e\}_{i,k} \right)$ (E.12)
5) Add factor λ to diagonal and compute parameter updates {Δβ} (E.14)
6) Update parameters $\{\beta\}_{k+1}$ (Equation 3)
7) Evaluate aggregate SSQ over all training pairs for new parameter estimates (E.9)
8) If aggregate SSQ has been reduced:
    a) Reduce factor $\lambda_{NEW} = \lambda_{OLD} / 10$
    b) Proceed with the next iteration at step 4)
9) If aggregate SSQ has increased:
    a) Discard the new parameter estimates and use immediate prior values
    b) Increasee factor $\lambda_{NEW} = \lambda_{OLD} * 10$
    c) Proceed with the next iteration at step 5)

Because of its robust performance, Levenberg-Marquardt method is often used with finite difference numerical approximations for the Jacobian [J] of the numerical model with respect to model parameters. Note that this Jacobian must be re-evaluated for each training pair for each iteration whether analytically or numerically. Penalty functions may be added to residuals to impose explicit or implicit inequality constraints on parameters. However as with any gradient technique, convergence may dither across constraint boundaries if the minimum SSQ is at a constraint boundary.

## F.1 CONTROLLER UNIT FOR DISTILLATION COLUMN

The controller unit works in automatic mode to control tray temperature to desired set point. In the present work PID controller unit is used so that the distillate composition can be controlled and also to generate temperature patterns with constant temperature of selected trays.

The three variables associated with the controller unit are:

- **Process Variable:** It is the temperature of the tray connected to the controller unit.
- **Set Point:** It is the desired tray temperature that is fed into the controller either directly or through the designed modules.
- **Control Output:** It is the controller output in the form of current signal, which is given to SCR based temperature controller. The SCR based temperature controller is connected to the reboiler heater. Therefore the controller signal indirectly controls the reboiler heaters to keep the temperature of the connected tray at the desired value; by controlling the average voltage applied to heater and in turn the heat input to reboiler. The schematic diagram for controller unit is shown in Fig. F.1. The working principle of SCR is shown in Fig. F.2.

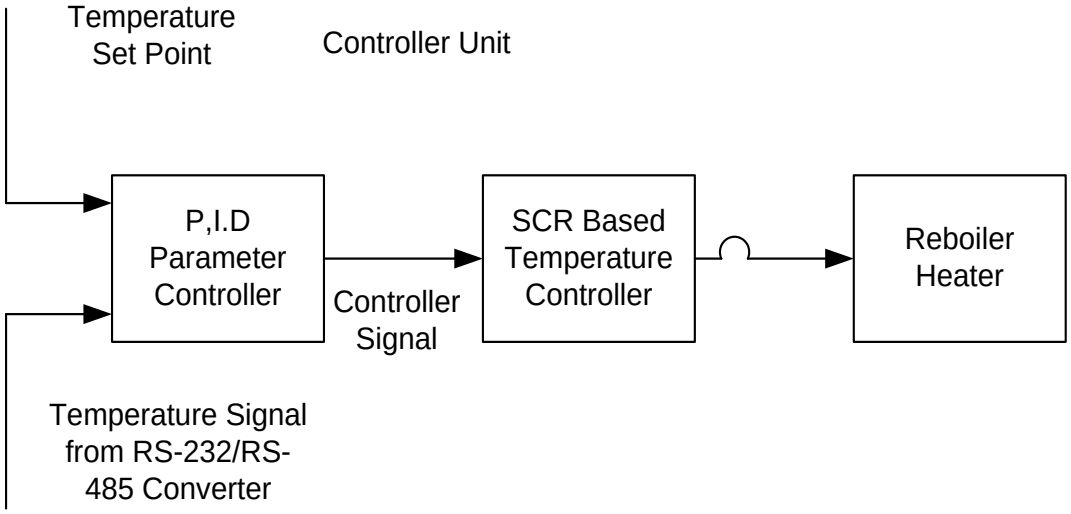


Fig. F.1 Schematic diagram of controller unit with distillation column

In the present work, digital indicating controller unit [99] model No. UT320 manufactured by Yokogawa is used. It has the following features

- Digital indicating controller
- Universal input process variable
- Programmable multiple set points and control output setting
- Three alarm facility available
- Fully programmable controller
- RS-485 interface available

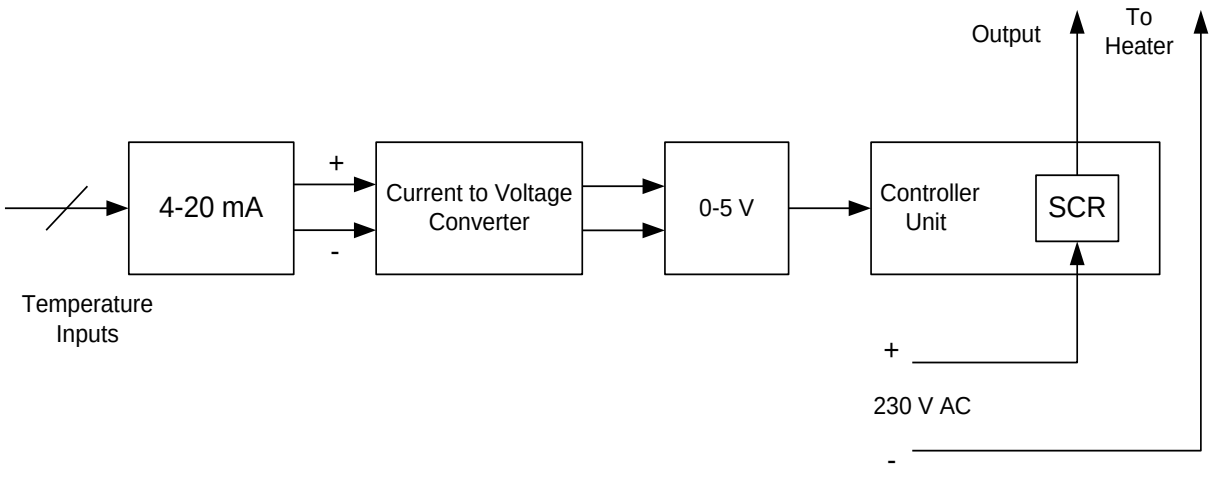


Fig. F.2 SCR interfacing for switching action

## G.1 Genetic Algorithms

Genetic algorithms (GA) were first introduced by John Holland in the 1970s (Holland 1975) as a result of investigations into the possibility of computer programs undergoing evolution in the Darwinian sense. GA is part of a broader soft computing paradigm known as evolutionary computation. They attempt to arrive at optimal solutions through a process similar to biological evolution. The GA methodology is particularly suited for *optimization*, a problem solving technique in which one or more very good solutions are searched for in a solution space consisting of a large number of possible solutions. GA reduces the search space by continually evaluating the current generation of candidate solutions. GA work on a population of individuals represents candidate solutions to the optimization problem. These individual are consists of a strings (called chromosomes) of genes. The genes are a practical allele (gene could be a bit, an integer number, a real value or an alphabet character etc. depending on the nature of the problem). GAs applying the principles of survival of the fittest, selection , reproduction , crossover (recombining) , and mutation on these individuals to get , hopefully , a new butter individuals (new solutions) . GAs are applied for those problems which either cannot be formulated in exact and accurate mathematical forms and may contain noisy or irregular data or it take so much time to solve or it is simply impossible to solve by the traditional computational methods.

## G.2 How Genetic Algorithms Work

Genetic algorithm maintains a population of individuals, say P(t), for generation t. Each individual represents a potential solution to the problem at hand. Each individual is evaluated to give some measure of its fitness. Some individuals undergo stochastic transformations by means of genetic operations to form new individuals. There are two type of transformation: 1) Mutation, which creates new individuals by making changes in a single individual. 2) Crossover, which creates new individuals by combining parts from two individuals. The new individuals, called offspring C(t), are then evaluated. A new population is formed by selecting the more fit individuals from the parent population and offspring population. After several generations, genetic algorithm converges to the best individual, which hopefully represents an optimal or suboptimal solution to the problem.

The general structure of the Genetic algorithms is as follow:

```
Begin
  {
  t=0;
  Initialize P(t);
  Evaluate P(t);
  While (not termination condition) do
```

```
Begin
        {
        Apply crossover and mutation to P(t) to yield C(t);
        Evaluate C(t);
        Select P(t+1) from P(t) and C(t);
              t=t+1;
        }
       End
 }
End
```

**G.3 Encoding**

How to encode the solutions of the problem into chromosomes is a key issue when using genetic algorithms. Various encoding methods have been created for particular problems to provide effective implementation of genetic algorithms. According to what kind of symbol is used as the alleles of a gene, the encoding methods can be classified as follows:1) Binary encoding, 2) Real-number encoding and, 3) Integer or literal permutation encoding. Binary encoding (i.e., the bit strings) method is used in the present problem.

**G.4 Genetic Algorithms Operators**

There are two basic genetic algorithms operators which are crossover and mutation. These two operators are work together to explore and exploit the search space by creating new variants in the chromosomes. There are many empirical studies on a comparison between crossover and mutation. It is confirmed that mutation operator play the same important role as that of the crossover.

**G.4.1 Crossover**

One of the unique aspects of the work involving genetic algorithms (GAs) is the important role that Crossover (recombination) plays in the design and implementation of robust evolutionary systems. In most GAs, individuals are represented by fixed-length strings and crossover operates on pairs of individuals (parents) to produce new strings (offspring) by exchanging segments from the parents' strings. Traditionally, the number of crossover points (which determines how many segments are exchanged) has been fixed at a very low constant value of 1 or 2. A commonly used method for crossover is called single point crossover. In this method, a single point crossover position (called cut-point) is chosen at random (e.g., between the 4th and 5th variables) and the parts of two parents after the crossover position are exchanged to form two offspring, as shown in figure (1). The other crossover methods are multi point crossover and uniform crossover method.

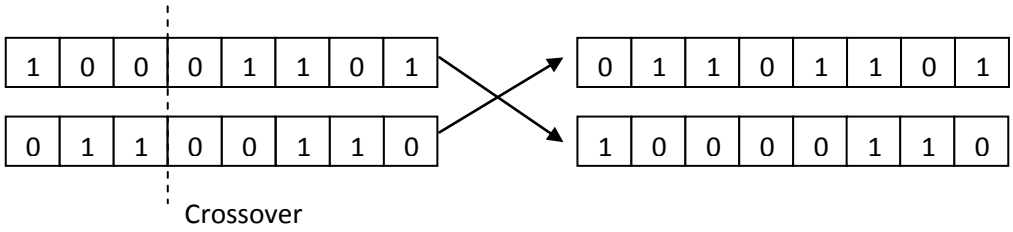


Fig. G.1 Single point crossover

### G.4.2 Mutation

Mutation is a common operator used to help preserve diversity in the population by finding new points in the search pace to evaluate. When a chromosome is chosen for mutation, a random change is made to the values of some locations in the chromosome. A commonly used method for mutation is called single point mutation. Though, a special mutation types used for varies problem kinds and encoding methods. Single gene (chromosome or even individual) is randomly selected to be mutated and its value is changed depending on the encoding type used, as shown in figure (2).

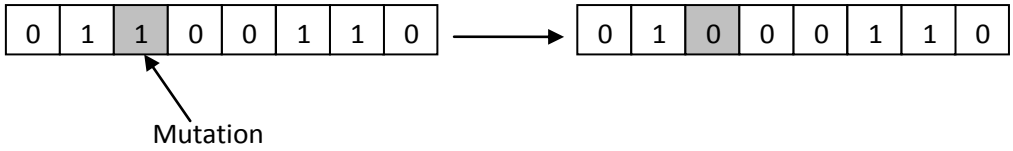


Fig. G.2 Single point mutation

### G.4.3 Selection

Selection is the process of determining the number of times a particular individual is chosen for reproduction and, thus, the number of offspring that an individual will produce. The principle behind genetic algorithms is essentially Darwinian natural selection. Selection provides the driving force in genetic algorithms. With too much force, genetic search will terminate prematurely. While with too little force, evolutionary progress will be slower than necessary.

Typically, a lower selection pressure is indicated at the start of genetic search in favor of a wide exploration of the search space, while a higher selection pressure is recommended at the end to narrow the search space. In this way, the selection directs the genetic search toward promising regions in the search space and that will improve the performance of genetic algorithms. Many selection methods have been proposed, examined and compared. The most common types are:

1) Roulette wheel selection,
2) Rank selection,
3) Tournament selection,
4) Steady state selection and,
5) Elitism.

In the present work, '*Roulette Wheel'* selection method is used for reproduction. For example as shown in figure 3, each individual in the population is allocated a section of a roulette wheel. The size of the section is proportional to the fitness of the individual. A pointer is spun and the pointed individual is selected. The number of times the roulette wheel is spun is equal to size of the population. This process continues until the selection criterion has been met. Thus, the probability of an individual being selected is related to its fitness. This ensures that fitter individuals are more likely to leave offspring. Multiple copies of the same string may be selected for reproduction and the fitter strings should begin to dominate. For example, there are three chromosomes 10001, 10000 and 01110 as shown in figure 3. The number of times the roulette wheel is spun is equal to size of the population. It is shown in figure 3 the way how wheel is now divided. Each time the wheel stops this gives the fitter individuals the greatest chance of being selected for the next generation.

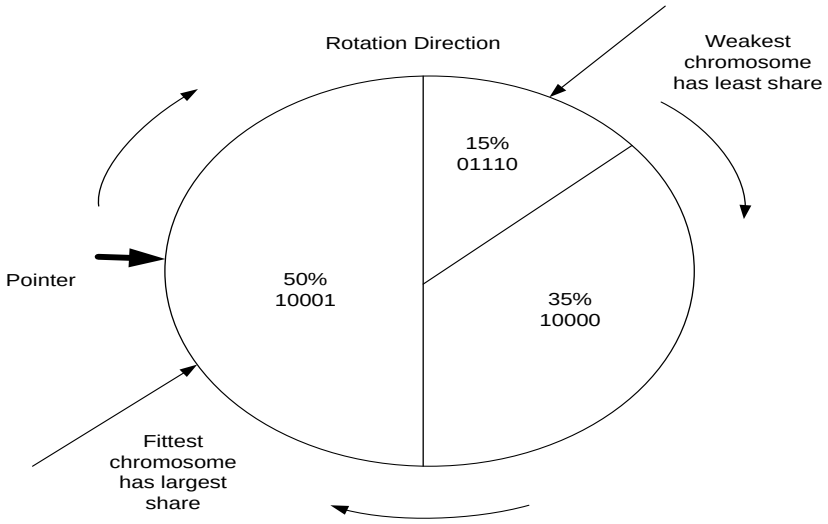


Fig. G.3 Roulette wheel approach: based on fitness

**G.5 Genetic Algorithms Parameters**

One of the more challenging aspects of using genetic algorithms is to choose the configuration parameter settings. Discussion of GA theory provides little guidance for proper selection of the settings. The population size, the mutation rate, and the type of recombination have the largest effect on search performance. They are used to control the run of a GA. They can influence the Population and the Reproduction part of the GAs. In traditional GAs the parameters has fixed values. Some guidelines are used in selecting these parameter settings are given in the following subsections.

**G.5.1 Population Size**

The population size is one of the most important parameters that play a significant role in the performance of the genetic algorithms. The population size dictates the number of individuals in the population. Larger population sizes increase the amount of variation present in the initial population at the expense of requiring more fitness evaluations. It is found that the best population size is both applications dependent and related to the

individual size (number of chromosomes within). For larger individuals and challenging optimization problems, larger population sizes are needed to maintain diversity (higher diversity can also be achieved through higher mutation rates and uniform crossover) and hence better exploration.

### G.5.2 Crossover Rate

Crossover rate determines the probability that crossover will occur. The crossover will generate new individuals in the population by combining parts of existing individuals. The crossover rate is usually high and 'application dependent'.

### G.5.3 Mutation Rate

Mutation rate determines the probability that a mutation will occur. Mutation is employed to give new information to the population (uncover new chromosomes) and also prevents the population from becoming saturated with similar chromosomes, simply said to avoid premature convergence. Large mutation rates increase the probability that good schemata will be destroyed, but increase population diversity.

## G.6 Advantages and Disadvantage of Genetic Algorithms

Crossover is a crucial aspect of any genetic algorithm as in biology; crossover can lead to new combinations of genes which are more fit than any in the previous generations. Creating new variants is the key to genetic algorithms, as there is a good chance of finding better solutions. This is why mutation is also a necessary part of the genetic algorithms. It will create offspring which would not have arisen otherwise, and may lead to a better solution.

Other optimization algorithms have the disadvantage that some kind of initial guess is required and this may bias the final result. GA on the other hand only requires a search range, which need only be constrained by prior knowledge of the physical properties of the system. Effectively they search the whole of the solution space, without calculating the fitness function at every point. This can help avoid a danger in any optimization problem which is being trapped in local maxima or minima. There are two main reasons for this:

1) The initial population, being randomly generated, will sample the whole of the solution space, and not just a small area.

2) Variation inducing tactics, i.e. crossover and mutation, prevent the algorithm being trapped in one part of the solution space.

Genetic algorithms can be employed for a wide variety of optimization problems. They perform very well for large scale optimization problems which may be very difficult or impossible to solve by other traditional methods.

The disadvantage of genetic algorithms is that it, Sometimes, have trouble finding the exact global optimum because there is no guaranty to find best solution. Another drawback is that GA requires large number of response (fitness) function evaluations depending on the number of individuals and the number of generations. Therefore, genetic algorithms may take long time to evaluate the individuals.